Defense Nuclear Agency
Alexandria, VA 22310-3398

DNA-TR-91-69

Advanced DAA Methods for Shock Response Analysis

Thomas L. Geers
Peizhen Zhang
Brett A. Lewis
University of Colorado
Department of Mechanical Engineering
Campus Box 427
Boulder, CO 80309

July 1992

Technical Report

CONTRACT No. DNA 001-88-C-0057

Destroy this report when it is no longer needed. Do not return to sender.

PLEASE NOTIFY THE DEFENSE NUCLEAR AGENCY, ATTN: CSTI, 6801 TELEGRAPH ROAD, ALEXANDRIA, VA 22310-3398, IF YOUR ADDRESS IS INCORRECT, IF YOU WISH IT DELETED FROM THE DISTRIBUTION LIST, OR IF THE ADDRESSEE IS NO LONGER EMPLOYED BY YOUR ORGANIZATION.

DISTRIBUTION LIST UPDATE

This mailer is provided to enable DNA to maintain current distribution lists for reports. (We would appreciate your providing the requested information.)

NOTE:
Please return the mailing label from the document so that any additions, changes, corrections or deletions can be made easily.

☐ Add the individual listed to your distribution list.

☐ Delete the cited organization/individual.

☐ Change of address.

NAME: _____

ORGANIZATION: _____

OLD ADDRESS	CURRENT ADDRESS
_____	_____
_____	_____
_____	_____

TELEPHONE NUMBER: ( ) _____

DNA PUBLICATION NUMBER/TITLE	CHANGES/DELETIONS/ADDITIONS, etc.) *(Attach Sheet if more Space is Required)*
_____	_____
_____	_____
_____	_____

DNA OR OTHER GOVERNMENT CONTRACT NUMBER: _____

CERTIFICATION OF NEED-TO-KNOW' BY GOVERNMENT SPONSOR (if other than DNA):

SPONSORING ORGANIZATION: _____

CONTRACTING OFFICER OR REPRESENTATIVE: _____

SIGNATURE: _____

CUT HERE AND RETURN

DEFENSE NUCLEAR AGENCY
ATTN: TITL
6801 TELEGRAPH ROAD
ALEXANDRIA, VA 22310-3398

DEFENSE NUCLEAR AGENCY
ATTN: TITL
6801 TELEGRAPH ROAD
ALEXANDRIA, VA 22310-3398

REPORT DOCUMENTATION PAGE

Form Approved OMB No. 0704-0188

1. AGENCY USE ONLY (Leave blank)	2. REPORT DATE	3. REPORT TYPE AND DATES COVERED
	920701	Technical 880601 – 910331

4. TITLE AND SUBTITLE

Advanced DAA Methods for Shock Response Analysis

5. FUNDING NUMBERS

C - DNA 001-88-C-0057
PE - 62715H
PR - RS
TA - RC
WU - DH048540

6. AUTHOR(S)

Thomas L. Geers, Peizhen Zhang, and Brett A. Lewis

7. PERFORMING ORGANIZATION NAME(S) AND ADDRESS(ES)

University of Colorado
Department o f Mechanical Engineering
Campus Box 427
Boulder, CO 80309

8. PERFORMING ORGANIZATION REPORT NUMBER

9. SPONSORING/MONITORING AGENCY NAME(S) AND ADDRESS(ES)

Defense Nuclear Agency
6801 Telegraph Road
Alexandria, VA 22310-3398
SPSD/Senseny

10. SPONSORING/MONITORING AGENCY REPORT NUMBER

DNA-TR-91-69

11. SUPPLEMENTARY NOTES

This work was sponsored by the Defense Nuclear Agency under RDT&E RMC Code B4662D RS RC 00074 SPSD 4300A 25904D.

12a. DISTRIBUTION/AVAILABILITY STATEMENT

Approved for public release; distribution is unlimited.

12b. DISTRIBUTION CODE

13. ABSTRACT *(Maximum 200 words)*

Doubly asymptotic approximations (DAA's) are approximate contact-surface relations for the dynamic interaction between a body and an adjacent medium. In this report, first- and second-order DAA's are formulated for an internal acoustic domain, and a first-order DAA is formulated and implemented in boundary-element form for a semi-infinite elastic domain. The new DAA's constitute extensions of DAA's previously formulated and implemented for external acoustic and infinite elastic domains. The accuracy of the internal DAA's is evaluated by comparing DAA and exact solutions for a canonical problem, namely, the excitation of a fluid-filled spherical shell submerged in an infinite acoustic medium by a plane step-wave; in this evaluation, the second-order DAA exhibits satisfactory accuracy. A preliminary evaluation of the first-order DAA for a semi-infinite elastic medium is conducted by comparing boundary-element DAA results with results in the literature for a suddenly pressurized spherical cavity; marginal accuracy is observed.

14. SUBJECT TERMS		15. NUMBER OF PAGES
Underwater Shock Acoustics Elasto-Dynamics	Ground Shock Medium-Structure Interaction	114
		16. PRICE CODE

17. SECURITY CLASSIFICATION OF REPORT	18. SECURITY CLASSIFICATION OF THIS PAGE	19. SECURITY CLASSIFICATION OF ABSTRACT	20. LIMITATION OF ABSTRACT
UNCLASSIFIED	UNCLASSIFIED	UNCLASSIFIED	SAR

CLASSIFIED BY:

N/A since Unclassified.

DECLASSIFY ON:

N/A since Unclassified.

SUMMARY

Doubly asymptotic approximations (DAA's) are approximate contact-surface relations for the dynamic interaction between a body and an adjacent medium. In this report, first- and second-order DAA's are formulated for an internal acoustic domain, and a first-order DAA is formulated and implemented in boundary-element form for a semi-infinite elastic domain. The new DAA's constitute extensions of DAA's previously formulated and implemented for external acoustic and infinite elastic domains. The accuracy of the internal DAA's is evaluated by comparing DAA and exact solutions for a canonical problem, *viz.* the excitation of a fluid-filled spherical shell submerged in an infinite acoustic medium by a plane step-wave; in this evaluation, the second-order DAA exhibits satisfactory accuracy. A preliminary evaluation of the first-order DAA for a semi-infinite elastic medium is conducted by comparing boundary-element DAA results with results in the literature for a suddenly pressurized spherical cavity; marginal accuracy is observed. The satisfactory performance exhibited by the second-order internal acoustic DAA calls for early implementation in production analysis codes for underwater shock analysis, but the development of second-order DAA's for elastic media should precede an implementation effort for ground shock analysis.

PREFACE

This study was performed under Contract Number DNA 001-88-C-0057 with Dr. Kent L. Goering as Contract Technical Monitor; The authors are grateful to Dr. Goering for his continued interest and confidence in doubly asymptotic methods.

TABLE OF CONTENTS

TABLE OF CONTENTS (Continued)

TABLE OF CONTENTS (Continued)

LIST OF ILLUSTRATIONS

LIST OF ILLUSTRATIONS (Continued)

LIST OF ILLUSTRATIONS (Continued)

SECTION 1

INTRODUCTION

Treating the transient dynamic interaction between a structure in contact with a fluid or elastic medium is a formidable task. Given the dynamical equations for the structure and a specification of the initial conditions, external dynamic forces and/or incident-wave field, a *doubly asymptotic approximation* (DAA) provides a link that greatly simplifies the analysis. This simplification allows the analyst to devote most of his/her computational resources to the structural model, which is the focus of interest, by minimizing the resources required for modelling the medium, which is rarely of interest.

1.1 MOTIVATION

In the 1970's, DAA's were first developed to treat the acoustic fluid-structure interaction in underwater shock problems (Geers, 1971, 1974, 1978). These approximations approach exactness in both the early-time/high-frequency and late-time/low-frequency limits; hence the name *doubly asymptotic*. Acoustic DAA's have been incorporated in a variety of production computer programs that are routinely used for engineering analysis (Ranlet, *et al.*, 1977; DeRuntz, *et al.*, 1980; DeRuntz and Brogan, 1980; Neilson, *et al.*, 1981; Vasudevan and Ranlet, 1982; Atkatsh, *et al.*,1987). In the 1980's, the acoustic DAA methodology was improved (Felippa, 1980; Geers and Felippa, 1983; Nicolas-Vullierme, 1989) and the DAA concept was extended to elastodynamics and electromagnetics (Underwood and Geers, 1981; Mathews and Geers, 1987; Geers and Zhang, 1988).

In solids and fluids, the general approach has been to regard the stress and displacement fields in the medium as the sum of those associated with the incoming incident wave (if there is one) and those associated with the outgoing scattered wave (of which there is always one--if there is no incident wave, the scattered wave is usually called the radiated wave). Compatibility of surface tractions and displacements provides all of the remaining relations needed save one:

a relation between the scattered-wave stress and the scattered-wave displacement over the surface of the structure in contact with the medium.

The Kirchhoff retarded-potential integral for an acoustic medium and the dynamic Somigliana identity for an elastic medium provide exact relations connecting scattered-wave tractions and displacements. Unfortunately, these relations are integral equations over the contact surface that involve field variables with retarded-time arguments; hence they are local neither in space nor in time, and they are complicated. These characteristics mitigate against computational efficiency, prompting the development of simpler relations. Singly asymptotic approximations have been developed that apply either at early time or at late time (but not both), but they are not sufficiently robust for diverse application. In contrast, doubly asymptotic approximations for external domains have been found easy to use and remarkably accurate in a broad apectrum of applications.

Recently, interest has developed in DAA's for *internal acoustic domains*, motivated by the following factors: (1) Internal domains of practical interest often possess exceedingly complex geometries, which makes 3-D mesh generation for finite-element modelling costly and cumbersome; (2) Numerical simulations of discontinuous wave fronts through 3-D finite-element meshes are typically plagued by non-physical osicillations, which compromise the value of the calculations: (3) An exact boundary-element treament based on Kirchhoff's retarded potential formulation would be computationally intensive, typically usurping resources that are needed for accurate structural modelling.

At the same time, interest continues in the advancement of DAA technology for ground shock analysis; of particular interest is the extension of the existing first-order DAA for the infinite elastic medium to treat the *semi-infinite elastic medium.* Because the constitutive behavior of soil is so often highly nonlinear, the placement of a DAA boundary directly on the soil-structure contact surface is not advisable. However, the use of such a boundary as a non-reflecting boundary at a modest distance from the contact surface is most attractive. As discussed by Mathews and Geers, 1987, a DAA nonreflecting boundary is superior to the singly asymptotic boundaries currently used in most codes.

This report documents recent advances in DAA technology. First, the methodology of formulating DAA's is systematized, which is essential for the development of high-order approximations. Second, first- and second-order DAA's are formulated for an internal acoustic

medium. Third, the internal DAA's are evaluated by comparing DAA solutions with exact solutions for a canonical underwater-shock problem; because solutions to this problem did not previously exist, the exact solutions are provided herein. Fourth, a first-order DAA for an elastic half-space is formulated. Fifth, this DAA is implemented in a boundary-element code and numerical results for two canonical problems are compared with results currently in the literature.

1.2 REPORT OUTLINE.

Section 2 of this report contains a review of the first-order DAA (DAA_1) for an *external acoustic medium* featuring the method of *operator matching*. Both integral-operator and matrix formulations are presented, and a *modal analysis* of the two formulations is performed.

DAA_1 for an *internal acoustic domain* is formulated in Section 3. The separation of low-frequency fluid motion into dilatational and equivoluminal components is shown to be essential to the formulation. Operator, matrix and modal developments are given, all based on operator matching.

Section 4 contains a straightforward formulation of the second-order DAA (DAA_2) for an *external acoustic medium* produced by operator matching. This extends the work of Felippa (1980a) and Nicolas-Vullierme (1989), avoiding the introduction of an impedance formalism and retaining the advantages of Laplace transformation. The corresponding matrix formulation is also presented, but a modal analysis is not, because the matched DAA_2 does not diagonalize.

The matched DAA_2 for an *internal acoustic domain* is formulated in Section 5. Again, the separation of low-frequency motion into dilatational and equivoluminal components is central. Both operator and matrix forms are given, but uncoupled modal analysis is not admissable.

Section 6 describes the specialization of the four matched DAA's to axisymmetric flow outside and inside a *spherical surface*. For this classical geometry, even the second-order DAA's submit to uncoupled modal decomposition in terms of Legendre polynomials. This yields modal DAA equations for each generalized harmonic. Also provided in this section are exact modal equations, which are substantially more complicated than the DAA equations.

In Section 7, exact modal response equations are derived for a previously unsolved *canonical problem*, namely, the response of a fluid-filled, submerged spherical shell to a transient acoustic wave. The modal equations are formulated by the residual potential method (Geers,

1969, 1971, 1972) and are solved by numerical integration in time. Physical responses are then obtained by modal superposition. Difficulties with poor modal convergence are successfully treated by obtaining partial closed-form solutions and using the Cesàro sum (Apostol, 1957). The numerical solutions thus obtained serve as basis for evaluating the internal DAA's developed in Sections 3 and 5.

Numerical results for the fluid-filled, submerged spherical shell excited by a plane step-wave are presented in Section 8. Exact, DAA_1, and DAA_2 results are compared to assess the accuracy of the internal DAA's. Also, the shock response of the fluid-filled shell is contrasted with that of an empty shell.

In Section 9, systematic DAA_1 formulations are given for infinite and semi-infinite *elastic media*, both in operator and matrix form. Implementation in a *boundary-element code* is described, and *numerical results* for two canonical problems are compared with corresponding results in the literature.

Section 10 concludes the report by summarizing the work conducted and listing the principal conclusions reached during the study.

1.3 TECHNOLOGY TRANSFER.

The implementation of external acoustic DAA's in production shock-analysis codes has improved the engineering design and analysis of many naval structures. The internal acoustic DAA_2 formulated in Section 5 is shown in Section 8 to be sufficiently accurate to warrant its early implementation in those codes. In the meantime, it is appropriate to seek improved internal DAA's in order to raise the level of accuracy to that exhibited by the external DAA_2.

More research is needed before elastic DAA's are ready for production analysis. The first-order DAA's for infinite and semi-infinite half-spaces are only marginally accurate, which calls for the development of second-order DAA's. Fortunately, such development can make good use of the formulation techniques used to develop acoustic DAA's.

DAA's can be formulated for shock response analyses involving other media, such as layered media, porous media, and air at moderate pressures; higher-order DAA's for electromagnetic scattering also hold promise. What was orignally developed as a method focused on underwater shock analysis is emerging as one of substantially broader scope.

SECTION 2

DAA_1 FOR AN EXTERNAL ACOUSTIC DOMAIN

Although the first-order doubly asymptotic approximation for an external acoustic domain was given some twenty years ago (Geers, 1971), a review is appropriate here, for two reasons. First, such a review provides the clearest picture of the DAA concept, and second, it introduces the operator matching method at the simplest level.

2.1 RETARDED POTENTIAL FORMULATION.

With the acoustic pressure $p(\mathbf{r},t)$ and fluid-particle displacement $\mathbf{u}(\mathbf{r},t)$ given in terms of a velocity potential $\phi(\mathbf{r},t)$ as

$$\begin{aligned} p(\mathbf{r},t) &= \rho\dot{\phi}(\mathbf{r},t) \\ \dot{\mathbf{u}}(\mathbf{r},t) &= -\nabla\phi(\mathbf{r},t) \end{aligned} \tag{2.1}$$

where ρ is the mass density of the fluid, an overdot denotes differentiation in time, and ∇ is the gradient operator, the wave equation for a uniform acoustic fluid is (see, *e.g.*, Pierce, 1981)

$$c^2\nabla^2\phi = \ddot{\phi} \tag{2.2}$$

where c is the speed of sound in the fluid and ∇^2 is the Laplacian operator.

With $\mathbf{n}$ as the normal going *into* the fluid at a point on a surface S that bounds the fluid domain, the inward fluid-particle displacement normal to that surface is defined by
$u = \mathbf{u}\cdot\mathbf{n}$.

An exact, integral-equation solution to (2.2) is given by Kirchhoff's retarded potential formulation (RPF) (see, *e.g.*, Baker and Copson, 1939, and Sobolev, 1964), which may be written for points P and Q on S

$$2\pi p_P(t) = \int_S \{\rho R_{PQ}^{-1} \ddot{u}_Q(t_R) - R_{PQ}^{-2} \cos\phi_{Rn}[p_Q(t_R) + c^{-1}R_{PQ}\dot{p}_Q(t_R)]\}\, dS_Q \qquad (2.3)$$

where $R_{PQ} = |r_P - r_Q|$, ϕ_{Rn} is the angle between $\mathbf{R}_{PQ}$ and $\mathbf{n}$, and t_R is the *retarded time* $t - c^{-1}R_{PQ}$; the line through the integral sign indicates that the point P is excluded from the integral. The constant 2π multiplying $p_P(t)$ on the left side of (2.3) indicates that the point P is located on a smooth portion of the surface S. If P is not on the surface, but is inside (or outside) the fluid domain, the multiplying constant becomes 4π (or zero); if S is not smooth at P, but instead has an edge or a corner there, the multiplying constant becomes the value of the solid angle subtended by the edge or corner.

For our purposes, it is convenient formally to incorporate the singular contribution $2\pi p_P(t)$ into the spatial integral of (2.3) and then take the Laplace transform of the result to obtain

$$\int_S R_{PQ}^{-2} \cos\phi_{Rn}(1+R_{PQ}s/c)\, e^{-(R_{PQ}s/c)}\, p_Q(s)\, dS_Q = \rho \int_S R_{PQ}^{-1} s^2\, e^{-(R_{PQ}s/c)}\, u_Q(s)\, dS_Q \qquad (2.4)$$

2.2 FIRST-ORDER EARLY-TIME APPROXIMATION: ETA_1.

Early-time approximations are the inverse Laplace transforms of algebraic equations to which (2.4) reduces when $R_{max}s/c \gg 1$, which corresponds in the time domain to $t \ll c^{-1}R_{max}$ (Geers, 1975). The first-order ETA for an external acoustic medium was first utilized by Mindlin and Bleich, 1953, for a problem in polar coordinates. In a systematic analysis, Felippa, 1980, found the same result for a general smooth surface, which is, in transform space,

$ETA_1(s)$: $$p_P(s) = \rho c s u_P(s) \qquad (2.5)$$

Inverse Laplace transformation yields as the first-order ETA in the time domain

$ETA_1(t)$: $$p_P(t) = \rho c \dot{u}_P(t) \qquad (2.6)$$

ETA_1 is clearly a *local approximation* in space, stating that each element of the surface S independently generates a plane wave that propagates normally into the fluid. In addition, it applies equally well to either an external or an internal fluid domain. Finally, because it approaches exactness only as $s \to \infty$, it is *singly asymptotic*. In the literature, ETA_1 is often referred to as the *plane wave approximation*.

2.3 FIRST-ORDER LATE-TIME APPROXIMATION: LTA_1.

Late-time approximations are the inverse Laplace transforms of integral equations in space to which (2.4) reduces when $R_{max}s/c << 1$, which corresponds in the time domain to $t >> c^{-1}R_{max}$ (Geers, 1975). The first-order LTA for an external acoustic domain was first utilized by Chertock, 1972. It may be readily obtained by merely expanding the exponentials in (2.4) in a Taylor's series as

$$e^{-R_{PQ}s/c} = 1 - R_{PQ}s/c + \frac{1}{2}(R_{PQ}s/c)^2 - \ldots \tag{2.7}$$

Introducing this into (2.4) and keeping only terms of order s^0 on the left and s^2 on the right, we obtain LTA_1 in transform space

$$\int_S R_{PQ}^{-2} \cos\phi_{Rn}\, p_Q(s)\, dS_Q = \rho \int_S R_{PQ}^{-1}\, s^2\, u_Q(s)\, dS_Q \tag{2.8}$$

Note that, unlike ETA_1, LTA_1 is not spatially local, and that, like ETA_1, it is singly asymptotic, but in the limit $s \to 0$ instead of $s \to \infty$. In the literature, LTA_1 is often referred to as the *added mass approximation* or the *virtual mass approximation*.

With the spatial operator definitions

$$\beta q_Q \equiv \int_S R_{PQ}^{-1}\, q_Q\, dS_Q \tag{2.9}$$

$$\gamma q_Q \equiv \int_S R_{PQ}^{-2} \cos\phi_{Rn}\, q_Q\, dS_Q$$

LTA_1 for an external domain may be expressed in transform space as

$LTA_1(s)$: $$\beta^{-1}\gamma p_Q(s) = \rho s^2 u_P(s) \tag{2.10}$$

or in the time domain as

$LTA_1(t)$: $$\beta^{-1}\gamma p_Q(t) = \rho \ddot{u}_P(t) \tag{2.11}$$

Here, β^{-1} denotes the inverse of the operator β, *i.e.*, if q_P produces $p_P = \beta q_Q$ through the first of (2.9), then p_P produces q_P through the relation $q_P = \beta^{-1} p_Q$. It can be shown that β is invertible.

By taking the Laplace transform of (2.2), considering $\nabla^2 \sim R_{max}^{-2}$, and then letting $R_{max}s/c \to 0$, one readily deduces that LTA_1 constitutes the integral-equation solution to Laplaces equation, $\nabla^2\phi = 0$. This means that LTA_1 pertains to the irrotational flow of an inviscid, incompressible fluid.

2.4 FIRST-ORDER DOUBLY ASYMPTOTIC APPROXIMATION: DAA_1.

An approximation that naturally reduces to ETA_1, (2.5), at early times ($s \to \infty$) and to LTA_1, (2.10), at late times ($s \to 0$) is

$$Cs^{j+2} p_P(s) + \gamma p_Q(s) = C\rho c s^{j+3} u_P(s) + \rho s^2 \beta u_Q(s) \tag{2.12}$$

where C is an arbitrary constant and $j \geq 0$. This approximation has two flaws: the constants C and j are undetermined and the inverse transform would possess derivatives higher than necessary. Hence we reject it as a first-order DAA.

An examination of (2.5) and (2.10) reveals that a relation with one term in $s^0p(s)$ and another in $s^1p(s)$ on the left, and with one term in $s^2u(s)$ on the right, is capable of reducing to the two singly asymptotic relations in the appropriate limits. Hence, as the first step in the *method of operator matching*, we introduce the DAA_1 *trial equation*

$$[sP_1 + cP_0]p_Q(s) = \rho c s^2 u_P(s) \tag{2.13}$$

where P_0 and P_1 are spatial operators (not functions of s!). For $s \to 0$, we write this equation as

$$[P_0 + O(s)]p_Q(s) = \rho s^2 u_P(s) \tag{2.14}$$

and match it to (2.10) as $s \to 0$, which yields $P_0 = \beta^{-1}\gamma$. For $s \to \infty$, we divide (2.13) through by s, write the result as

$$[P_1 + O(s^{-1})]p_Q(s) = \rho c s u_P(s) \tag{2.15}$$

and match it to (2.5) as $s \to \infty$, which yields $P_1 p_Q(s) = p_P(s)$. The introduction of these results into (2.13) produces the first-order DAA for an external acoustic domain, expressed in transform space as

$DAA_1(s)$: $$s p_P(s) + c\beta^{-1}\gamma p_Q(s) = \rho c s^2 u_P(s) \tag{2.16}$$

and in the time domain as

$DAA_1(t)$: $$\dot{p}_P(t) + c\beta^{-1}\gamma p_Q(t) = \rho c \ddot{u}_P(t) \tag{2.17}$$

We note that, as might be anticipated, DAA_1 is not a spatially local approximation.

2.5 MATRIX DAA_1 FOR BOUNDARY ELEMENT ANALYSIS.

The boundary element method has become a powerful tool for obtaining solutions to problems involving complex geometries (see, *e.g.*, Bannerjee, 1981). The method may be described with considerable generality as Petrov-Galerkin finite-element discretization over the boundary of a spatial domain (Hughes, 1986). To use the method, we first discretize the pressure and normal-displacement fields on the surface S as

$$p_Q(t) = \mathbf{v}_Q^T \mathbf{p}(t) \tag{2.18}$$

$$u_Q(t) = \mathbf{v}_Q^T \mathbf{u}(t)$$

where $\mathbf{v}_Q$ is the column vector of shape-functions, the superscript T denotes vector transposition, and $\mathbf{p}(t)$ and $\mathbf{u}(t)$ are, respectively, the column vectors for nodal-pressure and nodal-displacement response. To be able to represent a constant field, we require that $\mathbf{v}_Q^T\mathbf{1} = 1$, where $\mathbf{1}$ is the unit vector.

Next, we "preoperate" the DAA_1 equation, (2.17), through by the operator β, insert (2.18), and, with a column vector of weight-functions $\mathbf{w}_P$, form the weighted-residual equations

$$\int_S \mathbf{w}_P\, \beta \mathbf{v}_Q^T\, dS_P\, \dot{\mathbf{p}}(t) + c\int_S \mathbf{w}_P\, \gamma \mathbf{v}_Q^T\, dS_P\, \mathbf{p}(t) = \rho c \int_S \mathbf{w}_P\, \beta \mathbf{v}_Q^T\, dS_P\, \ddot{\mathbf{u}}(t) \tag{2.19}$$

which can be written more compactly as

$$\mathbf{B}\dot{\mathbf{p}}(t) + c\mathbf{C}\mathbf{p}(t) = \rho c \mathbf{B}\ddot{\mathbf{u}}(t) \tag{2.20}$$

where, from (2.9),

$$\mathbf{B} = \int_S\int_S \mathbf{w}_P\, R_{PQ}^{-1}\, \mathbf{v}_Q^T\, dS_Q\, dS_P$$

$$\mathbf{C} = \int_S\int_S \mathbf{w}_P\, R_{PQ}^{-2} \cos\phi_{Rn}\, \mathbf{v}_Q^T\, dS_Q\, dS_P \tag{2.21}$$

The NxN matrices **B** and **C** are full matrices of rank N, and are therefore invertible (see Section 2.6). They are most easily constructed if **v** corresponds to the assumption of a *constant field* over each element and **w** corresponds to *collocation at centroidal nodes* [see, *e.g.*, DeRuntz and Geers, 1978]. The elements of **B** and **C** are then given by

$$b_{ij} = \int_{S_j} R_{ij}^{-1} \, dS_j$$

$$c_{ij} = 2\pi\delta_{ij} + \int_{S_j} R_{ij}^{-2} \cos\phi_{ij} \, dS_j \tag{2.22}$$

where $R_{ij} = |\mathbf{R}_{ij}|$ is the distance from the centroid of element i to an integration point in element j, δ_{ij} is the Kronecker delta, and ϕ_{ij} is the angle between $\mathbf{R}_{ij}$ and the surface normal (going into the fluid) at an integration point in element j.

To obtain the semi-discretized form of (2.17), *i.e.*, that produced when (2.17) is discretized in space but not in time, we simply premultiply (2.20) through by $\mathbf{B}^{-1}$, which yields

$$\mathbf{DAA}_1(t): \qquad \dot{\mathbf{p}}(t) + c\mathbf{B}^{-1}\mathbf{C}\,\mathbf{p}(t) = \rho c\,\dot{\mathbf{u}}(t) \tag{2.23}$$

It would be advantageous if this relation were converted into a symmetric form. We accomplish this by first discretizing (2.11) to obtain the matrix $\mathbf{LTA}_1$

$$\mathbf{B}^{-1}\mathbf{C}\,\mathbf{p}(t) = \rho\,\ddot{\mathbf{u}}(t) \tag{2.24}$$

Next, we obtain a suitable boundary-element expression for the kinetic energy of an inviscid, incompressible fluid undergoing irrotational flow (see the last paragraph in Section 2.3). We start with the known continuum expression (see, *e.g.*, Milne-Thomson, 1960)

$$T(t) = \frac{1}{2} \int_S \overset{*}{p}_P(t)\, \dot{u}_P(t) \, dS_P \tag{2.25}$$

where the asterisk over $p_P(t)$ denotes a time integration. Introducing the discretization expressions (2.18), we then obtain

$$T(t) = \frac{1}{2}\, \dot{\mathbf{u}}^T(t)\mathbf{A}\,\overset{*}{\mathbf{p}}(t) \tag{2.26}$$

where the generalized area matrix **A** is given by

$$\mathbf{A} = \int_S \mathbf{v}_Q \, \mathbf{v}_Q^T \, dS_Q \tag{2.27}$$

Note that **A** is a diagonal matrix of element areas if **v** corresponds to the assumption of a constant field over each element.

Now, by (2.24), **p**(t) and **u**(t) cannot both be free vectors; hence we choose **u**(t) as the free vector and employ (2.24) to introduce $\overset{*}{\mathbf{p}}(t) = \rho \mathbf{C}^{-1}\mathbf{B}\dot{\mathbf{u}}$ into (2.26), which yields

$$T(t) = \frac{1}{2} \rho \dot{\mathbf{u}}^T(t) \, \mathbf{A}\mathbf{C}^{-1}\mathbf{B} \, \dot{\mathbf{u}}(t) \tag{2.28}$$

Then we separate the matrix $\mathbf{A}\mathbf{C}^{-1}\mathbf{B}$ into its symmetric and skew-symmetric parts and note that the latter contributes nothing to the kinetic energy. Hence (2.28) becomes

$$T(t) = \frac{1}{2} \rho \dot{\mathbf{u}}^T(t) \, \langle \mathbf{A}\mathbf{C}^{-1}\mathbf{B} \rangle \, \dot{\mathbf{u}}(t) \tag{2.29}$$

where the angular brackets denote symmetrization of the matrix within.

As the next step, we treat **p**(t) as a prescribed vector and write the fluid work-potential expression

$$\Pi(t) = \int_S p_P(t) \, u_P(t) \, dS_P = \mathbf{u}^T(t) \mathbf{A} \, \mathbf{p}(t) \tag{2.30}$$

Thus, on the basis of (2.29) and (2.30), Hamilton's Principle, $\delta\int(T+\Pi)dt = 0$, applied for variations $\delta\mathbf{u}$, yields

$$\rho \langle \mathbf{A}\mathbf{C}^{-1}\mathbf{B} \rangle \, \ddot{\mathbf{u}}(t) = \mathbf{A} \, \mathbf{p}(t) \tag{2.31}$$

The matrix $\rho\langle \mathbf{A}\mathbf{C}^{-1}\mathbf{B} \rangle$ is known as the *fluid mass matrix* (DeRuntz and Geers, 1978), which is a generalized form of Lamb's *inertia coefficients* for hydrodynamic flow about rigid bodies (Lamb, 1945). The fluid mass matrix is positive-definite.

For our purposes, we reverse (2.31) and then multiply through by $\mathbf{A}\langle\mathbf{A}\mathbf{C}^{-1}\mathbf{B}\rangle^{-1}$ to obtain

$$\mathbf{A}\langle\mathbf{A}\mathbf{C}^{-1}\mathbf{B}\rangle^{-1}\mathbf{A}\,\mathbf{p}(t) = \rho\mathbf{A}\ddot{\mathbf{u}}(t) \tag{2.32}$$

But because $\mathbf{A}$ is symmetric,

$$\begin{aligned}\mathbf{A}\langle\mathbf{A}\mathbf{C}^{-1}\mathbf{B}\rangle^{-1}\mathbf{A} &= \mathbf{A}^{T}\langle\mathbf{A}\mathbf{C}^{-1}\mathbf{B}\rangle^{-1}\mathbf{A}\\ &= \langle\mathbf{A}^{T}[\mathbf{A}\mathbf{C}^{-1}\mathbf{B}]^{-1}\mathbf{A}\rangle\\ &= \langle\mathbf{A}^{T}\mathbf{B}^{-1}\mathbf{C}\mathbf{A}^{-1}\mathbf{A}\rangle\\ &= \langle\mathbf{A}\mathbf{B}^{-1}\mathbf{C}\rangle\end{aligned} \tag{2.33}$$

Hence the symmetric-matrix LTA_1 becomes [*cf.* (2.24)]

$$\langle\mathbf{A}\mathbf{B}^{-1}\mathbf{C}\rangle\,\mathbf{p}(t) = \rho\mathbf{A}\ddot{\mathbf{u}}(t) \tag{2.34}$$

A way to get this result more directly is to use as a kinetic-energy expression equivalent to (2.26)

$$T(t) = \frac{1}{2}\dot{\mathbf{p}}^{T}(t)\mathbf{A}\dot{\mathbf{u}}(t) \tag{2.35}$$

and to choose $\mathbf{p}(t)$ as our free vector. Employing (2.24), we introduce $\dot{\mathbf{u}} = \rho^{-1}\mathbf{B}^{-1}\mathbf{C}\dot{\mathbf{p}}$ into (2.35) and retain only the symmetric part of $\mathbf{A}\mathbf{B}^{-1}\mathbf{C}$ to obtain

$$T(t) = \frac{1}{2}\rho^{-1}\dot{\mathbf{p}}^{T}(t)\langle\mathbf{A}\mathbf{B}^{-1}\mathbf{C}\rangle\dot{\mathbf{p}}(t) \tag{2.36}$$

Next, we treat $\mathbf{u}(t)$ as a prescribed vector and write for the fluid work potential

$$\Pi(t) = \int_{S} p_{P}(t)\,u_{P}(t)\,dS = \mathbf{p}^{T}(t)\mathbf{A}\,\mathbf{u}(t) \tag{2.37}$$

Then the application of Hamilton's Principle for variations $\delta\mathbf{p}$, followed by double

differentiation of the resulting equation in time, yields (2.34).

With (2.34) as our symmetric-matrix LTA_1, our symmetric-matrix DAA_1 is clearly [*cf.* (2.23)]

$$\langle \mathbf{DAA} \rangle_1(t): \qquad \mathbf{A}\dot{\mathbf{p}}(t) + c\langle \mathbf{A}\mathbf{B}^{-1}\mathbf{C} \rangle \mathbf{p}(t) = \rho c \mathbf{A}\ddot{\mathbf{u}}(t) \tag{2.38}$$

Using (2.33), we can write this equation in the form

$$\mathbf{M}\dot{\mathbf{p}}(t) + \rho c \mathbf{A}\mathbf{p}(t) = \rho c \mathbf{M}\ddot{\mathbf{u}}(t) \tag{2.39}$$

where $\mathbf{M} = \rho\langle \mathbf{A}\mathbf{C}^{-1}\mathbf{B} \rangle$ is the fluid mass matrix, discussed after (2.31). This is the original form of DAA_1, derived by inspection in Geers, 1971.

2.6 MODAL ANALYSIS OF THE EXTERNAL DAA_1.

Consider the following eigenproblem on the surface S:

$$c\beta^{-1}\gamma\psi_Q = \lambda\psi_P \tag{2.40}$$

This eigenproblem pertains to Laplace's equation for the conservative problem of irrotational sloshing of an inviscid, incompressible external fluid (see the last paragraph in Section 2.3). Furthermore, the sloshing problem is derivable from the kinetic energy expression for the external fluid, which is a positive quadratic form. Hence the eigenvalues λ_n are real and positive, and the eigenfunctions ψ_{Pn} are real and possess the orthogonality property

$$\int_S \psi_{Pm}\psi_{Pn}\, dS_P = A_n\delta_{mn} \tag{2.41}$$

where A_n is a normalization constant and δ_{mn} is the Kronecker delta.

Following standard modal analysis procedures, we expand $p_P(t)$ and $u_P(t)$ as

$$p_P(t) = \sum_{n=0}^{\infty} \psi_{Pn}\, p_n(t)$$

$$u_P(t) = \sum_{n=0}^{\infty} \psi_{Pn}\, u_n(t) \tag{2.42}$$

introduce them into (2.17), employ (2.40), multiply through by ψ_m, integrate over S, and utilize (2.41) to obtain the *modal DAA_1 equations* for an external acoustic domain

$$DAA_1^n(t): \qquad \dot{p}_n + \lambda_n p_n = \rho c \ddot{u}_n \tag{2.43}$$

This result shows that the *fluid boundary modes* for Laplace's equation in the external domain can be used to decompose the DAA_1 into uncoupled modal equations (Geers, 1978).

Modal analysis of the unsymmetric-matrix DAA_1, (2.23), proceeds in similar fashion. The pertinent eigenproblem is

$$c\mathbf{B}^{-1}\mathbf{C}\boldsymbol{\psi} = \lambda\boldsymbol{\psi} \tag{2.44}$$

and the orthogonality statement is

$$\boldsymbol{\psi}_m^T \boldsymbol{\psi}_n = \delta_{mn} \tag{2.45}$$

We expand $\mathbf{p}(t)$ and $\mathbf{u}(t)$ as

$$\mathbf{p}(t) = \sum_{n=0}^{\infty} \boldsymbol{\psi}_n\, p_n(t)$$

$$\mathbf{u}(t) = \sum_{n=0}^{\infty} \boldsymbol{\psi}_n\, u_n(t) \tag{2.46}$$

introduce them into (2.23), employ (2.44), premultiply through by $\boldsymbol{\psi}_m^T$, and utilize (2.45) to obtain (2.43).

Modal analysis of the symmetric-matrix DAA_1, (2.38), differs only slightly from that of its unsymmetric counterpart. Instead of (2.44), the pertinent eigenproblem is

$$c\langle \mathbf{A}\mathbf{B}^{-1}\mathbf{C}\rangle \boldsymbol{\psi} = \lambda \mathbf{A}\boldsymbol{\psi} \tag{2.47}$$

and the orthogonality statement is

$$\boldsymbol{\psi}_m^T \mathbf{A} \boldsymbol{\psi}_n = A_n \delta_{mn} \tag{2.48}$$

Proceeding as before, we introduce the modal expansions (2.46) into (2.38), employ (2.47), premultiply through by $\boldsymbol{\psi}_m^T$, and utilize (2.48) to obtain (2.43).

Although the continuum-operator, unsymmetric-matrix, and symmetric-matrix DAA_1's all produce (2.43), the three sets of modes all differ slightly from one another, depending upon the choice of shape functions v_P and weight functions w_P, and the degree of surface mesh refinement. The numerical determination of fluid boundary modes for surfaces of general geometry is discussed by DeRuntz and Geers, 1978.

SECTION 3

DAA_1 FOR AN INTERNAL ACOUSTIC DOMAIN

Development of the first-order DAA for an internal acoustic domain is complicated by the existence of low-frequency dilatational motion, which does not occur in an external domain. Hence, while ETA_1 is clearly the same for both internal and external domains, LTA_1 and thus DAA_1 for the internal domain differ from their external counterparts.

3.1 EQUIVOLUMINAL AND DILATATIONAL FIELDS AT LOW FREQUENCIES.

We recall the conservation-of-mass equation, the constitutive equation, and the small-perturbation assumption for an acoustic fluid (see, *e.g.*, Pierce, 1981)

$$\frac{\partial \rho}{\partial t} + \nabla\cdot(\rho \dot{u}) = 0 \quad , \qquad \frac{\partial p}{\partial t} = c^2 \frac{\partial \rho}{\partial t} \quad , \qquad \nabla\cdot(\rho \dot{u}) \cong \rho \nabla\cdot\dot{u} \tag{3.1}$$

These may be combined to yield

$$\nabla\cdot\dot{u} = -(\rho c^2)^{-1} \frac{\partial p}{\partial t} \tag{3.2}$$

In order to accommodate dilatational fluid motion in the internal domain, we take $p(r,t) = p^d(t)$, so that (3.2) becomes, after integration in time,

$$\nabla\cdot u(r,t) = -(\rho c^2)^{-1} p^d(t) \tag{3.3}$$

Note that $p^d(t) = 0$ for an external medium, in order that the boundary condition of zero acoustic pressure at infinity may be satisfied.

Now (3.3) is an equation that holds at every point in the fluid volume. Hence we may integrate it over the volume and apply the divergence theorem to the left side of the resulting equation to obtain

$$\int_S u(S,t)\, dS = (\rho c^2)^{-1} V p^d(t) \tag{3.4}$$

where we recall from Section 2.1 that $u = \mathbf{u}\cdot\mathbf{n}$ and where V is the volume of the internal fluid domain. Let us investigate the nature of the solutions to (3.4).

First, we take the fluid-particle displacement field as comprised of two parts: $u(\mathbf{r},t) = u^e(\mathbf{r},t) + u^d(\mathbf{r},t)$, where $u^e(\mathbf{r},t)$ is the homogeneous solution, *i.e.*, that for which $p^d(t) = 0$, and $u^d(\mathbf{r},t)$ is the particular solution produced by $p^d(t)$. On this basis, (3.4) yields

$$\int_S u^e(S,t)\, dS = 0$$

$$\int_S u^d(S,t)\, dS = (\rho c^2)^{-1} V p^d(t) \tag{3.5}$$

We recognize u^e and u^d as linearly independent equivoluminal and dilatational fluid-particle displacement fields, respectively. Similarly, $p(\mathbf{r},t) = p^e(\mathbf{r},t) + p^d(t)$, where $p^e(S,t)$ satisfies a zero-average equation like the first of (3.5).

Next, we show that u^d is constant over the surface S and determine its relationship to p_d. Suppose that

$$u^d(S,t) = u^d(t) + u^v(S,t) \tag{3.6}$$

in which $u^d(t)$ is the average of $u^d(S,t)$, given by $u^d(t) = \alpha u^d(S,t)$, where α is the *averaging operator* defined as

$$\alpha q_Q \equiv \frac{1}{A}\int_S q_Q\, dS \tag{3.7}$$

in which A is the area of the surface S. Then integration of (3.6) over S yields

$$\int_S u^v(S,t)\, dS = 0 \tag{3.8}$$

But if u^v satisfies this equation, then, from the first of (3.5), it must be part of the homogeneous solution u^e rather than part of the particular solution u^d. Hence $u^d(S,t) = u^d(t)$, and the second of (3.5) yields

$$p^d(t) = \rho c \Upsilon (A/V) u^d(t) \tag{3.9}$$

3.2 FIRST-ORDER LATE-TIME APPROXIMATION: LTA_1.

Determining LTA_1 for an internal acoustic domain requires separate consideration of equivoluminal motion and dilatational motion. For equivoluminal motion, where the flow is incompressible, LTA_1 is determined in the same manner as that used for general motion in the external domain, and is given by [*cf.* (2.10)]

$$\beta^{-1} \gamma p_Q^e(s) = \rho s^2 u_P^e(s) \tag{3.10}$$

Note, however, that γ here pertains to an inward normal, while γ in (2.10) pertains to an outward normal.

The preceding equation is not valid for dilatational motion, because $\gamma p_Q = 0$ when p_Q is constant over S. This is readily shown by introducing into Green's second identity

$$\int_V (p \nabla^2 q - q \nabla^2 p)\, dV = \int_S \left[p \frac{\partial q}{\partial n} - q \frac{\partial p}{\partial n} \right] dS \tag{3.11}$$

the particular functions $p = 1$ and $q = 1/R_{PQ}$, the latter being the singular solution to Laplace's equation. In this case, all terms vanish except that produced by the first integrand on the right, yielding

$$\begin{aligned} \int_S \frac{\partial}{\partial n}(1/R_{PQ})\, dS &= -\int_S R_{PQ}^{-2} \frac{\partial (R_{PQ})}{\partial n}\, dS \\ &= -\int_S R_{PQ}^{-2} \cos \phi_{Rn}\, dS = -\gamma 1 = 0 \end{aligned} \tag{3.12}$$

where we have used the second of (2.9).

To determine LTA_1 for dilatational motion, we take $p_Q(s) = p^d(s)$ and $u_Q(s) = u^d(s)$, introduce (2.7) into (2.4), and retain on both sides all terms through those of order s^2 to obtain

$$\left[0 - \tfrac{1}{2}(s/c)^2 \eta 1\right] p^d(s) = \rho s^2 \beta 1 \; u^d(s) \tag{3.13}$$

where the spatial operator η is defined as

$$\eta q_Q \equiv \int_S \cos\phi_{Rn} \; q_Q \; dS_Q \tag{3.14}$$

Because (3.13) must agree with (3.9), $\eta 1 = -2(V/A)\beta 1$.

To derive a first-order LTA for general motion in an internal domain, one might simply introduce (2.7) into (2.4), retain on both sides all terms through those of order s^2, and premultiply through by β^{-1} to get

$$\beta^{-1}\gamma p_Q(s) - \tfrac{1}{2}(s/c)^2 \beta^{-1}\eta p_Q(s) = \rho s^2 u_P(s) \tag{3.15}$$

For equivoluminal motion, this expression contains on the left both $O(s^0)$ and $O(s^2)$ terms; hence it is not a first-order LTA. The correct first-order LTA is

$LTA_1(s)$: $$\beta^{-1}\gamma p_Q(s) + (s/c)^2 L \alpha p_Q(s) = \rho s^2 u_P(s) \tag{3.16}$$

Where $L = V/A$. For equivoluminal motion, this relation becomes (3.10) because $\alpha p_Q^e(s) = 0$; for dilatational motion, it corresponds to (3.9) because $\gamma p_Q^d(s) = \gamma p^d(s) = 0$, $\alpha p_Q^d(s) = \alpha p^d(s) = p^d(s)$, and $u_P^d(s) = u^d(s)$. We note that (3.16) is spatially non-local and singly asymptotic in the limit $s \to 0$.

3.3 FIRST-ORDER DOUBLY ASYMPTOTIC APPROXIMATION: DAA_1.

We seek here an expression that naturally reduces to ETA_1, (2.5), and LTA_1, (3.16), in the limits $s \to \infty$ and $s \to 0$, respectively. One that does so is

$$Cs^{j+3}p_P(s) + \beta^{-1}\gamma p_Q(s) + (s/c)^2 L\alpha p_Q(s) = C\rho c s^{j+4}u_P(s) + \rho s^2 u_P(s) \tag{3.17}$$

where C is an arbitrary constant and $j \geq 0$. As discussed in Section 2.4, however, the indeterminacy of C and j, and the presence of high-order derivatives prompts us to reject it as a first-order DAA.

Having gained in Section 2.4 some experience in the method of operator matching, we propose a DAA_1 trial equation that immediately satisfies (2.5) for $s \to \infty$, *viz.*,

$$sp_P(s) + cP_0 p_Q(s) = \rho c s^2 u_P(s) + \rho c^2 s U_1 u_Q(s) \tag{3.18}$$

where P_0 and U_1 are unknown spatial operators.

For *equivoluminal motion* with $s \to 0$, we write (3.18) as

$$[P_0 + O(s)]p_Q^e(s) = \rho c s U_1 u_Q^e(s) + \rho s^2 u_P^e(s) \tag{3.19}$$

The only way in which this can match (3.16) with $p_Q(s) = p_Q^e(s)$ is if $U_1 = V_1\alpha$, which annihilates the first term on the right side of (3.19), and if $P_0 = \beta^{-1}\gamma$.

Next, we consider (3.18) as it would apply to *dilatational motion* with $s \to 0$. Dividing through by s, and noting that $p_P(s) = p^d(s)$, $P_0 p_Q^d(s) = \beta^{-1}\gamma p_Q^d(s) = 0$, and $U_1 u_Q^d(s) = V_1 \alpha u_Q^d(s) = V_1 u^d(s)$, we obtain

$$p^d(s) = \rho c^2 V_1 u^d(s) + O(s) \tag{3.20}$$

This matches (3.16) with $p_Q(s) = p^d(s)$ only if $V_1 = L^{-1}$.

The introduction of these results into (3.18) produces the first-order DAA for an internal acoustic domain, expressed in transform space as

$$DAA_1(s): \qquad sp_P(s) + c\beta^{-1}\gamma p_Q(s) = \rho c s^2 u_P(s) + \rho c^2 L^{-1} s\alpha u_Q(s) \tag{3.21}$$

and in the time domain as

$$DAA_1(t): \qquad \dot{p}_P(t) + c\beta^{-1}\gamma p_Q(t) = \rho c \dot{u}_P(t) + \rho c^2 L^{-1}\alpha \dot{u}_Q(t) \tag{3.22}$$

As expected, this is a spatially non-local approximation.

3.4 MATRIX DAA_1 FOR BOUNDARY ELEMENT ANALYSIS.

Petrov-Galerkin semi-discretization may be applied to the internal DAA_1 in the same manner in which it was applied in Section 2.5 to the external DAA_1. The DAA_1 equation (3.21) is preoperated through by β, the discretization formulas (2.18) are inserted, the weighted-residual procedure is implemented, and the resulting matrix equation is premultiplied through by $\mathbf{B}^{-1}$ to yield

$$\mathbf{DAA}_1(s): \qquad s\mathbf{p}(s) + c\mathbf{B}^{-1}\mathbf{C}\mathbf{p}(s) = \rho c s^2 \mathbf{u}(s) + \rho c^2 \mathbf{V}^{-1} s \mathbf{1}\mathbf{a}^T \mathbf{u}(s) \tag{3.23}$$

where **B** and **C** are given by (2.21), **1** is the unit vector, and

$$\mathbf{a} = \int_S \mathbf{v}_Q \, dS_Q \tag{3.24}$$

Note that, because $\mathbf{v}_Q^T \mathbf{1} = 1$ [see the discussion following (2.18)], $\mathbf{a}^T \mathbf{1} = A$. Equation (3.4.1) becomes in the time domain

$$\mathbf{DAA}_1(t): \qquad \dot{\mathbf{p}}(t) + c\mathbf{B}^{-1}\mathbf{C}\mathbf{p}(t) = \rho c \ddot{\mathbf{u}}(t) + \rho c^2 \mathbf{V}^{-1} \mathbf{1}\mathbf{a}^T \dot{\mathbf{u}}(t) \tag{3.25}$$

Because $\gamma p^d(t) = 0$ and $\gamma p_Q^e(t) \neq 0$, $\mathbf{C}\mathbf{p}_d(t) = \mathbf{C}\mathbf{1}p_d(t) = 0$ and $\mathbf{C}\mathbf{p}_e(t) \neq 0$. Hence the NxN matrix **C** is of rank N-1, transforming $\mathbf{p}(t)$ into a vector in the R^{N-1} subspace of equivoluminal solutions. Similarly, because $\alpha u_Q^e(t) = 0$ and $\alpha u^d(t) \neq 0$, $\mathbf{a}^T \mathbf{u}_e(t) = 0$ and $\mathbf{a}^T \mathbf{u}_d(t) = \mathbf{a}^T \mathbf{1} u_d(t) = A u_d(t) \neq 0$; hence the NxN rank-one matrix $\mathbf{1}\mathbf{a}^T$ transforms $\dot{\mathbf{u}}(t)$ into a vector in the R^1 subspace of dilatational solutions. As in the case of external fluid, **B** is of rank N.

Here too **B** and **C** are most easily constructed if **v** corresponds to the assumption of a *constant field* over each element and **w** corresponds to *collocation at centroidal nodes*. The elements of **B** and **C** are then given by (2.22), and **a** is a vector of element areas.

It is possible to symmetrize (3.23) and (3.25). To do so, we first consider (3.23) for late-time *equivoluminal motion* by taking $\mathbf{p}(s) = \mathbf{p}_e(s)$ and $\mathbf{u}(s) = \mathbf{u}_e(s)$ with $s \to 0$; the inverse Laplace transform of the resulting equation is [*cf.* (2.24)]

$$\mathbf{B}^{-1}\mathbf{C}\,\mathbf{p}_e(t) = \rho\ddot{\mathbf{u}}_e(t) \tag{3.26}$$

Then, using the arguments given after (2.34), we conclude that Hamilton's Principle yields instead of (3.26) [*cf.* (2.34)]

$$\langle \mathbf{A}\mathbf{B}^{-1}\mathbf{C}\rangle\,\mathbf{p}_e(t) = \rho\mathbf{A}\ddot{\mathbf{u}}_e(t) \tag{3.27}$$

Next, we note that the potential energy associated with *dilatational motion* of the fluid is

$$U(t) = \frac{1}{2}\int_S p_P^d(t)\, u_P^d(t)\, dS_P \tag{3.28}$$

which, after introduction of the discretization expressions (2.13), becomes

$$U(t) = \frac{1}{2}\mathbf{u}_d^T(t)\mathbf{A}\,\mathbf{p}_d(t) \tag{3.29}$$

But, for late-time dilatational motion, *i.e.*, for $\mathbf{p}(s) = \mathbf{p}_d(s)$ and $\mathbf{u}(s) = \mathbf{u}_d(s)$ with $s \to 0$, (3.23) yields

$$\mathbf{p}_d(s) = \rho c^2 \mathbf{V}^{-1}\mathbf{1}\,\mathbf{a}^T\mathbf{u}_d(s) \tag{3.30}$$

Inverse Laplace transforming this equation and introducing the result into (3.29), we obtain

$$U(t) = \frac{1}{2}\rho c^2 \mathbf{V}^{-1}\mathbf{u}_d^T(t)\langle \mathbf{A}\,\mathbf{1}\,\mathbf{a}^T\rangle\,\mathbf{u}_d(t) \tag{3.31}$$

where only the symmetric part of $\mathbf{A}\,\mathbf{1}\,\mathbf{a}^T$ has been retained.

Next, we treat $\mathbf{p}_d(t)$ as a prescribed vector and write the fluid work-potential expression

$$\Pi(t) = \int_S p_P^d(t)\, u_P^d(t)\, dS_P = \mathbf{u}_d^T(t)\mathbf{A}\,\mathbf{p}_d(t) \tag{3.32}$$

Then, using (3.31) and (3.32), we apply Hamilton's Principle to obtain

$$\mathbf{A}\,\mathbf{p}_d(t) = \rho c^2 \mathbf{V}^{-1} \langle \mathbf{A}\,\mathbf{l}\,\mathbf{a}^T \rangle \mathbf{u}_d(t) \tag{3.33}$$

From (3.25), (3.27), and (3.33), we conclude that the symmetric counterpart to (3.4.3) is

$$\langle \mathbf{DAA} \rangle_1(t): \qquad \mathbf{A}\,\dot{\mathbf{p}}(t) + c \langle \mathbf{A}\,\mathbf{B}^{-1}\mathbf{C} \rangle \mathbf{p}(t) = \rho c \mathbf{A}\,\ddot{\mathbf{u}}(t) + \rho c^2 \mathbf{V}^{-1} \langle \mathbf{A}\,\mathbf{l}\,\mathbf{a}^T \rangle \dot{\mathbf{u}}(t) \tag{3.34}$$

For the spatial discretization scheme in which **v** corresponds to the assumption of a constant field over each element and **w** corresponds to collocation at centroidal nodes, the elements of the diagonal matrix **A** and of the vector **a** are merely the areas of the finite elements, and $\mathbf{A}\,\mathbf{l}\,\mathbf{a}^T$ is already symmetric.

3.5 MODAL ANALYSIS OF THE INTERNAL DAA_1.

Consider for the internal domain the eigenproblem given over the surface S by

$$c\beta^{-1}\gamma\psi_Q = \lambda\psi_P \tag{3.35}$$

One solution to this eigenproblem pertains to dilatational motion, for which $\psi_Q = \psi^d$ (constant over S), $\gamma\psi^d = 0$, and so $\lambda^d = 0$. The remaining eigenvalues and eigenfunctions pertain to Laplace's equation for the conservative problem of irrotational sloshing of an inviscid, incompressible internal fluid. These equivoluminal modes derive from the kinetic energy of the internal fluid and hence possess real, positive eigenvalues and real eigenfunctions, as well as the orthogonality property (2.41). Orthogonality extends to the dilatational mode if we assign, say, the zero index to ψ^d and note that (2.41) becomes the first of (3.5) if either of the modal ψ-subscripts in (2.41) is zero.

In summary, then, the spectrum of the eigenproblem (3.35) is an infinite set of discrete eigenvalues, the first of which is zero and the rest of which are positive. The eigenfunction corresponding to the zero eigenvalue is a real constant over the surface S, which constitutes the dilatational mode. The rest of the eigenfunctions are real with zero average value, thus constituting the equivoluminal modes.

From the preceding, expansions given by (2.42) may be introduced into (3.22), and the orthogonalization process described after (2.42) may be employed to obtain the *modal* DAA_1

equations for an internal acoustic domain

$$p_o = \rho c \dot{u}_o + \rho c^2 L^{-1} u_o$$

$DAA_1(t)$: (3.36)

$$\dot{p}_n + \lambda_n p_n = \rho c \ddot{u}_n \ , \ n \geq 1$$

These equations demonstrate that the internal DAA_1 may be decomposed into uncoupled modal equations through the use of fluid boundary modes, the first equation pertaining to the dilatational mode and the second to the equivoluminal modes.

Modal analysis of the unsymmetric-matrix DAA_1 is similarly straightforward. The pertinent eigenproblem is written as (2.44), and yields eigenfunctions λ_n and eigenvectors ψ_n. The first eigenvalue $\lambda_o = 0$ and the corresponding eigenvector ψ_o is merely the unit vector 1 multiplied by a normalization constant; the remaining N-1 eigenvectors are equivoluminal. The orthogonality statement is (2.45) and the modal expansion is given by (2.46). Application to (3.25) of the orthogonalization process described after (2.46) then yields (3.36), inasmuch as the second term on the right in (3.25) yields $\psi_m^T 1 a^T \psi_n = A \delta_{no}$.

Modal analysis of the symmetric-matrix DAA_1 follows in like fashion. We know that $\psi_m \langle A 1 a^T \rangle \psi_n$ vanishes unless $m = n = 0$. We also know that $\psi_o = l_o 1$, where l_o is a normalization constant, and that the skew-symmetric part of an unsymmetric matrix contributes nothing to a generalized inner product; hence $\psi_o^T \langle A 1 a^T \rangle \psi_o = \psi_o^T A 1 a^T l_o 1 = \psi_o^T A \psi_o a^T 1 = A_o A$, where we have used (2.48) and the statement following (3.24). Therefore, application to (3.34) of the orthogonalization process described after (2.48) yields (3.36).

SECTION 4

DAA_2 FOR AN EXTERNAL ACOUSTIC DOMAIN

In the previous sections we dealt with first-order DAA's for both external and internal domains. In this section, we derive a second-order DAA for an external domain by the method of operator matching.

4.1 SECOND-ORDER EARLY-TIME APPROXIMATION: ETA_2.

The second-order early-time approximation (Felippa, 1980) is, in transform space, [*cf.* (2.5)]

$$\text{ETA}_2(s): \qquad (s+c\kappa_p)\,p_p(s)=\rho c s^2 u_p(s) \tag{4.1}$$

where κ_p is the local mean curvature of the surface. Like ETA_1, ETA_2 is a local approximation in space that has each element of the surface S independently generating a curved wave that propagates outwardly into the fluid. Hence (4.2) is often referred to in the literature as the *curved wave approximation.*

4.2 SECOND-ORDER LATE-TIME APPROXIMATION: LTA_2.

The derivation of LTA_2 consists merely of extending that of LTA_1, i.e., introducing (2.7) into (2.4) and retaining terms of order s^0 and s^1 on the left and s^2 and s^3 on the right. This yields

$$\int_S R_{PQ}^{-2} \cos\phi_{Rn}\, p_Q(s)\, dS_Q = \rho \int_S s^2 (R_{PQ}^{-1} - c^{-1} s)\, u_Q(s)\, dS_Q \tag{4.2}$$

Note that the term of order s^1 on the left has vanished identically.

With the spatial operator definitions (2.9) and (3.7), we can express (4.2) in operator form as [*cf.* (2.10)]

$LTA_2(s)$: $$\beta^{-1}\gamma\, p_Q(s) = \rho s^2 [u_P(s) - c^{-1} s A \beta^{-1}\alpha\, u_Q(s)] \tag{4.3}$$

4.3 SECOND-ORDER DOUBLY ASYMPTOTIC APPROXIMATION: DAA_2.

Pursuing a procedure similar to, but more complicated than, that for DAA_1, we assume the DAA_2 trial equation

$$s^2 p_P(s) + csP_1\, p_Q(s) + c^2 P_o\, p_Q(s) = \rho c s^3 u_P(s) + \rho c^2 s^2 U_2\, u_Q(s) \tag{4.4}$$

where P_o, P_1 and U_2 are spatial operators to be defined. For $s \to 0$, we write this as

$$[P_o + c^{-1} s\, P_1 + O(s^2)] p_Q(s) = \rho s^2 (U_2 + c^{-1} s) u_Q(s) \tag{4.5}$$

where *we adopt the convention that a scalar multiplying $u_Q(s)$ [or $p_Q(s)$] yields the product of that scalar and $u_P(s)$ [or $p_P(s)$]*. For $s \to \infty$, we divide (4.4) through by s^2 and write the result as

$$[1 + c s^{-1} P_1 + O(s^{-2})] p_Q(s) = \rho c (s + c\, U_2) u_Q(s) \tag{4.6}$$

In order to match (4.5) to (4.3) and (4.6) to (4.1), we need to invert the operator ensembles either on the left or right of (4.5) and (4.6). This leads to four possible solution procedures, which, as might be expected, are equivalent. For example, let us invert the operator on the left side of (4.5) to obtain, for $s \to 0$,

$$p_P(s) = \rho s^2 [1 - c^{-1} s P_o^{-1} P_1 + O(s^2)]\, P_o^{-1} (U_2 + c^{-1} s) u_Q(s) \tag{4.7}$$

inasmuch as $[1 - c^{-1} s P_o^{-1} P_1 + O(s^2)]\, P_o^{-1} [P_o + c^{-1} s\, P_1 + O(s^2)] = 1 + O(s^2)$. Hence, keeping terms of order s^0 and s^1, and then multiplying through by the operator $\beta^{-1}\gamma$, we obtain the result

$$\beta^{-1}\gamma\, p_Q(s) = \rho s^2 \beta^{-1}\gamma\, P_o^{-1} [U_2 + c^{-1} s(1 - P_1 P_o^{-1} U_2)]\, u_Q(s) \tag{4.8}$$

Matching this to (4.3), we find

$$\beta^{-1}\gamma P_o^{-1}U_2 = 1$$
$$\beta^{-1}\gamma P_o^{-1}(P_1P_o^{-1}U_2 - 1) = A\beta^{-1}\alpha \tag{4.9}$$

Similarly, we invert the operator on the right side of (4.6) to obtain

$$s^{-1}[1 - cs^{-1}U_2 + O(s^{-2})][1 + cs^{-1}P_1 + O(s^{-2})]p_Q(s) = \rho c u_P(s) \tag{4.10}$$

inasmuch as $s^{-1}[1 - cs^{-1}U_2 + O(s^{-2})](s + cU_2) = 1 + O(s^{-2})$. Hence, retaining terms of order s^{-1} and s^{-2}, and then multiplying through by s^2, we obtain

$$sp_P(s) + c(P_1 - U_2)p_Q(s) = \rho c s^2 u_P(s) \tag{4.11}$$

Matching this to (4.1), we find

$$P_1 - U_2 = \kappa_P \tag{4.12}$$

The unknown operators P_o, P_1 and U_2 may now be determined by solving (4.9) and (4.12) simultanously. This yields

$$P_o = \chi\beta^{-1}\gamma$$
$$P_1 = \chi + \kappa_P \tag{4.13}$$
$$U_2 = \chi$$

where

$$\chi = (\beta^{-1}\gamma - \kappa_P)(1 - A\beta^{-1}\alpha\beta^{-1}\gamma)^{-1} \tag{4.14}$$

The introduction of these results into (4.4) produces the second-order DAA for an external acoustic domain, expressed in transform space as

$$\text{DAA}_2(s): \quad s^2p_P(s) + cs\kappa_Pp_P(s) + cs\chi p_Q(s) + c^2\chi\beta^{-1}\gamma p_Q(s) = \rho c s^2[su_P(s) + c\chi u_Q(s)] \tag{4.15}$$

and in the time domain as

$$\text{DAA}_2(t): \qquad \ddot{p}_P(t) + c\kappa_P\dot{p}_P(t) + c\chi\dot{p}_Q(t) + c^2\chi\beta^{-1}\gamma p_Q(t) = \rho c[\ddot{u}_P(t) + c\chi\ddot{u}_Q(t)] \tag{4.16}$$

This result agrees with that of Nicolas-Vullierme, 1989. In his formulation the term $A\beta^{-1}\alpha\beta^{-1}\gamma$ in the expression for χ [see (4.14)] is replaced by $A\beta^{-1}\gamma(1/2\pi)\alpha\beta^{-1}\gamma$. This is due to a result obtained previously by Ohayon, 1983, which, in the present context, states that $\gamma^{-1}\alpha$ reduces to $(1/2\pi)\alpha$. Extending an idea outlined by Felippa in 1980, Nicolas-Vullierme was the first to formulate DAA's by operator matching, making use of the Fourier transform and the method of stationary phase. Although his formulation works well for non-concave surfaces, it becomes cumbersome for concave surfaces, a circumstance that is disadvantageous for internal domains. This is because high-frequency behavior does not correspond to early-time behavior when a ray departing from one surface element along the latter's normal intersects another surface element. In the time domain, causality prevents such early-time interaction.

4.4 MATRIX DAA_2 FOR BOUNDARY ELEMENT ANALYSIS.

We now apply Petrov-Galerkin semi-discretization to the external DAA_2. To avoid the discretization of inverse operators in (4.15), we spatially discretize ETA_2, given by (4.1), and LTA_2, given by (4.3), and then use the *method of matrix matching* to generate the matrix DAA_2.

We start with (4.1). Introducing the Laplace transforms of (2.18) and implementing the weighted-residual procedure described in section 2.5, we obtain the matrix ETA_2 in transform space

$$\text{ETA}_2(s): \qquad (s\mathbf{J} + c\mathbf{K})\,\mathbf{p}(s) = \rho c s^2 \mathbf{J}\,\mathbf{u}(s) \tag{4.17}$$

where

$$\mathbf{J} = \int_S \mathbf{w}_P \mathbf{v}_P^T dS_P$$
$$\mathbf{K} = \int_S \mathbf{w}_P \kappa_P \mathbf{v}_P^T dS_P \tag{4.18}$$

Applying the same procedure to (4.3) after it has been preoperated through by β, we find the matrix LTA_2

$$\mathbf{LTA_2}(s): \qquad \mathbf{C}\,\mathbf{p}(s) = \rho s^2 (\mathbf{B} - c^{-1} s \boldsymbol{a}\,\mathbf{a}^T)\mathbf{u}(s) \tag{4.19}$$

where **B** and **C** are given by (2.21), **a** is given by (3.24), and

$$\boldsymbol{a} = \int_S \mathbf{w}_P \, dS_P \tag{4.20}$$

For the simplest spatial discretization scheme, *i.e.*, that for a constant field asumed over each element and collocation at centroidal nodes, $\boldsymbol{a}$ becomes the unit vector, **a** becomes a vector of element areas, **J** becomes the identity matrix, and **K** becomes a diagonal matrix of local mean curvatures.

Following the procedure used in the method of operator matching, we propose here the trial equation [*cf.* (4.4)]

$$(s^2\mathbf{J} + cs\mathbf{P}_1 + c^2\mathbf{P}_o)\,\mathbf{p}(s) = \rho c s^2 (s\,\mathbf{J} + c\,\mathbf{U}_2)\,\mathbf{u}(s) \tag{4.21}$$

where $\mathbf{P}_o$, $\mathbf{P}_1$ and $\mathbf{U}_2$ are unknown matrices. For $s \to 0$, let us premultiply this equation through by **C** times the inverse of $(s^2\mathbf{J} + cs\mathbf{P}_1 + c^2\mathbf{P}_o)$ and then write

$$\begin{aligned}(s^2\mathbf{J} + cs\mathbf{P}_1 + c^2\mathbf{P}_o)^{-1} &= [c^2\mathbf{P}_o(\mathbf{I} + c^{-1}s\,\mathbf{P}_o^{-1}\mathbf{P}_1 + c^{-2}s^2\mathbf{P}_o^{-1}\mathbf{J})]^{-1} \\ &= c^{-2}[\mathbf{I} - c^{-1}s\,\mathbf{P}_o^{-1}\mathbf{P}_1 + O(s^2)]\mathbf{P}_o^{-1}\end{aligned} \tag{4.22}$$

to obtain

$$\mathbf{C}\,\mathbf{p}(s) = \rho s^2 \mathbf{C}\,\mathbf{P}_o^{-1}[\mathbf{U}_2 + c^{-1}s(\mathbf{J} - \mathbf{P}_1\mathbf{P}_o^{-1}\mathbf{U}_2) + O(s^2)]\,\mathbf{u}(s) \tag{4.23}$$

We then match this to (4.20) through order s^1, which gives

$$\begin{aligned}\mathbf{C}\,\mathbf{P}_o^{-1}\mathbf{U}_2 &= \mathbf{B} \\ \mathbf{C}\,\mathbf{P}_o^{-1}(\mathbf{J} - \mathbf{P}_1\mathbf{P}_o^{-1}\mathbf{U}_2) &= -\boldsymbol{a}\,\mathbf{a}^T\end{aligned} \tag{4.24}$$

For $s \to \infty$, let us premutilply (4.21) through by $\mathbf{J}$ times the inverse of $(s\mathbf{J} + c\mathbf{U}_2)$ and then write

$$(s\mathbf{J} + c\mathbf{U}_2)^{-1} = [s\mathbf{J}(\mathbf{I} + cs^{-1}\mathbf{J}^{-1}\mathbf{U}_2]^{-1} = s^{-1}[\mathbf{I} - cs^{-1}\mathbf{J}^{-1}\mathbf{U}_2 + O(s^2)]\mathbf{J}^{-1} \tag{4.25}$$

to obtain

$$[s\mathbf{J} + c(\mathbf{P}_1 - \mathbf{U}_2) + O(s^{-1})]\,\mathbf{p}(s) = \rho c s^2\,\mathbf{J}\,\mathbf{u}(s) \tag{4.26}$$

We match this to (4.17) through order s^0, which yields

$$\mathbf{P}_1 - \mathbf{U}_2 = \mathbf{K} \tag{4.27}$$

The unknown matrices $\mathbf{P}_0$, $\mathbf{P}_1$ and $\mathbf{U}_2$ may now be determined by solving (4.24) and (4.27) simultanously to obtain [*cf.* (4.13)]

$$\begin{aligned} \mathbf{P}_0 &= \mathbf{J}\mathbf{X}\mathbf{B}^{-1}\mathbf{C} \\ \mathbf{P}_1 &= \mathbf{J}\mathbf{X} + \mathbf{K} \\ \mathbf{U}_2 &= \mathbf{J}\mathbf{X} \end{aligned} \tag{4.28}$$

where [*cf.* (4.14)]

$$\mathbf{X} = (\mathbf{B}^{-1}\mathbf{C} - \mathbf{J}^{-1}\mathbf{K})\,(\mathbf{I} - \mathbf{B}^{-1}a\,\mathbf{a}^{T}\mathbf{B}^{-1}\mathbf{C})^{-1} \tag{4.29}$$

Substituting (4.28) into (4.22), we obtain the matrix $\mathbf{DAA}_2$ for an external acoustic domain, written in transform space as [*cf.* (4.15)]

$$\mathbf{DAA}_2(s): \quad \begin{aligned} &[s^2\mathbf{I} + cs(\mathbf{X} + \mathbf{J}^{-1}\mathbf{K}) + c^2\mathbf{X}\mathbf{B}^{-1}\mathbf{C}]\mathbf{p}(s) \\ &\qquad = \rho c s^2(s\mathbf{I} + c\mathbf{X})\,\mathbf{u}(s) \end{aligned} \tag{4.30}$$

and in the time domain as [*cf.* (4.16)]

$$\mathbf{DAA_2(t)}: \qquad \ddot{\mathbf{p}}(t) + c(\mathbf{X} + \mathbf{J}^{-1}\mathbf{K})\dot{\mathbf{p}}(t) + c^2\mathbf{X}\mathbf{B}^{-1}\mathbf{C}\mathbf{p}(t) = \rho c[\ddot{\mathbf{u}}(t) + c\mathbf{X}\ddot{\mathbf{u}}(t)] \tag{4.31}$$

This result differs somewhat from that of Felippa, 1980, who applied his matching procedure to a scalar representation of the true integral formulation. The extension to a matrix form was done inferentially, which incorrectly ordered some matrix multiplications. Also, in contrast to DAA_1, DAA_2 does not lend itself to symmetrization.

4.5 OTHER FORMULATIONS.

Matching is not the only way to derive higher-order DAA's. In 1978, Geers formulated a matrix DAA_2 for an external acoustic domain on the basis of fluid boundary modes. This procedure introduced a free parameter in each modal DAA_2 equation that could be used to optimize its accuracy across the intermediate frequency region. This has not been deemed necessary for external-domain problems, but may be found advantageous for internal domains (Geers, 1990).

In a modal DAA formulation, the fluid boundary modes remain uncoupled across the entire frequency range. This does not reflect the situation when an exact steady-state acoustic-radiation formulation is decomposed by fluid-boundary-mode analysis; in this circumstance, the modes are coupled across the intermediate frequency region. An examination of (4.15) from the viewpoint of (2.40) reveals that matched DAA_2's do not submit to fluid-boundary-mode decomposition, in consonance with the situation characterizing an exact steady-state analysis.

In addition to matched DAA formulations and modal DAA formulations, there are symmetric DAA formulations (Geers and Zhang, 1988). A symmetric formulation was found to be essential in achieving satisfactory performance by a first-order DAA in electromagnetic scattering problems. In the context of acoustic scattering, a symmetric DAA involves augmenting (2.4) with an equation obtained by taking the partial derivative of (2.4) with respect to the surface normal. Interesting work remains to be done here.

SECTION 5

DAA$_2$ FOR AN INTERNAL ACOUSTIC DOMAIN

From Section 3, we recall that the derivation of DAA's for an internal acoustic domain is complicated by the existence of low-frequency dilatational motion. Hence, LTA$_2$ and DAA$_2$ for the internal domain differ from their external counterparts, while ETA$_2$ is the same for both internal and external domains.

5.1 SECOND-ORDER LATE-TIME APPROXIMATION: LTA$_2$.

LTA$_2$ for *equivoluminal* motion in an internal domain is here determined by the procedure previously utilized for general motion in the external domain; it is given by [*cf.* (4.3)]

$$\beta^{-1}\gamma\, p_Q^e(s) = \rho s^2\, u_P^e(s) \tag{5.1}$$

where γ pertains to an inward normal and the inverse of γ does not exist. Note that the term corresponding to the last term in (4.3) is absent here because $\alpha u_Q^e(s) = 0$.

To determine LTA$_2$ for *dilatational* motion, we replace $p_Q(s)$ by $p^d(s)$ and $u_Q(s)$ by $u^d(s)$ in (2.4), introduce (2.7) into (2.4), and retain on both sides all terms through those of order s^3. We then introduce operator symbols to represent the spatial integrals and recall that $\gamma\, p^d(s) = 0$ and $\alpha\, u_Q(s) = u^d(s)$ to obtain

$$[\,0 - \frac{1}{2}(s/c)^2\eta\, 1 + \frac{1}{3}(s/c)^3\zeta\, 1\,]\, p^d(s) = \rho s^2\,[\beta\, 1 - (s/c)\,A]\, u^d(s) \tag{5.2}$$

where the spatial operators β and η have been defined in (2.9) and (3.14), and ς is defined as

$$\zeta\, q_Q \equiv \int_S R_{PQ} \cos\phi_{Rn}\, q_Q\, dS_Q \tag{5.3}$$

As discussed in Section 3.2, a naive derivation of LTA$_2$ for *general* motion in an internal domain consists merely of the introduction of (2.7) into (2.4) and the retention on both sides of

all terms through those of order s^3. This yields,

$$\gamma p_Q(s) - \frac{1}{2}(s/c)^2\eta\, p_Q(s) + \frac{1}{3}(s/c)^3\zeta\, p_Q(s) = \rho s^2[\beta u_Q(s) - (s/c)A\alpha u_Q(s)] \tag{5.4}$$

Comparing this with (5.1) and (5.2), we see that the $O(s^2)$ and $O(s^3)$ terms on the left side are not appropriate for equivoluminal motion but are needed for dilatational motion; hence we introduce the averaging operator α into these terms to obtain

$$\text{LTA}_2(s): \quad [\gamma + (s/c)^2 L\beta\alpha + \frac{1}{3}(s/c)^3\zeta\alpha]p_Q(s) = \rho s^2[\beta - (s/c)A\alpha]u_Q(s) \tag{5.5}$$

where we have used the fact that $\eta 1 = -2L\beta 1$, as established in Section 3.2.

5.2 SECOND-ORDER DOUBLY ASYMPTOTIC APPROXIMATION: DAA_2.

To construct a trial equation for internal DAA_2, we increase the order of the trial equation for the internal DAA_1, (3.18). Thus we try

$$(s^2 + csP_1 + c^2P_o)\, p_Q(s) = \rho cs\,(s^2 + csU_2 + c^2U_1)\, u_Q(s) \tag{5.6}$$

where P_o, P_1, U_1 and U_2 are spatial operators to be found. Determining these operators requires separate consideration of equivoluminal motion and dilatational motion, accompanied by extensive matching.

Let us first examine the trial equation (5.6) for *equivoluminal motion.* For $s\to 0$, the only way that this equation with $p_Q(s) = p_Q^e(s)$ and $u_Q(s) = u_Q^e(s)$ can match (5.1) is if $U_1 = V_1\alpha$; hence the trial equation (5.6) for $s\to 0$ becomes for equivoluminal motion,

$$[P_o + c^{-1}sP_1 + O(s^2)]\, p_Q^e(s) = \rho s^2(U_2 + c^{-1}s)\, u_Q^e(s) \tag{5.7}$$

For $s\to\infty$, (5.6) becomes, for equivoluminal motion,

$$[1 + cs^{-1}P_1 + O(s^{-2})]\, p_Q^e(s) = \rho c\,(s + cU_2)\, u_Q^e(s) \tag{5.8}$$

Following the same procedure as that used for general motion in an external domain (see Section 4.3), we determine the spatial operators P_o, $P_1$and U_2 by matching (5.7) to (5.1) and (5.8) to (4.1); the results are [*cf.* (4.13)]

$$\begin{aligned} P_o &= (\beta^{-1}\gamma - \kappa_p)\beta^{-1}\gamma \\ P_1 &= \beta^{-1}\gamma \\ U_2 &= \beta^{-1}\gamma - \kappa_p \end{aligned} \tag{5.9}$$

Let us remind ourselves that γ here pertains to an inward normal and the inverse of γ does not exist.

We now observe that the preceding development for equivoluminal motion would be unaffected if P_o, P_1 and U_2 were replaced by $P_o + Q_o\alpha$, $P_1 + Q_1\alpha$ and $U_2 + V_2\alpha$, respectively. Hence, remembering that $U_1 = V_1\alpha$, we write the updated trial equation

$$\begin{aligned} &[s^2 + cs(P_1 + Q_1\alpha) + c^2(P_o + Q_o\alpha)]\, p_Q(s) \\ &\qquad = \rho cs\,[s^2 + cs(U_2 + V_2\alpha) + c^2V_1\alpha]\, u_Q(s) \end{aligned} \tag{5.10}$$

where P_o, P_1 and U_2 are known, and Q_o, Q_1, V_1 and V_2 are unknown.

Let us now examine (5.10) for *dilatational motion.* With $p_Q(s) = p^d(s)$, $\alpha p^d(s) = p^d(s)$, $u_Q(s) = u^d(s)$, $\alpha u^d(s) = u^d(s)$ and $\gamma 1 = 0$, (5.10) may be expressed for dilatational motion as [note (5.9)]

$$\begin{aligned} &[s^2 + csQ_1 + c^2Q_o]\, p^d(s) \\ &\qquad = \rho cs\,[s^2 + cs(V_2 - c\kappa_p) + c^2V_1]\, u^d(s) \end{aligned} \tag{5.11}$$

Unique solutions for Q_o, Q_1, V_1 and V_2 can be found in the R^1 subspace of dilatational solutions. Hence, we project (5.11) into this R^1 subspace by preoperating through by α, which leads to the conclusion that Q_o, Q_1, V_1 and V_2 must be *scalars.* This yields the scalar equation

$$(s^2 + csQ_1 + c^2Q_o)\,p^d(s) = \rho cs\,[s^2 + cs(V_2 - c\bar{\kappa}) + c^2V_1)]\,u^d(s) \qquad (5.12)$$

where $\bar{\kappa}$ is the average curvature over the surface S. For future use, we write this equation for small s as

$$(c^2Q_o + csQ_1 + s^2)\,p^d(s) = \rho c^2 s\,[cV_1 + s(V_2 - c\bar{\kappa}) + O(s^2)]\,u^d(s) \qquad (5.13)$$

and for large s as

$$[1 + cs^{-1}Q_1 + O(s^{-2})]\,p^d(s) = \rho cs[1 + cs^{-1}(V_2 - c\bar{\kappa}) + O(s^{-2})]\,u^d(s) \qquad (5.14)$$

In order to determine Q_o, Q_1, V_1 and V_2 by second-order matching, we must also project (5.5) and (4.1) onto the R^1 subspace of dilatational solutions. Hence, with $p_Q(s) = p^d(s)$ and $u_Q(s) = u^d(s)$, we preoperate (5.5) through by α to obtain LTA_2 for dilatational motion

$$[Lb + \frac{1}{3}(s/c)z]\,p^d(s) = \rho c^2[b - (s/c)A]\,u^d(s) \qquad (5.15)$$

where $b = \alpha\beta 1$ and $z = \alpha\zeta 1$. Then we do the same to (4.1) to obtain ETA_2 for dilatational motion

$$(1 + cs^{-1}\bar{\kappa})\,p^d(s) = \rho cs\,u^d(s) \qquad (5.16)$$

We now perform second-order small-s maching of (5.13) and (5.15). First, we observe that (5.13) can match (5.15) as $s\to 0$ only if $Q_o = 0$. Then we multiply (5.13) through by $(cV_1)^{-1}[1 - (s/c)V_1^{-1}(V_2 - \bar{\kappa})]$ to obtain

$$\left\{V_1^{-1}Q_1 + (s/c)V_1^{-1}[1 - V_1^{-1}Q_1(V_2 - \bar{\kappa})] + O(s^2)\right\}p^d(s) = \rho c^2[1 + O(s^2)]u^d(s) \qquad (5.17)$$

Next, we multiply (5.15) through by $b^{-1}[1 + (s/c)b^{-1}A]$ to get

$$[L + (s/c)b^{-1}(V + \frac{1}{3}z) + O(s^2)]\,p^d(s) = \rho c^2[1 + O(s^2)]\,u^d(s) \tag{5.18}$$

Matching these two equations through O(s), we find

$$\begin{aligned} V_1^{-1}Q_1 &= L \\ V_1^{-1}[1 - V_1^{-1}Q_1(V_2 - \bar{\kappa})] &= b^{-1}(V + \frac{1}{3}z) \end{aligned} \tag{5.19}$$

We then perform second-order large-s matching of (5.14) and (5.16). Multiplying (5.14) through by $1 - cs^{-1}(V_2 - \bar{\kappa})$, we get

$$[1 + cs^{-1}(Q_1 - V_2 + \bar{\kappa}) + O(s^{-2})]\,p^d(s) = \rho cs[1 + O(s^{-2})]\,u^d(s) \tag{5.20}$$

Matching this to (5.16), we find

$$Q_1 - V_2 + \bar{\kappa} = \bar{\kappa} \tag{5.21}$$

Finally, we solve (5.19) and (5.21) simutaneously to obtain

$$\begin{aligned} Q_1 &= Ld \\ V_1 &= d \\ V_2 &= Ld \end{aligned} \tag{5.22}$$

where

$$d = \frac{1 + \bar{\kappa}L}{L^2 + (V + \frac{1}{3}z)/b} \tag{5.23}$$

Thus, by introducing (5.9), (5.22), and $Q_o = 0$ into (5.10), we obtain the second-order DAA for an internal acoustic domain, expressed in transform space as

$$\text{DAA}_2(s): \quad \begin{aligned} &s^2 p_P(s) + cs(\beta^{-1}\gamma + Ld\alpha)p_Q(s) + c^2(\beta^{-1}\gamma - \kappa_P)\beta^{-1}\gamma p_Q(s) \\ &\quad = \rho cs[(s^2 - cs\kappa_P)u_P(s) + cs(\beta^{-1}\gamma + Ld\alpha)u_Q(s) + c^2 d\alpha u_Q(s)] \end{aligned} \tag{5.24}$$

and in the time domain as

$$\text{DAA}_2(t): \quad \begin{aligned} &\ddot{p}_P(t) + c(\beta^{-1}\gamma + Ld\alpha)\dot{p}_Q(t) + c^2(\beta^{-1}\gamma - \kappa_P)\beta^{-1}\gamma p_Q(t) \\ &\quad = \rho c[\ddot{u}_P(t) - c\kappa_P \ddot{u}_P(t) + c(\beta^{-1}\gamma + Ld\alpha)\ddot{u}_Q(t) + c^2 d\alpha \dot{u}_Q(t)] \end{aligned} \tag{5.25}$$

5.3 MATRIX DAA_2 FOR BOUNDARY ELEMENT ANALYSIS.

We will now derive a matrix form of the second-order DAA for internal acoustic domains by Petrov-Galerkin semi-discretization. The matrix ETA_2 is given by (4.17). The matrix LTA_2 is obtained by introducing the Laplace transforms of (2.18) into (5.5) and then implementing the weighted residual procedure described in Section 2.5. The result is

$$\text{LTA}_2(s): \quad \begin{aligned} &[\mathbf{C} + (s/c)^2 L\mathbf{A}^{-1}\mathbf{B}\mathbf{1}\mathbf{a}^T + \frac{1}{3}(s/c)^3 \mathbf{A}^{-1}\mathbf{Z}\mathbf{1}\mathbf{a}^T]\mathbf{p}(s) \\ &\quad = \rho s^2 [\mathbf{B} - (s/c)\boldsymbol{a}\,\mathbf{a}^T]\mathbf{u}(s) \end{aligned} \tag{5.26}$$

where **B**, **C**, **a** and $\boldsymbol{a}$ have been given in (2.21), (3.24) and (4.21), respectively, and where

$$\mathbf{Z} = \int_S \int_S w_P R_{PQ} \cos\phi_{Rn} \mathbf{v}_Q^T \, dS_Q \, dS_P \tag{5.27}$$

For *equivoluminal motion*, $\mathbf{a}^T\mathbf{p}_e = 0$ and $\mathbf{a}^T\mathbf{u}_e = 0$, so (5.26) yields as LTA_2 for equivoluminal motion

$$\mathbf{C}\,\mathbf{p}_e(s) = \rho s^2 \mathbf{B}\,\mathbf{u}_e(s) \tag{5.28}$$

For *dilatational motion*, $\mathbf{p}_d(s) = \mathbf{1}p_d(s)$ and $\mathbf{u}_d(s) = \mathbf{1}u_d(s)$; also, because $\gamma\mathbf{1} = 0$, $\mathbf{C1} = 0$. Thus,

with $\mathbf{a}^T\mathbf{1} = A$, (5.26) becomes

$$[\mathbf{LB1} + \frac{1}{3}(s/c)\,\mathbf{Z\,1}]\,p_d(s) = \rho c^2[\mathbf{B\,1} - (s/c)\,\mathbf{A}a]\,u_d(s) \tag{5.29}$$

At this point, we introduce the DAA_2 trial equation [cf. (5.6)]

$$(s^2\mathbf{J} + cs\,\mathbf{P}_1 + c^2\mathbf{P}_o)\,\mathbf{p}(s) = \rho cs(s^2\mathbf{J} + cs\,\mathbf{U}_2 + c^2\mathbf{U}_1)\,\mathbf{u}(s) \tag{5.30}$$

where $\mathbf{P}_o$, $\mathbf{P}_1$ $\mathbf{U}_1$ and $\mathbf{U}_2$ are unknown matrices. To match, as $s\to 0$, LTA_2 for *equivoluminal motion, i.e.*, (5.28), $\mathbf{U}_1$ must be of the form $\mathbf{va}^T$ where $\mathbf{v}$ is an unknown vector, so that the last term on the right in (5.30) will vanish. Then the procedure used in Section 4.4 to obtain matrix DAA_2 for an external domain may be applied here to obtain [*cf.* (4.28) and (5.9)]

$$\begin{aligned} \mathbf{P}_o &= (\mathbf{J}\,\mathbf{B}^{-1}\mathbf{C} - \mathbf{K})\mathbf{B}^{-1}\mathbf{C} \\ \mathbf{P}_1 &= \mathbf{J}\,\mathbf{B}^{-1}\mathbf{C} \\ \mathbf{U}_2 &= \mathbf{J}\,\mathbf{B}^{-1}\mathbf{C} - \mathbf{K} \end{aligned} \tag{5.31}$$

Now the preceding equivoluminal development would be unaffected if $\mathbf{P}_o$, $\mathbf{P}_1$, $\mathbf{U}_1$ and $\mathbf{U}_2$ were replaced by $\mathbf{P}_o + Q_o\mathbf{1a}^T$, $\mathbf{P}_1 + Q_1\mathbf{1a}^T$, $V_1\mathbf{1a}^T$ and $\mathbf{U}_2 + V_2\mathbf{1a}^T$, respectively. Thus we write the updated trial equation

$$\begin{aligned} &[s^2\mathbf{J} + cs(\mathbf{P}_1 + Q_1\mathbf{1a}^T) + c^2(\mathbf{P}_o + Q_o\mathbf{1a}^T)]\,\mathbf{p}(s) \\ &\quad = \rho cs[s^2\mathbf{J} + cs(\mathbf{U}_2 + V_2\mathbf{1a}^T) + c^2V_1\mathbf{1a}^T]\mathbf{u}(s) \end{aligned} \tag{5.32}$$

where $\mathbf{P}_o$, $\mathbf{P}_1$ and $\mathbf{U}_2$ are known matrices, and Q_o, Q_1, V_1 and V_2 are unknown scalars.

Let us now consider *dilatational motion.* With $\mathbf{p}(s) = \mathbf{1}p_d(s)$, $\mathbf{u}(s) = \mathbf{1}u_d(s)$, $\mathbf{a}^T\mathbf{1} = A$, and $\mathbf{C1} = 0$, (5.32) yields [note (5.31) and *cf.* (5.11)]

$$\begin{aligned} &(s^2\mathbf{J1} + cs\mathbf{A}Q_1\mathbf{1} + c^2\mathbf{A}Q_0\mathbf{1})p_d(s) \\ &\quad = \rho cs[s^2\mathbf{J1} + cs(\mathbf{A}V_2\mathbf{1} - \mathbf{K1}) + c^2\mathbf{A}V_1\mathbf{1}]\,u_d(s) \end{aligned} \tag{5.33}$$

Premultiplication through by $\mathbf{N}^{-1}\mathbf{1}^T$, where N is the size of the discrete system (*i.e.*, the number

of degrees of freedom), then yields [*cf.* (5.12)]

$$(s^2J + csAQ_1 + c^2AQ_o)\,p_d(s) = \rho cs[s^2J + cs(AV_2 - K) + c^2AV_1]\,u_d(s) \tag{5.34}$$

where $J = N^{-1}\mathbf{1}^T\mathbf{J}\mathbf{1}$ and $K = N^{-1}\mathbf{1}^T\mathbf{K}\mathbf{1}$. For future use, we write this equation for small s as [*cf.* (5.13)]

$$(c^2Q_o + csQ_1 + s^2A^{-1}J)\,p_d(s) = \rho c^2s[cV_1 + s(V_2 - A^{-1}K) + O(s^2)]\,u_d(s) \tag{5.35}$$

and for large s as [*cf.* (5.14)]

$$[J + cs^{-1}AQ_1 + O(s^{-2})]p_d(s) = \rho cs[J + cs^{-1}(AV_2 - K) + O(s^{-2}]u_d(s) \tag{5.36}$$

In order to determine our unknown dilatational coefficients by matching, we must also project (5.29) and (4.17) onto the R^1 space of dilatational solutions, Hence, with $\mathbf{p}(s) = \mathbf{1}p_d(s)$ and $\mathbf{u}(s) = \mathbf{1}u_d(s)$, we premultiply (5.29) through by $N^{-1}\mathbf{1}^T$ to obtain LTA_2 for dilatational motion [*cf.* (5.15)]

$$[LB + \frac{1}{3}(s/c)Z]\,p_d(s) = \rho c^2[B - (s/c)L^{-1}Y]\,u_d(s) \tag{5.37}$$

where $B = N^{-1}\mathbf{1}^T\mathbf{B}\mathbf{1}$, $Z = N^{-1}\mathbf{1}^T\mathbf{Z}\mathbf{1}$, and $Y = N^{-1}V\mathbf{1}^T\mathbf{a}$. Then we do the same to (4.4.1), which yields ETA_2 for dilatational motion [*cf.* (5.16)]

$$(J + cs^{-1}K)\,p_d(s) = \rho csJ\,u_d(s) \tag{5.38}$$

We are now ready for matching. First, we note that (5.35) can match (5.37) for $s\to 0$ only if $Q_o = 0$. Then, we follow the same procedure as that employed in the previous section to obtain [*cf.* (5.22)]

$$Q_1 = LD$$
$$V_1 = D \tag{5.39}$$
$$V_2 = LD$$

where [*cf.* (5.23)]

$$D = \frac{(J + KL)/A}{L^2 + (Y + \frac{1}{3}Z)/B} \tag{5.40}$$

Thus, by introducing (5.31), (5.39) and $Q_o = 0$ into (5.32), we obtain the second-order matrix DAA for an internal acoustic domain, expressed in transform space as [*cf.* (5.24)]

$$\begin{aligned} \mathbf{DAA_2(s):}\quad & [s^2\mathbf{I} + cs(\mathbf{B}^{-1}\mathbf{C} + LD\mathbf{J}^{-1}\mathbf{1a}^T) + c^2(\mathbf{B}^{-1}\mathbf{C} - \mathbf{J}^{-1}\mathbf{K})\mathbf{B}^{-1}\mathbf{C}]\,\mathbf{p}(s) \\ & = \rho cs\{s^2\mathbf{I} + cs(\mathbf{B}^{-1}\mathbf{C} - \mathbf{J}^{-1}\mathbf{K}) + LD\mathbf{J}^{-1}\mathbf{1a}^T] + c^2D\mathbf{J}^{-1}\mathbf{1a}^T\}\mathbf{u}(s) \end{aligned} \tag{5.41}$$

and in the time domain as [*cf.* (5.25)]

$$\begin{aligned} \mathbf{DAA_2(t):}\quad & \ddot{\mathbf{p}}(t) + c(\mathbf{B}^{-1}\mathbf{C} + LD\mathbf{J}^{-1}\mathbf{1a}^T)\,\dot{\mathbf{p}}(s) + c^2(\mathbf{B}^{-1}\mathbf{C} - \mathbf{J}^{-1}\mathbf{K})\mathbf{B}^{-1}\mathbf{C}\,\mathbf{p}(t) \\ & = \rho c[\ddot{\mathbf{u}}(t) + c(\mathbf{B}^{-1}\mathbf{C} - \mathbf{J}^{-1}\mathbf{K} + LD\mathbf{J}^{-1}\mathbf{1a}^T)\,\ddot{\mathbf{u}}(t) + c^2D\mathbf{J}^{-1}\mathbf{1a}^T\dot{\mathbf{u}}(t)] \end{aligned} \tag{5.42}$$

In contrast to DAA_1, DAA_2 does not lend itself to symmetrization.

SECTION 6

MODAL EQUATIONS FOR A SPHERICAL GEOMETRY

In this section, modal exact and DAA equations are derived for axisymmetric flow in a spherical geometry, in which the wave equation separates, thereby admitting solution by separation of variables (Morse and Ingard, 1968). The derivation utilizes velocity-potential fields external and internal to a spherical surface and introduces residual potentials to facilitate the development (Geers, 1969, 1971, 1972). Exact modal equations linking the velocity potentials and their derivatives are first obtained, from which early-time and late time approximations are generated. Then modal DAA's of first and second order are constructed by scalar matching, the scalar form of operator and matrix matching. *A nondimensional formulation is used throughout the section,* with length normalized to a, the radius of the sphere, time normalized to a/c, and pressure to ρc^2.

6.1 EXACT MODAL EQUATIONS FOR THE EXTERNAL FLUID.

For axisymmetric flow, the wave equation in spherical coordinates admits solutions of the form (Morse and Ingard, 1968)

$$\phi(r,\theta,t) = \sum_{n=0}^{\infty} \phi_n(r,t) P_n(\cos\theta) \tag{6.1}$$

where r and θ are the radial and meridional coordinates, respectively, $\phi(r,\theta,t)$ is the velocity potential, and $P_n(\cos\theta)$ is the Legendre polynomial of order n (Abramowitz and Stegun, 1964). By taking the Laplace-transform of both sides of (6.1) and utilizing the orthogonality property of Legendre polynomials, one can obtain the following ordinary differential equation for each of the $\phi_n(r,s)$:

$$\xi^2 \frac{d^2\phi_n}{d\xi^2} + 2\xi \frac{d\phi_n}{d\xi} - [\xi^2 + n(n+1)]\phi_n = 0 \tag{6.2}$$

where $\xi = rs$. The solution to this equation that vanishes as $\xi \rightarrow \infty$ is

$$\phi_n(r,s) = f_n(s)\, k_n(rs) \tag{6.3}$$

where $f_n(s)$ is an underdetermined function and $k_n(\xi)$ is the nth-order modified spherical Bessel function of the third kind (Abramowitz and Stegun, 1964).

Geers (1969,1971,1972) has shown that ϕ_n at $r = 1$ is conveniently obtained as the solution of the equation

$$\underline{\phi}_{n,r}(s) + s\underline{\phi}_n(s) + \underline{\phi}_n(s) + \underline{\psi}_n(s) = 0 \tag{6.4}$$

where the r-subscript denotes radial differentiation, underlining indicates location on the surface $r = 1$, and the *modal residual potential* $\psi_n(s)$ is given by

$$\underline{\psi}_n(s) = -\left[s + 1 + s\frac{k_n'(s)}{k_n(s)}\right]\underline{\phi}_n(s) \tag{6.5}$$

in which k_n' is the derivative of k_n with respect to its argument. But $k_n(\xi)$ is given by

$$k_n(\xi) = \frac{\pi}{2} e^{-\xi} \sum_{m=0}^{n} \Gamma_{nm}\, \xi^{-(m+1)} \tag{6.6}$$

where $\Gamma_{nm} = (n+m)!\,[2^m m!\,(n-m)!\,]^{-1}$. Hence (6.5) and (6.6) yield

$$\sum_{m=0}^{n} \Gamma_{nm}\, s^{n-m} \underline{\psi}_n(s) = \sum_{m=0}^{n} m\, \Gamma_{nm}\, s^{n-m} \underline{\phi}_n(s) \tag{6.7}$$

Equations (6.4) and (6.7) constitute two equations for the two unknowns $\underline{\phi}_n(s)$ and $\underline{\psi}_n(s)$ in terms of the radial derivative $\underline{\phi}_{n,r}(s)$. They are key equations in the exact fluid-structure interaction formulation of Section 7.

6.2 EXACT MODAL EQUATIONS FOR THE INTERNAL FLUID.

We now apply the approch of the preceding section to the internal acoustic fluid. Equation (6.1) and (6.2) carry over, but (6.3) become

$$\phi_n(r,s) = f_n(s)\, i_n(rs) \tag{6.8}$$

where $f_n(s)$ is again an unknown function and $i_n(\varsigma)$ is the nth-order modified spherical Bessel function of the first kind, which remains finite at r = 0 (Abramowitz and Stegun, 1964).

Proceding as before, we find that ϕ_n at r = 1 is conveniently obtained as the solution of equation [*cf.* (6.4)]

$$\underline{\phi}_{n,r}(s) - s\underline{\phi}_n(s) + \underline{\phi}_n(s) + \underline{\Psi}_n(s) = 0 \tag{6.9}$$

where the modal residual potential $\underline{\Psi}_n(s)$ is given by [*cf.* (6.5)]

$$\underline{\Psi}_n(s) = [s - 1 - s\frac{i_n'(s)}{i_n(s)}]\underline{\phi}_n(s) \tag{6.10}$$

where i_n' is the derivative of i_n with respect to its argument. But $i_n(\xi)$ is given by

$$i_n(\xi) = \frac{1}{2}\xi^{-(n+1)}\sum_{m=0}^{n}\Gamma_{nm}\xi^{n-m}[(-1)^m - (-1)^n e^{-2\xi}]\, e^{\xi} \tag{6.11}$$

so that (6.10) is equivalent to the delayed-differential equation

$$\begin{aligned}\sum_{m=0}^{n}(-1)^m\Gamma_{nm}s^{n-m}\underline{\Psi}_n(s) &= \sum_{m=0}^{n}(-1)^m m s^{n-m}\Gamma_{nm}\underline{\phi}_n(s) \\ &+ (-1)^n\sum_{m=0}^{n}s^{n-m}\Gamma_{nm}[\underline{\Psi}_n(s) - 2s\underline{\phi}_n(s) - m\underline{\phi}_n(s)]\, e^{-2s}\end{aligned} \tag{6.12}$$

where e^{-2s} indicates evaluation in the time domain of the quantity in brackets at the retarded time t - 2.

Equations (6.9) and (6.12) constitute two equations for the two unknowns $\underline{\phi}_n(1,s)$ and $\underline{\Psi}_n(s)$ in terms of the radial derivative $\underline{\phi}_{n,r}(1,s)$. They too are key equations in the exact fluid-structure interaction formulation of Section 7.

6.3 MODAL DAA EQUATIONS FOR THE EXTERNAL FLUID.

The definitions $p = \dot{\phi}$ and $\dot{u} = -\nabla\phi$, along with (6.1) and (6.3), yield as the relation between the nth components of nondimensional pressure and radial fluid-particle displacement on the unit sphere

$$\frac{k_n'(s)}{k_n(s)} \underline{p}_n(s) = -s\underline{u}_n(s) \tag{6.13}$$

where k_n is given in (6.6). This relation is the starting point for the approximations derived below. Although the derivations are carried out in transform space, the resulting approximations are all simple polynomials in s, so that inversion to the time domain, which yields ordinary differential equations, is straightforward.

First, we derive approximations valid at early time, which corresponds to $s\to\infty$, and other approximations valid at late time, which corresponds to $s\to 0$. For $s\to\infty$, (6.6) yields

$$\begin{aligned} k_n(s) &= \frac{\pi}{2} e^{-s}(1 + \Gamma_{n1}s^{-1} + \Gamma_{n2}s^{-2} + \ldots) \\ k_n'(s) &= -\frac{\pi}{2} e^{-s}[1 + \Gamma_{n1}s^{-1} + (\Gamma_{n1} + \Gamma_{n2})s^{-2} + \ldots] \end{aligned} \tag{6.14}$$

Long division then gives the $s\to\infty$ ratio

$$\frac{k_n'(s)}{k_n(s)} = -1 - s^{-1} + O(s^{-2}) \tag{6.15}$$

For $s\to 0$, we premultiply (6.6) through by s^{n+1}, which yields

$$s^{n+1}k_n(s) = \frac{\pi}{2} e^{-s}(\Gamma_{nn} + \Gamma_{n(n-1)}s + \Gamma_{n(n-2)}s^2 + \ldots) \tag{6.16}$$

from which we obtain

$$s^{n+1}k_n'(s) = -\frac{\pi}{2}e^{-s}s^{-1}\Big\{(n+1)\Gamma_{nn} + (\Gamma_{nn} + n\Gamma_{n(n-1)})s + [\Gamma_{n(n-1)} + (n-1)\Gamma_{n(n-2)}]s^2 + \ldots\Big\} \tag{6.17}$$

Long division then gives the $s\to 0$ ratio

$$\frac{k_n(s)}{k_n'(s)} = -\frac{1}{n+1}s + O(s^3) \tag{6.18}$$

First- and second-order early-time approximations are obtained by keeping terms in (6.15) through s^0 or s^{-1}, and introducing each result, one at a time, into (6.13). The two ETA's are

$$\begin{aligned} &ETA_1^n(s): && \underline{p}_n(s) = s\,\underline{u}_n(s) \\ &ETA_2^n(s): && (s+1)\,\underline{p}_n(s) = s^2\underline{u}_n(s) \end{aligned} \tag{6.19}$$

Similarly, first- and second-order late-time approximations are obtained by retaining terms in (6.18) through s^1 or s^2 and introducing each result, one at a time, into (6.13). The results are

$$\begin{aligned} &LTA_1^n(s): && (n+1)\,\underline{p}_n(S) = s^2\underline{u}_n(s) \\ &LTA_2^n(s): && \text{same as } LTA_1^n(s) \end{aligned} \tag{6.20}$$

DAA's will now be derived by scalar matching. As in the previous sections, the method consists of selecting a suitable trial equation in transform space that contains an appropriate number of arbitrary coefficients, and then determining those coefficients by forcing the trial equation to fit both the corresponding ETA and LTA for large and small s, respectively.

As will soon be evident, the trial equation for the first-order DAA is

$$(P_1^n s + P_o^n)\,\underline{p}_n(s) = s^2\underline{u}_n(s) \tag{6.21}$$

where P_1^n and P_o^n are coefficients to be determined. This equation will match the first of (6.19) for arbitrarily large s only if $P_1^n = 1$, and it will match (6.20) for arbitrarily small s only if $P_o^n = n + 1$. Thus we have the first-order modal DAA in transform space

$$\text{DAA}_1^n(s): \qquad (s + n + 1)\underline{p}_n(s) = s^2\underline{u}_n(s) \tag{6.22}$$

and in the time domain

$$\text{DAA}_1^n(t): \qquad \dot{\underline{p}}_n(t) + (n + 1)\underline{p}_n(t) = \ddot{\underline{u}}_n(t) \tag{6.23}$$

A logical extension of (6.21) that satisfies ETA_1^n as $s\to\infty$ and LTA_1^n as $s\to 0$ produces the trial equation for the second-order DAA, *viz.*,

$$[s^2 + P_1^n s + (n + 1)P_o^n]\underline{p}_n(s) = (s^3 + P_o^n s^2)\underline{u}_n(s) \tag{6.24}$$

To match $\text{ETA}_2^n(s)$, we divide this equation through by s^2 and the second of (6.19) through by s; then we match the resulting equations through order s^{-1} to obtain $P_o^n = P_1^n - 1$. To match $\text{LTA}_2^n(s)$, we divide (6.24) through by $(n+1)P_o^n$, divide (6.20) through by n + 1, and match the resulting equations through order s; this yields $P_1^n = (n+1)$. Thus, introducing these results into (6.24), we obtain the second-order DAA in transform space as

$$\text{DAA}_2^n(s): \qquad [s^2 + (n + 1)s + n(n + 1)]\underline{p}_n(s) = (s + n)s^2\underline{u}_n(s) \tag{6.25}$$

and in the time domain as

$$\text{DAA}_2^n(t): \qquad \ddot{\underline{p}}_n(t) + (n + 1)\dot{\underline{p}}_n(t) + n(n + 1)\underline{p}_n(t) = \ddot{\underline{u}}_n(t) + n\ddot{\underline{u}}_n(t) \tag{6.26}$$

6.4 MODAL DAA EQUATIONS FOR THE INTERNAL FLUID.

For the internal fluid, the equation analogous to (6.13) is

$$\frac{i_n'(s)}{i_n(s)}\underline{p}_n(s) = s\,\underline{u}_n(s) \tag{6.27}$$

where $i_n(s)$ is given in (6.11) and $\underline{u}(s)$ is defined for the internal fluid as *possitive inward.* Following the procedure of Section 6.3, we determine the singly asymptotic approximations by examining (6.27) as $s\to\infty$ and $s\to 0$.

For $s\to\infty$, (6.11) yields

$$i_n(s) = \frac{1}{2}s^{-1}e^{s}[1 - \Gamma_{n1}s^{-1} + \Gamma_{n2}s^{-2} - \ldots]$$
$$i_n'(s) = \frac{1}{2}s^{-1}e^{s}[1 - (\Gamma_{n1} + 1)s^{-1} + (\Gamma_{n2} + 2\Gamma_{n1})s^{-2} - \ldots] \tag{6.28}$$

Long division then gives the $s\to\infty$ ratio

$$\frac{i_n'(s)}{i_n(s)} = 1 - s^{-1} + O(s^{-2}) \tag{6.29}$$

For $s\to 0$, (6.11) gives

$$i_n(s) = \sum_{m=0}^{\infty} \gamma_{nm} s^{n+2m} \tag{6.30}$$

where

$$\gamma_{nm} = \frac{1}{[1\cdot 3\cdot 5\cdots(2n + 2m + 1)]\,2^m m!} \tag{6.31}$$

Differentiation followed by long division then gives the $s\to 0$ ratio

$$\frac{i_n'(s)}{i_n(s)} = n s^{-1} + 2(\gamma_{n1}/\gamma_{no})s + O(s^3) \tag{6.32}$$

ETA_1^n and ETA_2^n are obtained by keeping terms through s^0 or s^{-1} in (6.29) and introducing each result, one at a time, into (6.27). The first two ETA's are

$$ETA_1^n(s): \qquad \underline{p}_n(s) = s\,\underline{u}_n(s)$$
$$ETA_2^n(s): \qquad (s - 1)\,\underline{p}_n(s) = s^2\,\underline{u}_n(s) \tag{6.33}$$

LTA_1^n and LTA_2^n are obtained by retaining terms in (6.32) through s or s^2 for $n=0$ and s^{-1} or s^0 for $n>0$, and introducing each result, one at a time, into (6.27). The results are

$LTA_1^n(s)$:

$$\underline{p}_o(s) = 3\,\underline{u}_o(s)$$

$$n\,\underline{p}_n(s) = s^2\underline{u}_n(s), \quad n>0 \tag{6.34}$$

$LTA_2^n(s)$: same as $LTA_1^n(s)$

Because the LTA's for n = 0 are distinct from their counterparts for n > 0, DAA derivations will be performed in pairs. The trial equation for the first-order DAA for n = 0 is

$$\underline{p}_o(s) = (U_1^\circ s + U_o^\circ)\,\underline{u}_o(s) \tag{6.35}$$

where U_1° and U_o° are coefficients to be determined. This equation will match the first of (6.33) for arbitrarily large s only if $U_1^\circ = 1$; it will match the first of (6.34) for arbitrarily small s only if $U_o^\circ = 3$. Thus we have the first-order DAA for n=0 in transform space

$DAA_1^n(s)$ for n=0:

$$\underline{p}_o(s) = (s + 3)\,\underline{u}_o(s) \tag{6.36}$$

and in the time domain

$DAA_1^n(t)$ for n=0:

$$\underline{p}_o(t) = \dot{\underline{u}}_o(t) + 3\,\underline{u}_o(t) \tag{6.37}$$

The trial equation for the first-order DAA for n > 0 is

$$(P_1^n s + P_o^n)\,\underline{p}_n(s) = s^2\underline{u}_n(s) \tag{6.38}$$

This equation will match the first of (6.33) for arbitrary large s only if $P_1^n = 1$, and it will match the second of (6.34) for arbitrary small s only if $P_o^n = n$. Thus we have the first-order DAA in transform space

$DAA_1^n(s)$ for n>0:

$$(s + n)\,\underline{p}_n(s) = s^2\underline{u}_n(s) \tag{6.39}$$

and in the time domain

$DAA_1^n(t)$ for n>0:

$$\dot{\underline{p}}_n(t) + n\,\underline{p}_n(t) = \ddot{\underline{u}}_n(t) \tag{6.40}$$

For the second-order DAA, the trial equation for n=0 is constructed by extension of (6.35) as

$$(s + P_o^o)\,\underline{p}_o(s) = (s^2 + U_1^o s + 3P_o^o)\,\underline{u}_o(s) \tag{6.41}$$

To match ETA_2, we divide both this equation and the second of (6.33) through by s, and then require that the resulting equations match through order s^{-1}. That is, we require $(1 + P_o^o s^{-1})\underline{p}_o(s) = s(1 + U_1^o s^{-1})\underline{u}_o(s)$ to match $(1 - s^{-1})\underline{p}_o(s) = s\underline{u}_o(s)$ through order s^{-1}; long division and matching yields $U_1^o = P_o^o + 1$. To match LTA_2, we divide (6.41) through by P_o^o and match through order s^{-1} the resulting equation to the first of (6.34); this yields $P_o^o = 2$. With P_o^o and U_1^o thus determined, (6.41) becomes

$DAA_2^n(s)$ for n=0: $$(s + 2)\,\underline{p}_o(s) = (s^2 + 3s + 6)\,\underline{u}_o(s) \tag{6.42}$$

In the time domain, this equation is

$DAA_2^n(t)$ for n=0: $$\dot{\underline{p}}_o(t) + 2\underline{p}_o(t) = \ddot{\underline{u}}_o(t) + 3\dot{\underline{u}}_o(t) + 6\underline{u}_o(t) \tag{6.43}$$

Similarly, by referring to (6.38), the trial equation for the second-order DAA for $n > 0$ is constructed as

$$(s^2 + P_1^n s + nP_o^n)\,\underline{p}_n(s) = (s^3 + P_o^n s^2)\,\underline{u}_n(s) \tag{6.44}$$

By following here the same matching procedure as that applied to (6.38), we obtain $P_o^n = P_1^n + 1$ and $P_1^n = n$. Thus, introducing these results into (6.44), we find the second-order internal DAA for $n > 0$ in transform space to be

$DAA_2^n(s)$ for n>0: $$[s^2 + ns + n(n + 1)]\,\underline{p}_n(s) = (s + n + 1)\,s^2\underline{u}_n(s) \tag{6.45}$$

and in the time domain to be

$DAA_2^n(t)$ for n>0: $$\ddot{\underline{p}}_n(t) + n\dot{\underline{p}}_n(t) + n(n+1)\underline{p}_n(t) = \dddot{\underline{u}}_n(t) + (n+1)\ddot{\underline{u}}_n(t) \tag{6.46}$$

SECTION 7

TRANSIENT EXCITATION OF A FLUID-FILLED, SUBMERGED SPHERICAL SHELL: EXACT AND DAA FORMULATIONS

A canonical problem in transient fluid-structure interaction is the excitation of a submerged spherical shell by a plane acoustic wave. Exact shell-response solutions for an empty spherical shell were first provided by Huang, 1969; the results produced by these solutions contained small errors, which were subsequently found and corrected by Huang, *et al.*, 1977, and by Geers, 1978. In 1979, Huang also obtained solutions for the problem of plane-wave-excited concentric spherical shells with fluid present in the annular region between the shells and absent inside the inner shell. The plane-wave excitation problem for a submerged single shell filled with fluid has apparently never been solved.

In this section, exact shell-response and acoustic-pressure solutions are obtained for a fluid-filled, submerged spherical shell excited by a plane acoustic wave. The method of separation of variables is used to construct generalized Fourier series expressions. For some response quantities, especially surface pressures, convergence of the series is not satisfactory, so special techniques are employed, with gratifying results. As in Section 6, *nondimensional variables are used*, with length normalized to a, time to a/c_e, and pressure to $\rho_e c_e^2$, where ρ_e and c_e pertain to the external fluid.

DAA Fourier series solutions are also obtained for the purpose of evaluating the doubly asymptotic approximations for internal acoustic domains developed in Sections 3 and 5. Numerical results produced by the exact and DAA Fourier series are presented in Section 8.

7.1 DESCRIPTION OF THE PROBLEM.

A diagram of the problem appears in Figure 1. For generality, the internal and external acoustic fluids are regarded as having different mass densities, ρ_i and ρ_e, and different sound speeds, c_i and c_e. The shell material is elastic and isotropic, with density ρ_0 and plate velocity $c_0 = [E/(1-\nu^2)]^{1/2}$, where E is Young's modulus and ν is Poisson's ratio. The shell's thickness-to-radius ratio h/a is sufficiently small that thin-shell theory suffices. The response equations are formulated in terms of four field variables: the meridional and radial shell displacements $v(\theta,t)$ and $w(\theta,t)$, and the internal and external velocity potentials $\phi^i(r,\theta,t)$ and $\phi^e(r,\theta,t)$.

The expansions in generalized Fourier series of the internal and external velocity potentials are given by (6.1), and those of the shell displacements are given by

$$v(\theta,t) = -\sum_{n=1}^{\infty} v_n(t)\frac{d}{d\theta}P_n(\cos\theta)$$
$$w(\theta,t) = \sum_{n=0}^{\infty} w_n(t)P_n(\cos\theta) \tag{7.1}$$

Acoustic pressure and *radial* fluid-particle velocity at the external shell surface are related to the external velocity potential there by $\underline{p}^e = \underline{\dot{\phi}}^e$ and $\underline{\dot{u}}^e = -\underline{\dot{\phi}}^e_{,r}$, where a dot denotes partial differentiation with respect to nondimensional time and the r-subscript denotes partial differentiation with respect to the nondimensional radial coordinate; we recall that an underline means evaluation at r = 1. The corresponding relations for the internal acoustic medium are $\underline{p}^i = (\rho_i/\rho_e)\underline{\dot{\phi}}^i$ and $\underline{\dot{u}}^i = \underline{\dot{\phi}}^i_{,r}$, where $\dot{u}^i$ is positive *inward*.

7.2 MODAL EQUATIONS OF MOTION FOR THE SPHERICAL SHELL.

The equations of motion for the n*th* Fourier component of shell response may be written [Junger and Feit, 1972]

$$n(n+1)\ddot{v}_n + \lambda_n^{vv} v_n + \lambda_n^{vw} w_n = 0$$
$$\ddot{w}_n + \lambda_n^{vw} v_n + \lambda_n^{ww} w_n = \mu \underline{p}_n \tag{7.2}$$

in which $\mu = (\rho_e/\rho_0)(a/h)$, $\underline{p}_n$ is the n*th* Fourier component of net pressure acting radially outward on the shell, and

$$\lambda_n^{vv} = n(n+1)(1+\varepsilon)\xi_n\gamma_o$$
$$\lambda_n^{vw} = n(n+1)(1+\nu+\varepsilon\xi_n)\gamma_o \tag{7.3}$$
$$\lambda_n^{ww} = [2(1+\nu) + n(n+1)\varepsilon\xi_n]\gamma_o$$

where $\varepsilon = (h/a)^2/12$, $\gamma_0 = (c_0/c_e)^2$, $\xi_n = n(n+1)-1+\nu$.

7.3 EXACT FLUID-STRUCTURE-INTERACTION EQUATIONS.

Force compatibility at the surface of the shell requires that $\underline{p}_n = \underline{p}^i_n - \underline{p}^e_n$, where $\underline{p}^i_n$ and $\underline{p}^e_n$ are the pressures exerted by the internal and external fluid, respectively. But $\underline{p}^e_n$ is the sum of the known incident pressure $\underline{p}^o_n$ and an unknown scattered pressure $\underline{p}^s_n$; furthermore, modal surface pressures are related to corresponding velocity potentials as $\underline{p}^i_n = (\rho_i/\rho_e)\underline{\dot{\phi}}^i_n$ and $\underline{p}^e_n = \underline{\dot{\phi}}^e_n$. Hence $\underline{p}_n$ may be expressed as

$$\underline{p}_n = (\rho_i/\rho_e)\underline{\dot{\phi}}^i_n - \underline{p}^o_n - \underline{\dot{\phi}}^s_n \tag{7.4}$$

With modal radial fluid-particle velocities related to corresponding velocity potentials as $\underline{\dot{u}}^i_n = \underline{\dot{\phi}}^i_{n,r}$ and $\underline{\dot{u}}^s_n = -\underline{\dot{\phi}}^s_{n,r}$, and with $\underline{\dot{u}}^e_n = \underline{\dot{u}}^o_n + \underline{\dot{u}}^s_n$, geometric compatibility at the inner and outer surfaces of the shell requires that

$$\underline{\dot{\phi}}^i_{n,r} = -\dot{w}_n \qquad\qquad \underline{\dot{u}}^o_n - \underline{\dot{\phi}}^s_{n,r} = \dot{w}_n \tag{7.5}$$

Note that circumferential geometric compatibility is not enforced, as the fluid is inviscid.

Now (6.9) for the internal fluid and (6.4) for the external fluid enable us to eliminate $\underline{\dot{\phi}}^i_{n,r}$ and $\underline{\dot{\phi}}^s_{n,r}$ from (7.5), which yields

$$\begin{aligned} (c_e/c_i)\underline{\dot{\phi}}^i_n - \underline{\dot{\phi}}^i_n - \underline{\psi}^i_n &= -\dot{w}_n \\ \underline{\dot{\phi}}^s_n + \underline{\dot{\phi}}^s_n + \underline{\psi}^s_n &= \dot{w}_n - \underline{\dot{u}}^o_n \end{aligned} \tag{7.6}$$

Also, we observe from (6.7) that each scattered residual potential $\underline{\psi}^s_n(t)$ is related to the corresponding velocity potential $\underline{\dot{\phi}}^s_n(t)$ through the differential equation

$$\sum_{m=0}^{n} \Gamma_{nm}\underline{\psi}^s_{n,n-m} = \sum_{m=1}^{n} m\Gamma_{nm}\underline{\dot{\phi}}^s_{n,n-m} \tag{7.7}$$

where the subscript n-m denotes (n-m)-fold differentiation in time. Finally, we see from (6.12) that each internal residual potential $\underline{\Psi}^{i}_{n}(t)$ is related to the corresponding velocity potential $\underline{\Phi}^{i}_{n}(t)$ and historical data through the delayed-differential equation

$$\sum_{m=0}^{n}(-1)^{m}(c_e/c_i)^{n-m}\Gamma_{nm}\underline{\Psi}^{i}_{n,n-m} = \sum_{m=1}^{n}(-1)^{m}m(c_e/c_i)^{n-m}\Gamma_{nm}\underline{\Phi}^{i}_{n,n-m}$$

$$+(-1)^{n}\sum_{m=0}^{n}(c_e/c_i)^{n-m}\Gamma_{nm}\left[\underline{\Psi}^{i}_{n,n-m} - 2(c_e/c_i)\underline{\Phi}^{i}_{n,n-m+1} - m\underline{\Phi}^{i}_{n,n-m}\right]_{t-2c_e/c_i} \tag{7.8}$$

7.4 ASSEMBLY OF THE EXACT RESPONSE EQUATIONS.

The ensemble of equations (7.2), (7.4), (7.6), (7.7) and (7.8) constitutes a set of seven equations for the seven unknowns $v_n(t)$, $w_n(t)$, $\underline{p}_n(t)$, $\underline{\Phi}^{s}_{n}(t)$, $\underline{\Psi}^{s}_{n}(t)$, $\underline{\Phi}^{i}_{n}(t)$ and $\underline{\Psi}^{i}_{n}(t)$, given the incident-wave functions $\underline{p}^{o}_{n}(t)$ and $\underline{\dot{u}}^{o}_{n}(t)$. However, (7.8) presents a problem in that the highest derivative of $\underline{\Phi}^{i}_{n}(t)$ in the time-delayed term would be one order higher than the highest derivative of $\underline{\Phi}^{i}_{n}(t)$ previously calculated. This problem can be overcome by numerical differentiation of the *nth* derivative of $\underline{\Phi}^{i}_{n}(t)$, which is not particularly appealing. Fortunately, it can also be overcome by (n-m)-fold differentiation of the first of (7.6), which permits the replacement of $\underline{\Phi}^{i}_{n-m+1}$ in (7.8) by means of the relation

$$(c_e/c_i)\underline{\Phi}^{i}_{n,n-m+1} = \underline{\Phi}^{i}_{n,n-m} + \underline{\Psi}^{i}_{n,n-m} - w_{n,n-m+1} \tag{7.9}$$

Unfortunately, this equation brings with it, for n > 0, unacceptably high derivatives of w_n, which we avoid by introducing the *integrated variables* $V_n(t)$, $W_n(t)$, $\underline{\Phi}^{s}_{n}(t)$, $\underline{\Psi}^{s}_{n}(t)$, $\underline{\Phi}^{i}_{n}(t)$ and $\underline{\Psi}^{i}_{n}(t)$, defined by

$$v_n = V_{n,n} \quad w_n = W_{n,n} \quad \underline{\phi}^s_n = \underline{\Phi}^s_{n,n}$$

$$\underline{\psi}^s_n = \underline{\Psi}^s_{n,n} \quad \underline{\phi}^i_n = \underline{\Phi}^i_{n,n} \quad \underline{\psi}^i_n = \underline{\Psi}^i_{n,n} \tag{7.10}$$

Thus, inserting (7.4) into (7.2), integrating (7.7) and (7.8) n times, and introducing the integrated variables into the resulting equations and into (7.6), we obtain the following six equations for six unknowns:

$$n(n+1)V_{n,n+2} + \lambda^{vv}_n V_{n,n} + \lambda^{vw}_n W_{n,n} = 0$$

$$W_{n,n+2} + \lambda^{vw}_n V_{n,n} + \lambda^{ww}_n W_{n,n} + \mu[\underline{\Phi}^s_{n,n+1} - (\rho_i/\rho_e)\underline{\Phi}^i_{n,n+1}] = -\mu \underline{p}^o_n$$

$$W_{n,n+1} - \underline{\Phi}^s_{n,n+1} - \underline{\Phi}^s_{n,n} - \underline{\Psi}^s_{n,n} = \underline{\dot{u}}^o_n$$

$$W_{n,n+1} + (c_e/c_i)\underline{\Phi}^i_{n,n+1} - \underline{\Phi}^i_{n,n} - \underline{\Psi}^i_{n,n} = 0 \tag{7.11}$$

$$\sum_{m=0}^{n} \Gamma_{nm}(m\underline{\Phi}^s_{n,n-m} - \underline{\Psi}^s_{n,n-m}) = 0$$

$$\sum_{m=0}^{n} (-1)^m (c_i/c_e)^m \Gamma_{nm}(m\underline{\Phi}^i_{n,n-m} - \underline{\Psi}^i_{n,n-m}) =$$

$$(-1)^n \sum_{m=0}^{n} (c_i/c_e)^m \Gamma_{nm}\left[\underline{\Psi}^i_{n,n-m} + (m+2)\underline{\Phi}^i_{n,n-m} - 2W_{n,n-m+1}\right]_{t-2c_e/c_i}$$

Once the solutions to these equations have been obtained for several values of n and the desired modal response histories have been determined in accordance with (7.10), Fourier superposition yields response histories for surface pressures and shell responses at desired locations in accordance with (6.1) and (7.1).

7.5 ASSEMBLY OF THE DAA_1 RESPONSE EQUATIONS.

To obtain a set of equations corresponding to (7.11) that are based on a DAA_1 treatment of the fluid-structure interaction, we first use (6.37) and (6.40) for the internal fluid along with the compatibility relation $\dot{\underline{u}}_n^i = -\dot{w}_n$ to get [*cf.* the first of (7.6)]

$$\begin{aligned} (c_e/c_i)\underline{\phi}_o^i &= -\left[\dot{w}_o + 3(c_i/c_e)w_o\right] \\ (c_e/c_i)\underline{\phi}_n^i + n\underline{\phi}_n^i &= -\dot{w}_n \qquad (n > 0) \end{aligned} \tag{7.12}$$

Next, we use (6.23) for the external fluid along with the compatibility relation $\dot{\underline{u}}_n^o + \dot{\underline{u}}_n^s = \dot{w}_n$ to obtain [*cf.* the second of (7.6)]

$$\underline{\phi}_n^s + (n+1)\underline{\phi}_n^s = \dot{w}_n - \dot{\underline{u}}_n^o \tag{7.13}$$

Finally, we introduce (7.4) into (7.2) to eliminate $\underline{p}_n$ as an unknown. Thus we obtain four equations for the four unknowns $v_n(t)$, $w_n(t)$, $\underline{\phi}_n^s(t)$ and $\underline{\phi}_n^i(t)$:

$$\begin{aligned} n(n+1)\ddot{v}_n + \lambda_n^{vv} v_n + \lambda_n^{vw} w_n &= 0 \\ \ddot{w}_n + \lambda_n^{vw} v_n + \lambda_n^{ww} w_n + \mu[\underline{\phi}_n^s - (\rho_i/\rho_e)\underline{\phi}_n^i] &= -\mu \underline{p}_n^o \\ \dot{w}_n - \underline{\phi}_n^s - (n+1)\underline{\phi}_n^s &= \dot{\underline{u}}_n^o \\ \dot{w}_o + (c_e/c_i)\underline{\phi}_o^i + 3(c_i/c_e)w_o &= 0 \\ \dot{w}_n + (c_e/c_i)\underline{\phi}_n^i + n\underline{\phi}_n^i &= 0 \qquad (n > 0) \end{aligned} \tag{7.14}$$

7.6 ASSEMBLY OF THE DAA_2 RESPONSE EQUATIONS.

To obtain a set of equations corresponding to (7.11) that are based on a DAA_2 treatment of the fluid-structure interaction, we first use (6.43) and (6.46) for the interior fluid along with the compatibility relation $\dot{\underline{u}}_n^i = -\dot{w}_n$ to get [*cf.* (7.12) and the first of (7.6)]

$$(c_e/c_i)\ddot{\underline{\phi}}_o^i + 2\dot{\underline{\phi}}_o^i = -[\ddot{w}_o + 3(c_i/c_e)\dot{w}_o + 6(c_i/c_e)^2 w_o] \tag{7.15}$$

$$(c_e/c_i)\ddot{\underline{\phi}}_n^i + n\dot{\underline{\phi}}_n^i + n(n+1)(c_i/c_e)\underline{\phi}_n^i = -[\ddot{w}_n + (n+1)(c_i/c_e)\dot{w}_n] \qquad (n \geq 1)$$

Next, we use (6.27) for the external fluid along with the compatibility relation $\dot{\underline{u}}_n^o + \dot{\underline{u}}_n^s = \dot{w}_n$ to obtain [*cf.* (7.13) and the second of (7.6)]

$$\ddot{\underline{\phi}}_n^s + (n+1)\dot{\underline{\phi}}_n^s + n(n+1)\underline{\phi}_n^s = \ddot{w}_n - \ddot{\underline{u}}_n^o + n(\dot{w}_n - \dot{\underline{u}}_n^o) \tag{7.16}$$

Finally, we introduce (7.4) into (7.2) to eliminate $\underline{p}_n$ as an unknown. This yields the following four equations for the four unknowns $v_n(t)$, $w_n(t)$, $\underline{\phi}_n^s(t)$ and $\underline{\phi}_n^i(t)$:

$$\begin{aligned}
&n(n+1)\dot{v}_n + \lambda_n^{vv} v_n + \lambda_n^{vw} w_n = 0 \\
&\ddot{w}_n + \lambda_n^{vw} v_n + \lambda_n^{ww} w_n + \mu[\dot{\underline{\phi}}_n^s - (\rho_i/\rho_e)\dot{\underline{\phi}}_n^i] = -\mu \underline{p}_n^o \\
&\ddot{w}_n - \ddot{\underline{\phi}}_n^s + n\dot{w}_n - (n+1)\dot{\underline{\phi}}_n^s - n(n+1)\underline{\phi}_n^s = \ddot{\underline{u}}_n^o + n\dot{\underline{u}}_n^o \\
&\ddot{w}_o + (c_e/c_i)\ddot{\underline{\phi}}_o^i + 3(c_i/c_e)\dot{w}_o + 2\dot{\underline{\phi}}_o^i + 6(c_i/c_e)^2 w_o = 0 \\
&\ddot{w}_n + (c_e/c_i)\ddot{\underline{\phi}}_n^i + (n+1)(c_i/c_e)\dot{w}_n + n\dot{\underline{\phi}}_n^i + n(n+1)(c_i/c_e)\underline{\phi}_n^i = 0 \qquad (n > 0)
\end{aligned} \tag{7.17}$$

In contrast to (7.11), (7.14) and (7.17) are low-order ordinary differential equations in the direct, not integrated, variables. Once modal solutions to these equations have been obtained for

several values of n, Fourier superposition yields results for surface pressures and shell responses at desired locations in accordance with (6.1) and (7.1).

7.7 MODIFIED CESÀRO SUMMATION FOR IMPROVED CONVERGENCE.

As mentioned above, the generalized Fourier series calculated for some of the response quantities of interest do not converge satisfactorily. This is certainly to be expected in response histories that contain discontinuities, where pronounced non-physical oscillations appear (Gibb's phenomenon). A superposition technique that has proven effective in reducing these oscillations is due to Cesàro (Apostol, 1957).

With S_N as the partial sum of an infinite series through the first N+1 terms, the N*th* Cesàro sum, σ_N, of that series is the arithmetic mean of the first N+1 partial sums S_N, *i.e.*,

$$S_N = \sum_{n=0}^{N} x_n \qquad \sigma_N = \frac{1}{N+1} \sum_{M=0}^{N} S_M \tag{7.18}$$

Introducing the first of these into the latter and expanding, we find that the Cesàro sum may be written explicitly as

$$\sigma_N = x_0 + \frac{N}{N+1} x_1 + \frac{N-1}{N+1} x_2 + \cdots + \frac{1}{N+1} x_N \tag{7.19}$$

A useful interpretation of partial and Cesàro summation consists of regarding each as a digital weighting filter for an infinite series. In this interpretation, partial summation employs unit weights for the first n+1 terms and zero weights for the rest, and Cesàro summation employs weights that decrease linearly from one for the first term to zero for x_{n+1} and beyond. Clearly, the filter characteristic for Cesàro summation is more gradual than that for partial summation.

Standard Cesàro summation is not appropriate in the present problem because weights less than unity for n=1 and n=2 produce inaccurate late-time asymptotic results for translational velocity and deformational displacement of the shell [Geers, 1974]. The procedure is easily modified, however, to produce unit weighting for modes 0, 1, and 2, and linearly decreasing weights for modes 3 through N. The resulting filter characteristics for N = 5 and N = 8 are shown in Figure 2; also shown are the corresponding filter characteristics for partial summation.

Cesàro summation can dramatically improve convergence, as demonstrated in Figures 3 and 4. The figures show pressure histories generated for a free-field step-wave by the

superposition of modal pressure histories in accordance with (6.1). Each modal pressure history is given, for $0 \le t \le 2$, by

$$\underline{p}_n(t) = (n + \tfrac{1}{2})P_I \int_0^{\pi} H(t - \cos\theta - 1)\, P_n(\cos\theta)\, \sin\theta\, d\theta \tag{7.20}$$

For $t \ge 2$, $\underline{p}_n(t) = \underline{p}_n(2)$. The integral in (7.20) is easily evaluated by the change of variable $\tau = \cos\theta$. Pressure histories are shown at three points on the locus $r = 1$ in the spherical geometry. The true histories, of course, are step-functions, with discontinuities at $t = 0$, 1 and 2 for $\theta = \pi$, $\pi/2$ and 0, respectively.

Figures 3 and 4 also provide values of integrated mean-square error, given by

$$e = (2P_I^2)^{-1} \int_0^2 [\underline{p}_{\Sigma n}(t) - \underline{p}_{Ex}(t)]^2\, dt \tag{7.21}$$

where $\underline{p}_{\Sigma n}(t)$ is the summed history and $\underline{p}_{Ex}(t)$ is the exact history. The values indicate that, while modified Cesàro sums may be superior to standard partial sums at some points, they may be inferior at others. This is demonstrated more comprehensively in Figure 5, which shows integrated mean-square error characterizing modified Cesàro and standard partial sums for step-wave pressure histories on the locus $r = 1$. As one would expect from the overall optimality attribute of Fourier series, the average integrated mean-square error for standard partial summation is less than that for modified Cesàro summation. However, the maximum error produced by the latter is less than that produced by the former. Furthermore, standard partial summation incurs its largest errors at $\theta = 0$ and $\theta = \pi$, which are often the points of greatest interest.

From the preceding, modified Cesàro summation yields for shell velocities and surface pressures

$$\dot{v}(\theta,t) = -\sum_{n=1}^{N} C_n \dot{v}_n(t) \frac{d}{d\theta} P_n(\cos\theta)$$

$$\dot{w}(\theta,t) = \sum_{n=0}^{N} C_n \dot{w}_n(t) P_n(\cos\theta) \tag{7.22}$$

$$\underline{p}^e(\theta,t) = \underline{p}^o(\theta,t) + \sum_{n=0}^{N} C_n \underline{\phi}_n^s(t)\, P_n(\cos\theta)$$

$$\underline{p}^i(\theta,t) = \sum_{n=0}^{N} C_n \underline{\phi}_n^i(t)\, P_n(\cos\theta)$$

where $C_0 = C_1 = C_2 = 1$ and $C_n = (N+1-n)/(N-1)$ for $n > 2$.

7.8 PARTIAL CLOSED-FORM SOLUTION FOR IMPROVED CONVERGENCE.

It is clear from Figures 3 and 4 that no superposition of modal solutions can reproduce the jump in pressure at a discontinuous wave front. This deficiency is even more pronounced in the vicinity of the point of first contact between the wave front and the spherical shell, where the pressure initially doubles. Hence we introduce here a method to alleviate this convergence problem by assembling the complete solution as the sum of a closed-form initial solution and a complementary series solution.

The *first step* in the method involves retention of the terms in (7.11) that dominate early-time response; this yields the *initial-response equations*

$$\begin{aligned} W^*_{n,n+2} + \mu[\underline{\Phi}^{s*}_{n,n+1} - (\rho_i/\rho_e)\underline{\Phi}^{i*}_{n,n+1}] &= -\mu \underline{p}^o_n \\ W^*_{n,n+1} - \underline{\Phi}^{s*}_{n,n+1} &= \underline{\dot{u}}^o_n \\ W^*_{n,n+1} + (c_e/c_i)\underline{\Phi}^{i*}_{n,n+1} &= 0 \end{aligned} \tag{7.23}$$

where the asterisk denotes initial-response quantities. It is apparent that these equations neglect all stiffness effects in the shell and invoke the first-order early-time (plane-wave) approximation for the fluid-structure interaction. Because they do not involve the modal index n as an explicit parameter, *they can be summed in closed form.* Thus, eliminating the two integrated velocity potentials from the first equation by using the other two, and then utilizing (7.10), we may write the summed equations in terms of the direct variables $w^*(\theta,t)$, $\underline{\phi}^{s*}(\theta,t)$ and $\underline{\phi}^{i*}(\theta,t)$ as

$$\ddot{w}^* + \upsilon\dot{w}^* = -\mu(\underline{p}^o - \underline{\dot{u}}^o)$$

$$\underline{\phi}^{s*} = \dot{w}^* - \underline{\dot{u}}^o \tag{7.24}$$

$$\underline{\phi}^{i*} = -(c_i/c_e)\dot{w}^*$$

where $\upsilon = \mu(1 + \rho_i c_i/\rho_e c_e)$.

The *second step* consists of solving (7.24) for a prescribed incident wave. For example, an incident step wave propagating to the right that at $t = 0$ first contacts the shell at $\theta = \pi$ yields

$$\underline{p}^o(\theta,t) = P_I H(t - \cos\theta - 1)$$

$$\underline{\dot{u}}^o(\theta,t) = P_I \cos\theta\, H(t - \cos\theta - 1) \tag{7.25}$$

where $H(\,)$ is the Heaviside step-function. For this excitation, the closed-form solutions to (7.24) with quiescent initial conditions are

$$\dot{w}^*(\theta,t) = -\mu\upsilon^{-1}P_I(1 - \cos\theta)[1 - e^{-\upsilon(t-\cos\theta-1)}]H(t - \cos\theta - 1)$$

$$\begin{aligned}\underline{\phi}^{s*}(\theta,t) = &-\mu\upsilon^{-1}P_I[1 - e^{-\upsilon(t-\cos\theta-1)}]H(t - \cos\theta - 1)\\ &- P_I\cos\theta\{1 - \mu\upsilon^{-1}[1 - e^{-\upsilon(1-\cos\theta-1)}]\}H(t - \cos\theta - 1)\end{aligned} \tag{7.26}$$

$$\underline{\phi}^{i*}(\theta,t) = \mu\upsilon^{-1}(c_i/c_e)P_I(1 - \cos\theta)[1 - e^{-\upsilon(t-\cos\theta-1)}]H(t - \cos\theta - 1)$$

The *third step* requires that the closed-form solutions be used to compute modal initial-response histories from the standard formula

$$\{\dot{w}_n^*(t), \underline{\phi}_n^{s*}(t), \underline{\phi}_n^{i*}(t)\} = (n + \tfrac{1}{2})\int_0^\pi \{\dot{w}^*(\theta,t), \underline{\phi}^{s*}(\theta,t), \underline{\phi}^{i*}(\theta,t)\}P_n(\cos\theta)\sin\theta\, d\theta \tag{7.27}$$

Then these histories are numerically integrated in time to tabulate the modal initial responses $w_n^*(t)$, $\underline{\Phi}^{s*}_{n,n}(t), \underline{\Phi}^{s*}_{n,n-1}(t), \cdots, \underline{\Phi}^{s*}_{n,1}(t), \underline{\Phi}^{s*}_{n}(t)$, $\underline{\Phi}^{i*}_{n,n}(t), \underline{\Phi}^{i*}_{n,n-1}(t), \cdots, \underline{\Phi}^{s*}_{n,1}(t), \underline{\Phi}^{s*}_{n}(t)$.

The *fourth step* involves associating with each modal initial response [*e.g.*, $w_n^*(t)$] a modal complementary response [*e.g.*, $w_n^+(t)$] such that the sum of the two yields the true modal response [*e.g.*, $w_n(t) = w_n^*(t) + w_n^+(t)$], subtracting each of (7.23) from its counterpart in (7.11), expressing the last two of (7.11) in terms of initial and complementary responses, and invoking the second of (7.10). This yields, <u>for $t < 2c_e/c_i$</u>, the *complementary-response equations*

$$n(n+1)V^{+}_{n,n+2} + \lambda_n^{vv} V_{n,n} + \lambda_n^{vw} W^{+}_{n,n} = -\lambda_n^{vw} w_n^*$$

$$W^{+}_{n,n+2} + \lambda_n^{vw} V_{n,n} + \lambda_n^{ww} W^{+}_{n,n} + \mu[\underline{\Phi}^{s+}_{n,n+1} - (\rho_i/\rho_e)\underline{\Phi}^{i+}_{n,n+1}] = -\lambda_n^{ww} w_n^*$$

$$W^{+}_{n,n+1} - \underline{\Phi}^{s+}_{n,n+1} - \underline{\Phi}^{s+}_{n,n} - \underline{\Psi}^{s}_{n,n} = \underline{\Phi}^{s*}_{n,n}$$

$$W^{+}_{n,n+1} + (c_e/c_i)\underline{\Phi}^{i+}_{n,n+1} - \underline{\Phi}^{i+}_{n,n} - \underline{\Psi}^{i}_{n,n} = \underline{\Phi}^{i*}_{n,n} \tag{7.28}$$

$$\sum_{m=0}^{n} \Gamma_{nm}(m\Phi^{s+}_{n,n-m} - \Psi^{s}_{n,n-m}) = \sum_{m=1}^{n} m\Gamma_{nm}\Phi^{s*}_{n,n-m}$$

$$\sum_{m=0}^{n} (-1)^m (c_i/c_e)^m \Gamma_{nm}(m\Phi^{i+}_{n,n-m} - \Psi^{i}_{n,n-m}) = \sum_{m=1}^{n} (-1)^{m-1}(c_i/c_e)^m m\Gamma_{nm}\Phi^{i*}_{n,n-m}$$

The *final step* consists of the addition of initial and complementary solutions, and the use of modified Cesàro summation, which yields for shell velocities and surface pressures [*cf.* (7.22)]

$$\dot{v}(\theta,t) = -\sum_{n=1}^{\infty} C_n \dot{v}_n(t) \frac{d}{d\theta} P_n(\cos\theta)$$

$$\dot{w}(\theta,t) = \dot{w}^*(\theta,t) + \sum_{n=0}^{N} C_n \dot{w}_n^+(t) P_n(\cos\theta) \tag{7.29}$$

$$\underline{p}^e(\theta,t) = \underline{p}^o(\theta,t) + \underline{\phi}^{s*}(\theta,t) + \sum_{n=0}^{N} C_n \underline{\phi}_n^{s+}(t)\, P_n(\cos\theta)$$

$$\underline{p}^i(\theta,t) = \underline{\phi}^{i*}(\theta,t) + \sum_{n=0}^{N} C_n \underline{\phi}_n^{i+}(t)\, P_n(\cos\theta)$$

where, again, $C_0 = C_1 = C_2 = 1$ and $C_n = (N+1-n)/(N-1)$ for $n > 2$. Because the delayed term in the last of (7.11) was dropped in the process of deriving (7.28), (7.29) are only valid for $t < 2c_e/c_i$. This is generally satisfactory, in that $\underline{p}^s(\theta,t)$ contains no discontinuity for $\theta > \pi/2$ [Friedlander, 1958], which the incident wave front reaches at $t = 1$. Hence it is appropriate to use (7.29) for t less than unity or $2c_e/c_i$, whichever is smaller.

The first-order early-time (plane-wave) approximation, on which (7.29) are based, is only accurate for $t << 1$. The region of validity of this approximation is readily assessed by noting that the second of (7.26) predicts a wave-front jump in scattered pressure of $-P_I\cos\theta_o$ at the circle on the shell defined by $r = 1$, $\theta = \arccos(t-1)$. In contrast, at points on the shell reached first by the incident wave, the true jump is unity [Geers, 1972]. Hence we would expect (7.29) to predict discontinuous scattered-wave response accurately over the region $180^o \leq \theta < 155^o$.

Partial-closed-form solution with modified Cesàro summation is also used to obtain DAA results. The initial-response solutions for DAA_1 are (7.26), but only $w_n^*(t)$ needs to be tabulated using (7.27). The complementary-response equations are

$$\begin{aligned}
&n(n+1)\tilde{v}_n + \lambda_n^{vv} v_n + \lambda_n^{vw} w_n^+ = -\lambda_n^{vw} w_n^* \\
&\ddot{w}_n^+ + \lambda_n^{vw} v_n + \lambda_n^{ww} w_n^+ + \mu[\underline{\phi}_n^{s+} - (\rho_i/\rho_e)\underline{\phi}_n^{i+}] = -\lambda_n^{ww} w_n^* \\
&\dot{w}_n^+ - \underline{\phi}_n^{s+} - (n+1)\underline{\phi}_n^{s+} = (n+1)(w_n^* - \underline{u}_n^o) \\
&\dot{w}_o^+ + (c_e/c_i)\underline{\phi}_o^{i+} + 3(c_i/c_e) w_o^+ = -3(c_i/c_e) w_o^* \\
&\dot{w}_n^+ + (c_e/c_i)\underline{\phi}_n^{i+} + n\underline{\phi}_n^{i+} = n(c_i/c_e) w_n^* \qquad (n > 0)
\end{aligned} \tag{7.30}$$

The initial-response solutions for DAA_2 are (7.26) also, but the only modal initial responses that must be tabulated using (7.27) are $w_n^*(t)$ and $\dot{w}_n^*(t)$. The complementary-response equations are

$$n(n+1)\ddot{v}_n + \lambda_n^{vv} v_n + \lambda_n^{vw} w_n^+ = -\lambda_n^{vw} w_n^*$$

$$\ddot{w}_n^+ + \lambda_n^{vw} v_n + \lambda_n^{ww} w_n^+ + \mu[\underline{\phi}_n^{s+} - (\rho_i/\rho_e)\underline{\phi}_n^{i+}] = -\lambda_n^{ww} w_n^*$$

$$\ddot{w}_n^+ - \underline{\phi}_n^{s+} + n\dot{w}_n^+ - (n+1)\underline{\phi}_n^{s+} - n(n+1)\underline{\phi}_n^{s+} = (\dot{w}_n^* - \underline{u}_n^o) + n(n+1)(w_n^* - \underline{u}_n^o)$$

$$\ddot{w}_o^+ + (c_e/c_i)\underline{\phi}_o^{i+} + 3(c_i/c_e)\dot{w}_o^+ + 2\underline{\phi}_o^{i+} + 6(c_i/c_e)^2 w_o^+ = -(c_i/c_e)[\dot{w}_o^* + 6(c_i/c_e)w_o^*] \tag{7.31}$$

$$\ddot{w}_n^+ + (c_e/c_i)\underline{\phi}_n^{i+} + (n+1)(c_i/c_e)\dot{w}_n^+ + n\underline{\phi}_n^{i+} + n(n+1)(c_i/c_e)\underline{\phi}_n^{i+}$$
$$= -(c_i/c_e)[\dot{w}_n^* - n(n+1)(c_i/c_e)w_n^*] \qquad (n > 0)$$

The partial-closed-form DAA solutions are obtained in accordance with (7.29) for $t < 1$.

7.9 INTERNAL ACOUSTIC FIELDS.

From (6.8) and from $p^i(r,\theta,t) = (\rho_i/\rho_e)\dot{\phi}^i(r,\theta,t)$ and $\mathbf{u}^i(r,\theta,t) = -\nabla\phi^i(r,\theta,t)$, the Fourier components of Laplace-transformed acoustic pressure, radial fluid-particle velocity, and meridional fluid-particle velocity at any point in the internal fluid may be expressed as

$$p_n^i(r,s) = (\rho_i/\rho_e)\, s f_n^i(s) i_n(rsc_e/c_i)$$

$$su_{rn}^i(r,s) = -(sc_e/c_i) f_n^i(s) i_n'(rsc_e/c_i) \tag{7.32}$$

$$su_{\theta n}^i(r,s) = -r^{-1} f_n^i(s) i_n(rsc_e/c_i)$$

where, again, $i_n(\,)$ is the nth-order modified spherical Bessel function of the first kind and $i_n'(\,)$

is the derivative of $i_n(\ )$ with respect to its argument. But the *nth* Fourier component of inward normal surface displacement is just $\underline{u}^i_n(s) = - u^i_{rn}(1,s)$. Hence we may use (7.32) to relate each Fourier component of the internal acoustic field to the corresponding component of inward normal surface displacement as

$$p^i_n(r,s) = (\rho_i c_i/\rho_e c_e)\frac{i_n(rsc_e/c_i)}{i'_n(sc_e/c_i)}\, s\underline{u}^i_n(s)$$

$$u^i_{rn}(r,s) = -\frac{i'_n(rsc_e/c_i)}{i'_n(sc_e/c_i)}\underline{u}^i_n(s) \tag{7.33}$$

$$u^i_{\theta n}(r,s) = -\, r^{-1}\frac{i_n(rsc_e/c_i)}{i'_n(sc_e/c_i)}\underline{u}^i_n(s)$$

The inverse transform of each of these relations is a delayed-differential equation, which can be solved numerically. With solutions for several values of n thus obtained, Fourier superposition yields response histories for the internal fields as

$$p^i(r,\theta,t) = \sum_{n=0}^{\infty} p^i_n(r,t)P_n(\cos\theta)$$

$$u^i_r(r,\theta,t) = \sum_{n=0}^{\infty} u^i_{rn}(r,t)P_n(\cos\theta) \tag{7.34}$$

$$u^i_\theta(r,\theta,t) = \sum_{n=1}^{\infty} u^i_{\theta n}(r,t)\frac{d}{d\theta}P_n(\cos\theta)$$

It is particularly easy to obtain response histories at the center of the internal fluid domain, *viz.*, at r = 0. At this point, symmetry arguments allow us to conclude that only the n = 0 component of surface displacement contributes to pressure and only the n = 1 component contributes to fluid-particle displacement. For these modes, inverse transformation of the first and second of (7.33) yields, with geometric compatibility requiring that $\underline{u}^i_n(t) = - w_n(t)$ and with integrated variables avoiding high derivatives,

$$\dot{\phi}^{i}_{o}(0,t) - (c_i/c_e)\dot{\phi}^{i}_{o}(0,t) = -2\tilde{w}_o(t - c_e/c_i) - \dot{\phi}^{i}_{o}(0,t - c_e/c_i)$$

$$\ddot{U}^{i}_{r1}(0,t) - 2(c_i/c_e)\dot{U}^{i}_{r1}(0,t) + 2(c_i/c_e)^2 U^{i}_{r1}(0,t) = \frac{2}{3}(c_e/c_i)\ddot{w}^{i}_{1}(t - c_e/c_i) \tag{7.35}$$

$$+ \ddot{U}^{i}_{r1}(0,t - 2c_e/c_i) + 2(c_i/c_e)\dot{U}^{i}_{r1}(0,t - 2c_e/c_i) + 2(c_i/c_e)^2\dot{U}^{i}_{r1}(0,t - 2c_e/c_i)$$

where $U^{i}_{r1}(0,t)$ is defined by $\dot{U}^{i}_{r1}(0,t) = u^{i}_{r1}(0,t)$. From the solutions to these equations, we obtain for pressure and fluid-particle velocity at $r = 0$

$$p^{i}(0,0,t) = (\rho_i/\rho_e)\dot{\phi}^{i}_{o}(0,t)$$

$$\dot{u}^{i}_{r}(0,0,t) = \ddot{U}^{i}_{r1}(0,t) \tag{7.36}$$

$$\dot{u}_{\theta}(0,0,t) = 0$$

SECTION 8

NUMERICAL RESULTS

Computed transient response histories are presented in this section for a steel spherical shell filled with and submerged in water, and excited by a plane step-wave. The thickness-to radius ratio is h/a = 0.01, the mass-density ratio is $\rho_o/\rho = 7.7$, and the sound-velocity ratio is $c_o/c = (13.8)^{1/2}$. Fifth-order Runge-Kutta integration was used to solve (7.11), (7.14), (7.17), (7.28), (7.30), (7.31) and (7.35), and Simpson's rule was used to perform the numerical integrations in space and time discussed in connection with (7.27). Partial closed-form solution with modified Cesàro summation, *i.e.*, (7.29), was used during $0 \leq t < 2$, and modal superposition with modified Cesàro summation, *i.e.*, (7.22), was used during $2 \leq t < 10$, As many as nine Fourier meriodonal harmonics were used; response histories for both N = 5 and N = 8 are displayed in the figures to indicate the degree of modal convergence.

The computer coding was validated by first performing response computations for a shell with mass-density and sound-velocity ratios of unity. The results showed the shell to be essentially transparent, as desired. Computations were also performed for an empty submerged shell, and the results were compared with the previous results of Geers, 1978; excellent agreement was found. Finally, early- and late-time responses were checked against easily calculated early-time jump and late-time static values; proper behavior was obtained in all cases.

8.1 EXACT RESULTS.

Response histories corresponding to an exact treatment of the fluid-structure interaction are displayed in Figure 6 through 15. Figure 6 shows surface-pressure histories at $\theta = \pi$ that were generated *without* the use of partial closed-form solution; the absence of the requisite jump in $\underline{p}_e$ and the poor convergence for $0 \leq t < 2$ are clearly seen. Figure 7 shows the same histories generated *with* partial closure; the improvement is obvious.

The pressure histories of Figure 7 exhibit considerable texture produced by complex wave-

propagation effects. The external-pressure history drops rapidly following its initial jump to two, which is characteristic of a thin shell (Geers, 1972); at late time, $\underline{p}_e$ approaches its late-time asymptote of unity. The internal-pressure history initially rises rapidly from zero, almost reaching the external-pressure history, and then oscillates irregularly about its late-time asymptote of 0.52.

Figure 8 shows surface-pressure histories at the deep-shadow point $\theta = 0$. Virtually no response is seen until $t \approx 0.75$, which demonstrates the effectiveness of Cesàro summation and partial closure for modal convergence enhancement. After the arrival of stress waves in the shell, which generate shell motion and thus surface pressures and before the arrival at $t = 2$ of the acoustic wave that travels through the internal fluid, the external-pressure history exhibits a modest hump and the internal-pressure history shows a substantial negative excursion. At $t = 2$, both pressure histories rise rapidly and then oscillate irregularly about their late-time asymptotes of 1.0 and 0.52, respectively.

Shell radial-velocity histories at $\theta = \pi$ and $\theta = 0$ are displayed in Figure 9. In keeping with the plane-wave approximation, the latter history matches the internal surface-pressure history in Figure 7 at early time; the two are even quite similar until $t \approx 2$. A brief, but prominent, oscillation appears in the $\theta = \pi$ velocity history during $2.5 < t < 4$, which is caused by the internal pressure wave reflected back from the rear portion of the shell. The motion after $t \approx 4$ consists of low-frequency oscillation about the asymptotic value of 0.87 (the filled shell is slightly negatively buoyant). As expected, no response is seen at $\theta = 0$ until $t \approx 0.75$, when shell stress waves arrive. The velocity history shows a modest hump during $0.75 \leq t < 2$ (*cf.* the $\underline{p}_e$ history in Figure 8), after which it rises rapidly to a peak value at $t \approx 3$ that exceeds the incident wave's fluid-particle velocity by nearly 50%. Subsequent motion consists of low-frequency oscillation about the 0.87 asymptote.

It is interesting to compare transient response histories for a fluid-filled shell with their counterparts for an empty shell, as done in Figure 10 through 14. External-surface pressure histories at $\theta = \pi$, which are displayed in Figure 10, exhibit rather modest differences, with the empty-shell history initially dropping from two at twice the rate of the filled-shell history, reaching a substantially lower minimum, and exhibiting more oscillation at late time. Differences are also modest at $\theta = \pi/2$. as seen in Figure 11; here, the filled-shell history rises rapidly after

$t = 1$, which the empty-shell history does not do, and the latter exhibits more oscillation at late time. Substantial differences between empty-shell and filled-shell pressure histories appear at $\theta = 0$, however, as shown in Figure 12. The empty-shell history rises rapidly at $t \approx 0.75$; the filled-shell history rises even more rapidly at $t \approx 2$. Also, the empty-shell history exhibits large oscillation at late time, which is not matched by filled-shell history. In all three figures, the empty-shell histories are quite smooth after $t = 3.5$, while the filled-shell histories exhibit continuing wave reflections in the internal fluid; in all cases, of course, the late-time asymptote is unity.

Velocity histories for the fluid-filled and empty shells are compared in Figure 13 and 14. In the former figure, which pertains to $\theta = \pi$, the empty-shell history initially rises at twice the rate of its filled-shell counterpart, reaches a substantially higher initial peak, and then oscillates with much higher amplitude about an asymptotic value of 2.05 (the empty shell is very positively buoyant). At $\theta = 0$, to which Figure 14 pertains, the empty-shell history rises immediately after $t \approx 0.75$ to reach peak values more than triple the fluid-particle velocity of the incident wave. Both figures fulfill the expectation that, at late time, the empty shell oscillates at a frequency higher than that characterizing the filled-shell oscillation; also, the empty-shell histories are smoother than the filled-shell histories after $t = 2$.

Finally, Figure 15 shows acoustic-pressure and fluid-particle-velocity histories at the center point in the internal fluid. Plane-wave propagation governs for $1 \leq t \leq 1.3$, during which time the pressure and velocity histories coincide, but the two histories diverge rapidly after that. At no time does the shell appear transparent to the incident wave, the pressure and velocity histories for which would appear in the figure as a unit step-function at $t = 1$. Strong focusing effects at $t = 3$, 5, 7 and 9 are apparent in the figure, and the two histories properly approach their late-time asymptotes of 0.87 and 0.52.

8.2 DAA RESULTS.

Response histories corresponding to DAA treatments of the fluid-structure interaction are exhibited in Figure 16 through 24 . At $\theta = \pi$, to which Figure 16 pertains, DAA results for external-surface pressure are quite satisfactory, with the DAA_2 history following the exact history

very closely everywhere except for $2.5 < t < 4$, during which the exact history exhibits its brief oscillation. As seen in Figure 17, DAA performance is not as good for internal pressure, with $2 \leq t \leq 4$ being the period of greatest difficulty, also because of the brief oscillation. Here DAA_2 clearly emerges as superior to DAA_1, reaching the initial peak with greater accuracy and exhibiting the correct frequency of oscillation at late time; DAA_2 does not, however, capture the fine texture of the exact history.

External- and internal-surface pressure histories at $\theta = \pi/2$ are shown in Figures 18 and 19. DAA performance is quite satisfactory, with DAA_2 doing slightly better than DAA_1. The situation is somewhat different at $\theta = 0$, as seen in Figures 20 and 21. In Figure 20, which shows external-surface pressure histories, the DAA humps between $t = 1$ and $t = 2$ are too high, and the rise times immediately after $t = 2$ are too long relative to their exact-history counterparts. Even so, the DAA_2 history captures the physics rather well, exhibiting accurate peak values and correct late-time oscillation. In Figure 21, which shows internal-surface pressure histories, the DAA histories cannot manage the deep negative excursion of the exact history during $0.75 < t < 2$ and the abrupt rise at $t \approx 2$. DAA_2 performs better than DAA_1, producing a deeper negative excursion and producing correct late-time oscillation.

Exact and DAA shell-velocity histories are shown in Figure 22 through 24. DAA_2 clearly outperforms DAA_1, the latter producing histories in Figure 22 and 24 that deviate substantially from the exact histories at late time; this derives from DAA_1's tendency to introduce too much acoustic damping (Geers, 1978). DAA_2 fails to reproduce the brief oscillation during $2 < t < 4$ in Figure 22 and 23, and to rise rapidly enough at $t \approx 2$ in Figure 24; generally, however, it does quite well, producing good general response with accurate peaks and correct late-time oscillation.

SECTION 9
FIRST ORDER DAA FOR ELASTIC MEDIA

This section contains formulations of first–order doubly asymptotic approximations for infinite and semi-infinite, homogenous, elastic media. The formulation for the infinite domain is a generalization of the matrix form given in Underwood and Geers, 1981, and then implemented and evaluated by Mathews and Geers, 1987. Here, the method of operator matching is used as in Sections 2 through 5 for an acoustic fluid.

First, we write down the dynamic extension of Somigliana's identity. Next, we present the first–order early–time approximation for infinite and semi–infinite domains. Then we develop the first–order late–time approximation for the infinite domain, which is followed by a similar development for the semi–infinite domain. Finally, we formulate first–order DAAs for infinite and semi-infinite domains by operator matching.

The section concludes with a transformation of the DAAs from operator form into matrix form, and the application of the matrix forms to some canonical problems. Numerical results are compared with corresponding "exact" results in the literature.

9.1 DYNAMIC SOMIGLIANA IDENTITY.

With the displacement vector $\vec{u}(x,y,z,t)$ expressed through a Helmholtz decomposition in terms of a scalar potential $\phi(x,y,z,t)$ and a vector potential $\vec{\psi}$(x,y,z,t) as (see, *e.g.*, Achenbach, 1973)

$$\vec{u} = \nabla\phi + \nabla \times \vec{\psi}, \qquad \nabla \cdot \vec{\psi} = 0, \tag{9.1}$$

the wave equations for a uniform elastic medium are

$$\begin{aligned} c_D^2 \nabla^2 \phi &= \ddot{\phi}, \\ c_S^2 \nabla^2 \vec{\psi} &= \ddot{\vec{\psi}} \end{aligned} \tag{9.2}$$

where c_D and c_S are the dilatational– and shear– wave speeds, respectively, given by

$$c_D^2 = \frac{\lambda + 2\mu}{\rho}, \qquad c_S^2 = \frac{\mu}{\rho}. \tag{9.3}$$

An exact integral-equation solution to (9.1) and (9.3) for the displacement field on the smooth surface or surfaces of the elastic medium is provided by a extension of Somigliana's identity, which may be written in Laplace-transform space as (Cruze & Rizzo, 1968)

$$\vec{u}_P(s) + \int_S \vec{u}_Q(s)\tilde{T}_{PQ}(s)dS_Q = \int_S \vec{t}_Q(s)\tilde{U}_{PQ}(s)dS_Q \tag{9.4}$$

In this equation, P and Q denote points on the surface S, $\vec{u}_P$ and $\vec{t}_P$ are surface displacement and traction vectors, respectively, and $\tilde{T}_{PQ}(s)$ and $\tilde{U}_{PQ(s)}$ are second-order tensor operators with components

$$\begin{aligned} U_{ij}(s) &= \frac{1}{4\pi\mu}(\psi\delta_{ij} - \chi R_{,i}R_{,j}) \\ T_{ij}(s) &= \frac{1}{4\pi}[(\frac{d\psi}{dR} - \frac{1}{R}\chi)(\delta_{ij}\frac{\partial R}{\partial n}R_{,j}n_i) \\ &\quad -\frac{2}{R}\chi(n_jR_{,i} - 2R_{,i}R_{,j}\frac{\partial R}{\partial n}) - 2\frac{d\chi}{dR}R_{,i}R_{,j}\frac{\partial R}{\partial n} \\ &\quad +(\frac{c_D^2}{c_T^2} - 2)(\frac{d\psi}{dR} - \frac{d\chi}{dR} - \frac{2}{R}\chi)R_{,i}n_j] \end{aligned} \tag{9.5}$$

where the usual Cartesian tensor notation applies, where the PQ subscript for R_{PQ}, defined after (2.3), has been omitted for notational simplicity, and where $\psi(R,s)$ and $\chi(R,s)$ are defined for three dimensions as:

$$\begin{aligned} \psi(R,s) &= (1 + \frac{c_S}{sR} + \frac{c_S^2}{s^2R^2})\frac{e^{-sR/c_S}}{R} - \frac{c_S^2}{c_D^2}(\frac{c_D}{sR} + \frac{c_D^2}{s^2R^2})\frac{e^{-sR/c_D}}{R} \\ \chi(R,s) &= (1 + \frac{3c_S}{sR} + \frac{3c_S^2}{s^2R^2})\frac{e^{-sR/c_S}}{R} - \frac{c_S^2}{c_D^2}(1 + \frac{3c_D}{sR} + \frac{3c_D^2}{s^2R^2})\frac{e^{-sR/c_D}}{R} \end{aligned} \tag{9.6}$$

9.2 FIRST-ORDER EARLY-TIME APPROXIMATION: ETA_1.

The first-order ETA for an elastic medium is a vector extension of that for an acoustic medium [see (2.5)]. It is given in transform space for an infinite domain by (Underwood and Geers, 1981)

$$ETA_1: \qquad \vec{t}_P(s) = \rho\tilde{C}s\vec{u}_P(s) \tag{9.7}$$

where $\tilde{C}$ is a second-order tensor that involves the dilatational- and shear-wave speeds defined in (9.3). For a semi-infinite domain, (9.7) also applies if the DAA boundary is somewhat removed from the flat traction-free surface of the semi-infinite domain, or if it intersects the flat surface at angles equal to or exceeding 90°; we restrict ourselves to such situations.

ETA_1 is a *local approximation* , stating that each element of the surface S independently generates three plane waves, one dilatational and two shear, which propagate normally outward into the elastic medium. Because it approaches exactness only as $s \rightarrow \infty$, it is singly asymptotic.

9.3 FIRST-ORDER LATE-TIME APPROXIMATION FOR A WHOLE-SPACE: LTA_1^W.

Here, we apply to (9.4) the procedure described in Section 2.3, keeping terms through s^0 throughout. This yields the standard Somigliana identity.

$$\vec{u}_P + \int_S \vec{u}_Q \tilde{T}_{PQ}(0) dS_Q = \int_S \vec{t}_Q \tilde{U}_{PQ}(0) dS_Q, \tag{9.8}$$

where the tensor components are given by [*c.f.* (9.4) and (9.6)]

$$U_{ij}(0) = \frac{1}{4\pi\mu(1-\nu)R}[(3-4\nu)\delta_{ij}R_{,i}R_{,j}]$$

$$T_{ij}(0) = \frac{1}{8\pi(1-\nu)R^2}\left\{\frac{dR}{dn}[(1-2\nu)\delta_{ij}+3R_{,i}R_{,j}]-(1-2\nu)(R_{,i}n_j-R_{,j}n_i)\right\} \tag{9.9}$$

The static relation (9.8) is based on the Green's function for an infinite elastic medium obtained by Kelvin in 1848. With the spatial-operator definitions

$$\tilde{B}\vec{q}_Q = \int_S \vec{q}_Q \tilde{U}_{PQ} dS_Q$$

$$\tilde{G}\vec{q}_Q = \int_S \vec{q}_Q[\delta(P-Q)+\tilde{T}_{PQ}]dS_Q \tag{9.10}$$

where $\delta(P-Q)$ is the Dirac delta-function, (9.8) may be expressed in the form

$$LTA_1^W: \qquad \vec{t}_Q = \tilde{B}^{-1}\tilde{G}\vec{u}_P \tag{9.11}$$

LTA_1^W is a *non-local, singly asymptotic, quasi-static* approximation.

9.4 FIRST-ORDER LATE-TIME APPROXIMATION FOR A HALF-SPACE: LTA_1^H.

The first–order LTA for a semi-infinite space is also a quasi–static approximation expressed by (9.8), but with $\tilde{T}_{PQ}$ and $\tilde{U}_{PQ}$ given by expressions corresponding to the half–space Green's function of Mindlin, 1936, rather than that of Kelvin. These expressions are constructed by augmenting (9.9) with additional terms (Brebbia,1984). For $\tilde{U}$, the augmentation is

$$\tilde{U}^H_{PQ} = \tilde{U}_{PQ} + \tilde{U}^*_{PQ} \tag{9.12}$$

in which the components of $\tilde{U}^*_{PQ}$ are;

$$\begin{aligned}
U^*_{11} &= K_d\left[8(1-\nu)^2-(3-4\nu)+\frac{(3-4\nu)r_1^2-2c\bar{x}}{R'^2}+\frac{6c\bar{x}r_1'^2}{R'^4}\right]\\
U^*_{12} &= K_d r_2\left[\frac{(3-4\nu)r_1}{R'^2}-\frac{4(1-\nu)(1-2\nu)}{R'+r_1'}+\frac{6c\bar{x}r_1'}{R'^4}\right]\\
U^*_{21} &= K_d r_2\left[\frac{(3-4\nu)r_1}{R'^2}+\frac{4(1-\nu)(1-2\nu)}{R'+r_1'}-\frac{6c\bar{x}r_1'}{R'^4}\right]\\
U^*_{22} &= K_d\left[1+\frac{(3-4\nu)r_2'^2}{R'^2}+\frac{2c\bar{x}}{R'^2}\left(\frac{1-3r_2'^2}{R'^2}\right)\right.\\
&\qquad\left.+\frac{4r(1-\nu)(1-2\nu)}{R'+r_1'}\left(1-\frac{r_2'^2}{R'(R'+r_1')}\right)\right]\\
U^*_{23} &= K_d r_2 r_3\left[\frac{(3-4\nu)}{R'^2}-\frac{4(1-\nu)(1-2\nu)}{R'(R'+r_1')^2}-\frac{6c\bar{x}}{R'^4}\right]\\
U^*_{13} &= \frac{r_3 U^*_{12}}{r_2}\\
U^*_{31} &= \frac{r_3 U^*_{21}}{r_2}\\
U^*_{32} &= U^*_{23}\\
U^*_{33} &= K_d\left[1+\frac{(3-4\nu)r_3'^2}{R'^2}+\frac{2c\bar{x}}{R'^2}\left(1-\frac{3r_3'^2}{R'^2}\right)\right.\\
&\qquad\left.+\frac{4r(1-\nu)(1-2\nu)}{R'+r_1'}\left(1-\frac{r_3'^2}{R'(R'+r_1')}\right)\right]
\end{aligned} \tag{9.13}$$

where (see Figure 25)

$$
\begin{aligned}
r_i &= x_i(P) - x_i(Q) \\
R &= (r_i r_i)^{\frac{1}{2}} \\
r_i' &= x_i(P) - x_i(Q') \\
R' &= (r_i' r_i')^{\frac{1}{2}} \\
\bar{x} &= x_1(P) \\
c &= x_1(Q) \\
K_d &= \frac{1}{16\pi(1-\nu)\mu R'}
\end{aligned}
\tag{9.14}
$$

$\tilde{T}$ is augmented as

$$
\tilde{T}^H_{PQ} = \tilde{T}_{PQ} + \tilde{T}^*_{PQ} \tag{9.15}
$$

in which the components of $\tilde{T}^*_{PQ}$ are given by

$$
T^*_{ij} = \sigma^*_{jki} n_k \tag{9.16}
$$

where n_k is the surface normal (defined as positive going *into* the medium), and where the components of σ^* are, with $K_t = \frac{1}{8\pi(1-\nu)}$,

$$
\sigma^*_{111} = \frac{K_t}{R'^3}\left[1 - 2\nu r_1 - \frac{3(3-4\nu)\bar{x}r_1'^2 - 3cr_1'(5\bar{x}-c)}{R'^2} - \frac{30c\bar{x}r_1'r_1'^2}{R'^4}\right]
$$

$$
\sigma^*_{121} = \frac{K_t r_2}{R'^3}\left[1 - 2\nu - \frac{3(3-4\nu)\bar{x}r_1' - 9c\bar{x} - 3c^2}{R'^2} - \frac{30c\bar{x}r_1'^2}{R'^4}\right]
$$

$$
\sigma^*_{131} = \frac{K_t r_3}{R'^3}\left[1 - 2\nu - \frac{3(3-4\nu)\bar{x}r_1' - 9c\bar{x} - 3c^2}{R'^2} - \frac{30c\bar{x}r_1'^2}{R'^4}\right]
$$

$$
\begin{aligned}
\sigma^*_{221} = \frac{K_t}{R'^3}\Bigg[&(1-2\nu)\frac{(3r_1 - 4\nu r_1') - 3(3-4\nu)r_1 r_2'^2}{R'^2} \\
&+ 6cr_1'\frac{(1-2\nu\bar{x}-2\nu c)}{R'^2} - \frac{30c\bar{x}r_2'^2 r_1'}{R'^4} - \frac{4R'^2(1-\nu)(1-2\nu)}{R'+r_1'}\left(1 - \frac{r_2'^2}{R'(R'+r_1')} - \frac{r_2'^2}{R'^2}\right)\Bigg]
\end{aligned}
$$

$$
\sigma^*_{231} = \frac{K_t r_2 r_3}{R'^2}\left[-\frac{3(3-4\nu)r_1}{R'^3} + \frac{4(1-\nu)(1-2\nu)}{R'+r_1'}\left(\frac{1}{R'+r_1'} + \frac{1}{R'}\right) - \frac{30c\bar{x}r_1'}{R'^5}\right]
$$

$$\sigma^*_{331} = \frac{K_t}{R'^3}\left[(1-2\nu)(3r_1-4\nu r'_1) - \frac{3(3-4\nu)r_1 r'^2_3}{R'^2} - \frac{6cr'_1[(1-2\nu)\bar{x}-2\nu c]}{R'^2}\right.$$
$$\left. - \frac{30c\bar{x}r'^2_3 r'_1}{R'^4} - \frac{4R'^2(1-\nu)(1-2\nu)}{R'+r'_1}\left(1-\frac{r'^2_3}{R'(R'+r'_1)}-\frac{r'^2_3}{R'^2}\right)\right]$$

$$\sigma^*_{112} = \frac{K_t r_2}{R'^3}\left[-(1-2\nu)-\frac{3(3-4\nu)r'^2_1}{R'^2}+\frac{6c}{R'^2}\left(c+(1-2\nu)r'_1+\frac{5\bar{x}r'^2_1}{R'^2}\right)\right] \qquad (9.17)$$

$$\sigma^*_{122} = \frac{K_t}{R'^3}\left[(1-2\nu)r_1-\frac{3(3-4\nu)r'^2_2 r'_1}{R'^2}-\frac{6c}{R'^2}\left(\bar{x}r'_1-(1-2\nu)r'^2_2-\frac{5\bar{x}r'^2_2 r'_1}{R'^2}\right)\right]$$

$$\sigma^*_{132} = \frac{K_t r_2 r_3}{R'^5}\left[-3(3-4\nu)r'_1+6c\left(1-2\nu+\frac{5\bar{x}r'_1}{R'^2}\right)\right]$$

$$\sigma^*_{222} = \frac{K_t r_2}{R'^3}\left[(1-2\nu)(5-4\nu)-\frac{3(3-4\nu)r'^2_2}{R'^2}-\frac{4R'^2(1-\nu)(1-2\nu)}{(R'+r'_1)^2}\left(3-\frac{r'^2_2(3r+r'_1)}{R'^2(R'+r'_1)}\right)\right.$$
$$\left. + \frac{6c}{R'^2}\left(3c-3-2\nu r'_1+\frac{5\bar{x}}{R'^2}r'^2_2\right)\right]$$

$$\sigma^*_{232} = \frac{K_t r_3}{R'^3}\left[1-2\nu-\frac{3(3-4\nu)r'^2_2}{R'^2}-\frac{4R'^2(1-\nu)(1-2\nu)}{(R'+r'_1)^2}\left(1-\frac{r'^2_2(3r+r'_1)}{R'^2(R'+r'_1)}\right)\right.$$
$$\left. - \frac{6c\bar{x}}{R'^2}\left(1-\frac{5r'^2_2}{R'^2}\right)\right]$$

$$\sigma^*_{332} = \frac{K_t r_2}{R'^3}\left[(1-2\nu)(3-4\nu)-\frac{3(3-4\nu)r'^2_3}{R'^2}-\frac{4R'^2(1-\nu)(1-2\nu)}{(R'+r'_1)^2}\left(1-\frac{r'^2_3(3r+r'_1)}{R'^2(R'+r'_1)}\right)\right.$$
$$\left. + \frac{6c}{R'^2}\left(c-(1-2\nu)r'_1+\frac{5\bar{x}}{R'^2}r'^2_3\right)\right]$$

$$\sigma^*_{113} = \sigma^*_{112}\frac{r_3}{r_2}$$

$$\sigma^*_{123} = \sigma^*_{132}$$

$$\sigma^*_{133} = \frac{K_t}{R'^3}\left[(1-2\nu)r_1-\frac{3(3-4\nu)r'^2_3 r'_1}{R'^2}-\frac{6c}{R'^2}\left(\bar{x}r'_1-(1-2\nu)r'^2_3-\frac{5\bar{x}r'^2_3 r'_1}{R'^2}\right)\right]$$

$$\sigma^*_{223} = \frac{K_t r_3}{R'^3}\left[(1-2\nu)(3-4\nu)-\frac{3(3-4\nu)r'^2_2}{R'^2}-\frac{4R'^2(1-\nu)(1-2\nu)}{(R'+r'_1)^2}\left(1-\frac{r'^2_2(3r+r'_1)}{R'^2(R'+r'_1)}\right)\right.$$
$$\left. + \frac{6c}{R'^2}\left(c-(1-2\nu)r'_1+\frac{5\bar{x}}{R'^2}r'^2_2\right)\right]$$

$$\sigma^*_{233} = \frac{K_t r_2}{R'^3}\left[1-2\nu-\frac{3(3-4\nu)r'^2_3}{R'^2}-\frac{4R'^2(1-\nu)(1-2\nu)}{(R'+r'_1)^2}\left(1-\frac{r'^2_3(3r+r'_1)}{R'^2(R'+r'_1)}\right)-\frac{6c\bar{x}}{R'^2}\left(1-\frac{5r'^2_3}{R'^2}\right)\right]$$

$$\sigma^*_{333} = \frac{K_t r_3}{R'^3}\left[(1-2\nu)(5-4\nu) - \frac{3(3-4\nu)r_3'^2}{R'^2} - \frac{4R'^2(1-\nu)(1-2\nu)}{(R'+r_1')^2}\left(3 - \frac{r_3'^2(3r+r_1')}{R'^2(R'+r_1')}\right)\right.$$
$$\left. + \frac{6c}{R'^2}\left(3c - (3-2\nu)r_1' + \frac{5\bar{x}}{R'^2}r_3'^2\right)\right].$$

In operator notation, LTA_1 for the semi-infinite domain appears the same as that for the infinite domain, given by (9.11).

9.5 FIRST-ORDER DOUBLY ASYMPTOTIC APPROXIMATIONS FOR WHOLE- AND HALF-SPACES: DAA_1.

Because the only differences between the first-order early- and late-time approximations for infinite and semi-infinite domains reside in the operators $\tilde{T}_{PQ}$ and $\tilde{U}_{PQ}$, we can formally develop first-order DAA's for the two domains simultaneously. We will use the method of operator matching for this purpose. The appropriate trial equation is

$$[s\tilde{P}_1 + \tilde{P}_0]\vec{u}_P(s) = \vec{t}_Q(s) \tag{9.18}$$

where the spatial operators $\tilde{P}_0$ and $\tilde{P}_1$ are not functions of s.

For s$\rightarrow$ 0 we write (9.18) as

$$[\tilde{P}_0 + 0(s)]\vec{u}_P(s) = \vec{t}_Q(s) \tag{9.19}$$

and match with (9.11) as s$\rightarrow$ 0, which yields $\tilde{P}_0 = \tilde{B}^{-1}\tilde{G}$. This the asymptotic match for the static limit. For s$\rightarrow \infty$ we divide (9.18) through by s to get

$$[\tilde{P}_1 + 0(s^{-1})]\vec{u}_P(s) = s^{-1}\vec{t}_Q(s) \tag{9.20}$$

Now we match with (9.7) as s$\rightarrow \infty$ to give $\tilde{P}_1 = \rho\tilde{C}$. Introducing these results into (9.18), we obtain, in transform space,

$$DAA_1(s): \qquad \vec{t}_Q(s) = \left[\rho\tilde{C}s + \tilde{B}^{-1}\tilde{G}\right]\vec{u}_P(s) \tag{9.21}$$

and in the time domain

$$DAA_1(t): \qquad \vec{t}_Q(t) = \rho\tilde{C}\ddot{\vec{u}}_P(t) + \tilde{B}^{-1}\tilde{G}\vec{u}_P(t) \tag{9.22}$$

Note that the DAA_1 for elastic domains is not spatially local, because of the late-time approximation term.

9.6 MATRIX DAA_1 FOR BOUNDARY ELEMENT ANALYSIS.

The most direct way to obtain the matrix DAA_1 for either whole- or half-spaces is to discretize the singly asymptotic approximations (9.7) and (9.11) and then employ the method of matrix matching. Thus, we preoperate (9.11) through by $\tilde{B}$ and introduce into the resulting equation and into (9.7) the finite element approximations

$$\begin{aligned} \vec{t}_Q(t) &= \mathbf{v}_Q^T \mathbf{t}(t) \\ \vec{u}_Q(t) &= \mathbf{v}_Q^T \mathbf{u}(t), \end{aligned} \tag{9.23}$$

Then, with a column vector of weight-functions $\mathbf{w}_P$ we form the weighted-residual equations

$$\mathbf{LTA_1}(t): \qquad \mathbf{Bt}(t) = \mathbf{Gu}(t) \tag{9.24}$$

$$\mathbf{ETA_1}(t): \qquad \mathbf{t}(t) = \rho \mathbf{C} \ddot{\mathbf{u}}(t)$$

in which

$$\begin{aligned} \mathbf{B} &= \int_S \mathbf{w}_p \tilde{B} \mathbf{v}_Q^T dS_P \\ \mathbf{G} &= \int_S \mathbf{w}_p \tilde{G} \mathbf{v}_Q^T dS_P \\ \mathbf{C} &= \int_S \mathbf{w}_p \tilde{C} \mathbf{v}_Q^T dS_P \end{aligned} \tag{9.25}$$

If we now follow in a matrix context the operator - based matching procedure carried out in the previous section, we obtain the matrix DAA_1 in an elastic whole- or half-space

$$\mathbf{DAA_1}(t): \qquad \mathbf{t}(t) = \rho \mathbf{C} \dot{\mathbf{u}}(t) + \mathbf{B}^{-1} \mathbf{G} \mathbf{u}(t). \tag{9.26}$$

9.7 CANONICAL PROBLEMS.

It is useful to compare DAA based and "exact" results for canonical problems, as done previously by Underwood and Geers, 1981, and by Mathews and Geers, 1987. Here we consider two canonical problems, both pertaining to a spherical cavity subjected to sudden internal pressurization.

The first problem is a *spherical cavity embedded in an infinite elastic medium and excited by an internal step pressure.* This problem possesses radial symmetry, and has a well-known analytical solution (Timoshenko & Goodier 1970). With a as the cavity radius and P_0 as the pressure magnitude, the radial displacement of the cavity is given by

$$\begin{aligned} u(t) &= -\frac{P_0 a}{4\mu}\left\{\alpha e^{-\alpha t}(\cos \alpha s t + \frac{1}{s'}\sin \alpha s' t)\right. \\ &\quad -\alpha e^{-\alpha t}(-\sin \alpha s' t + \cos \alpha s' t) \\ &\quad \left. +1 - e^{-\alpha t}(\cos \alpha s' t + \frac{1}{s'}\sin \alpha s' t)\right\}. \end{aligned} \tag{9.27}$$

where

$$\begin{aligned} \alpha &= \frac{c_D(1-2\nu)}{a(1-\nu)} \\ s' &= \sqrt{\frac{1}{1-2\nu}} \end{aligned} \tag{9.28}$$

The corresponding analytical DAA solution is simply

$$u_{DAA}(t) = \frac{P_0 a}{4\mu}\left(1 - e^{-4\mu t/a\rho C_D}\right). \tag{9.29}$$

In order to generate numerical DAA solutions, a dynamic boundary element program has been built that is based upon the program constructed by Mathews (Mathews and Geers, 1987). The program uses eight node quadratic quadrilaterals for spatial discretization and the trapezoidal rule for time integration. For the present problem, the boundary-element model for the cavity boundary consists of 24 eight node elements over the entire spherical surface. The analytical exact, analytical DAA_1, and numerical DAA_1 solutions are shown in Figure 26 for the parameters $\rho = 1.00$, $\mu = 1/6$, $\nu = 1/4$, $a = 1$, and $P_0 = 1$. The analytical DAA_1 and numerical DAA_1 solutions are seen to be almost identical, and the DAA_1 solutions agree well with the analytical exact solution at both early and late times. As previously observed by Underwood and Geers, 1987, the DAA_1 solutions do not exhibit the response overshoot seen in the exact solution. This is characteristic of solutions to first-order differential equations like (9.26). A second-order DAA is capable of accommodating such overshoot.

The second problem is a *spherical cavity embedded in a semi-infinite elastic medium and excited by an internal step pressure.* This problem does not posses radial symmetry, and

does not posses an analytical solution. However, a boundary–element solution based on numerical inversion of Laplace transforms has been generated (Manolis and Ahmad, 1988), and an analytical solution to the related static problem exists (Bonefed, 1990). In terms of the geometry shown in Figure 27, the latter solution is

$$u_r = P_0 a^3 \left\{ (1-2\nu)\frac{r}{R^{*3}} - \frac{3z(z+d)r}{R^{*5}} + \frac{1}{2}\left[\frac{r}{R'^3} + \frac{r}{R^{*3}} \right] \right\}$$

$$u_z = P_0 a^3 \left\{ 2(1-2\nu)\frac{(z+d)}{R^{*3}} - \frac{z}{R^{*3}} + \frac{3z(z+d)^2}{R^{*5}} + \frac{1}{2}\left[\frac{(z+d)}{R'^3} + \frac{(z+d)}{R^{*3}} \right] \right\} \tag{9.30}$$

where

$$R' = \sqrt{r^2 + (z - z_0)^2}$$

$$R^* = \sqrt{r^2 + (z + z_0)^2}.$$

Numerical DAA_1 and numerical inversion solutions for this problem are shown in Figures 28–30, along with the late–time static asymptotes given by (9.30); the physical parameters specified are the same as those previously used for the infinite–domain problem. Figure 28 pertains to the top of the cavity, *i.e.*, the point on the cavity surface closest to the free surface of the elastic half–space, Figure 29 pertains to a point 90° around, and Figure 30 pertains to the bottom of the cavity. These figures show that the DAA_1 solutions agree with the numerical inversion solutions at early time and appear to approach the correct late–time asymptotes; unfortunately, the numerical inversion solutions do not extend far enough in time to allow a completely satisfactory comparison.

SECTION 10

CONCLUSION

This report documents the formulation and evaluation of new doubly asymptotic approximations for simplifying the analysis of transient medium-structure interaction problems. More specifically,

1. The formulation of first- and second-order DAA's for an external acoustic medium has been systematized; finite-element discretization has been introduced to configure the operator-based formulation for boundary-element solution.

2. First- and second-order DAA's for an internal acoustic medium have been systematically formulated on an operator basis; finite-element discretization has been introduced to configure the formulation for boundary-element solution.

3. The canonical problem of a spherical shell filled with an acoustic fluid, submerged in an acoustic medium, and excited by a plane step-wave has been solved by modal analysis; special techniques have been developed and applied to achieve satisfactory convergence.

4. Extensive numerical results for the canonical problem have been generated for exact, DAA_1 and DAA_2 treatments of the internal and external fluid-structure interactions; the numerical results have been compared to assess DAA accuracy.

5. The formulation of the first-order DAA for an infinite elastic medium has been systematized; finite-element discretization has been implemented to configure the operator-based formulation for boundary-element solution.

6. The first-order DAA for a semi-infinite elastic medium has been systematically formulated

on an operator basis; finite-element discretization has been implemented to configure the formulation for boundary-element solution.

7. Boundary-element DAA results for suddenly pressurized spherical cavities embedded in infinite and semi-infinite elastic media have been generated; the DAA results have been compared with corresponding results by other investigators.

The principal conclusions reached during this study are:

1. First-order DAA's are marginally satisfactory for approximating transient medium-structure interactions involving external and internal acoustic domains and external elastic domains.

2. Second-order DAA's are highly satisfactory for treating external acoustic domains; they are satisfactory for treating internal acoustic domains.

3. The second-order DAA for an internal acoustic medium is sufficiently accurate to warrant early implementation in production codes for underwater shock analysis.

4. Second-order DAA's are needed for treating infinite and semi-infinite elastic media; the techniques used herein to formulate second-order DAA's for an acoustic medium may be applied to an elastic medium as well.

5. Further DAA development is desirable in order to obtain approximations of higher accuracy and broader application.

SECTION 11

LIST OF REFERENCES

1. Apostol, T.M., 1957, "Mathematical Analysis: A Modern Approach to Advanced Calculus", Addison-Wesley Pub. Co..

2. Abramowitz, M. and Stegun, I.A., 1964, "Handbook of Mathematical Functions", NBS Appl. Math. Ser. 55 (U.S. Dept. of Commerce, Washington, DC).

3. Atkash, R., et al., 1987, "Developments for the EPSA Computer Code", DNA-TR-87-155, Defense Nuclear Agency, Washington, DC.

4. Baker, B.B. and Copson, E.T., 1939, "The Mathematical Theory of Huygen's Principle", Clarendon Press, Oxford.

5. Bannerjee, P.K. and Butterfield, R., 1981, "Boundary Element Methods in Enginnering Science", McGraw-Hill Book Company (UK) Limited, London.

6. Bonefed, M., 1990, "Axisymmetric Deformation of a Thermo-poro-elastic Halfspace; Inflation of a Magma Chamber", Geophys. T. Inter, Vol. 103, pp. 289-299.

7. Chertock, G., 1971, "Integral Equation Methods in Sound Radiation and Scattering from Arbitrary Surfaces", Rep. No. 3538, Naval Ship Research and Development Center, Carderock, MD.

8. Cruse, T.A. and Rizzo, F.T., 1968, "A Direct Formulation and Numerical Solution of the General Transient Elastodynamic Problem", Math. Analysis & Appl., Vol. 22, pp. 244-259.

9. DeRuntz, J.A. and Geers, T.L., 1978, "Added Mass Computation by the Boundary Integral Method", Int. J. Numer. Meth. Eng., Vol. 12, pp. 531-549.

10. DeRuntz, J.A., Geers, T.L. and Felippa, C.A., 1980, "The Underwater Shock Analysis Code (USA-Version 3)", DNA 5615F, Defense Nuclear Agency, Washington, DC.

11. DeRuntz, J.A., and Brogan, F.A., 1980, "Underwater Shock Analysis of Nonlinear Structures, A Reference Manual for the USA-STAGS Code (Version 3)", DNA 5545F, Defense Nuclear Agency, Washington, DC.

12. Felippa, C.A., 1980, "A Family of Early-Time Approximations for Fluid Structure Interaction", J. Appl. Mech., Vol. 47, pp. 703-708.

13. Felippa, C.A., 1980a, "Top-down Derivation of Doubly Asymptotic Approximations for Structure-fluid Interaction Analysis", in "Innovative Numerical Analysis for the Engineering Sciences", edited by R.P. Shaw et al., U.P. of Virginia, Charlottesville, pp 79-88.

14. Friedlander, F.G., 1958, "Sound Pulses", Cambridge University Press, Cambridge.

15. Geers, T.L., 1969, "Excitation of an Elastic Cylindrical Shell by a Transient Acoustic Wave", J. Appl. Mech., Vol. 36, pp. 459-469.

16. Geers, T.L., 1971, "Residual Potential and Approximate Methods for Three-dimensional Fluid-structure Interaction Problems", J. Acoust. Soc. Am., Vol. 49, pp. 1505-1510.

17. Geers, T.L., 1972, "Scattering of a Transient Acoustic Wave by an Elastic Cylindrical Shell", J. Acoust. Soc. Am., Vol. 51, pp. 1640-1651.

18. Geers, T.L., 1974, "Shock Response Analysis of Submerged Structures", Shock and Vibration Bulletin, Vol. 44, Supp. 3, pp. 17-32.

19. Geers, T.L., 1975, "Transient Response Analysis of Submerged Structures", in "Finite Element Analysis of Transient Nonlinear Structural Behavior', edited by T. Belytschko and T.L. Geers, AMD-vol. 14, ASME, New York, pp. 59-84.

20. Geers, T.L., 1976, "Submerged Structure Survivability (U)", Proc. AIAA 3rd Joint Strategic Sciences Meeting, San Diego, CA.

21. Geers, T.L., 1978, "Doubly Asymptotic Approximation for Transient Motions of Submerged Structures", J. Acoust. Soc. Am., Vol. 64, pp. 1500-1508.

22. Geers, T.L. and Felippa, C.A., 1983, "Doubly Asymptotic Approximations for Vibration Analysis of Submerged Structures", J. Acoust. Soc. Am., Vol. 73, pp. 1152-1159.

23. Geers, T.L. and Ruzicka, G.C., 1984, "Finite-Element / Boundary-Element Analysis of Multiple Structures Excited by Transient Acoustic Waves", in "Numerical Methods for Transient and Coupled Problems", edited by R.W. Lewis, *et al.* Pineridge Press, Swansea, UK, pp. 150-162.

24. Geers, T.L. and Zhang, P., 1988, "Doubly Asymptotic Approximations for Electromagnetic Scattering Problems", in "Boundary Element Methods in Applied Mechanics", edited by M. Tanaka and T.A. Cruse, Pergamon Press, Oxford, pp. 357-369.

25. Geers, T.L. and Zhang, P., 1989, "Response of a Fluid-filled Spherical Shell in an Infinite Fluid Medium to a Transient Acoustic Wave", presented at the 118th Meeting of Acoust. Soc. Am., St. Louis, Missouri.

26. Geers, T.L., 1990, "Doubly Asymptotic Approximations for a spherical Acoustic Domain", Appendix A to a DNA report submitted in draft form by NKF Engineering, Inc. in November 1990.

27. Huang, H., 1969, "Transient Interaction of Plane Waves with a Spherical Elastic Shell", J. Acoust. Soc. Am., Vol. 45, pp. 661-670.

28. Huang, H. 1979, "Transient Response of Two Fluid-coupled Spherical Elastic Shells to an Incident Pressure Pulse", J. Acoust. Soc. Am., Vol. 65, pp. 881-887.

29. Hughes, T.J.R. and Hinton, E., 1986, "Finite Element Methods for Plate and Shell Structures", Pineridge Press International, Swansea, U.K.

30. Junger, M.C. and Feit, D. 1972, "Sound, Structures, and Their Interaction", (MIT press, Cambridge, MA).

31. Lamb, H.S., 1945, "Hydrodynamics", Dover Publications, New York.

32. Mathews, I.C., and Geers, T.L., 1987, " A Doubly Asymptotic, Non-Reflecting Boundary for Ground-Shock Analysis", J. Appl. Mech., Vol. 54, pp. 489-497.

33. Milne-Thomson, L.M., 1960, "Theoretical Hydrodynamics", Macmillan, New York.

34. Morse, P.M. and Ingard, K.U., 1968, "Theoretical Acoustics", McGraw-Hill, New York.

35. Neilson, H.C. et al., 1981, "Transient Response of a Submerged, Fluid-Coupled, Double-Walled Shell Structure to a Pressure Pulse", J. Acoust. Soc. Am., Vol. 70, pp. 1776-1782.

36. Nicolas-Vullierme, B., 1989, "A Contribution to Doubly Asymptotic Approximations: An Operator Top-down Approach", Numerical Techniques in Acoustic adiation, NCA-Vol.6, ASME, New York, pp. 7-13.

37. Pierce, A.D., 1981, "Acoustics: an Introduction to its Physical Principles and Applications", McGraw-Hill Book Co., New York.

38. Ranlet, D., et al., 1977, "Elastic Response of Submerged Shells with Internally Attached Structures to Shock Loading", Int. J. Computers and Structures, Vol. 7, pp. 355-364.

39. Sobolev, S.L., 1964, "Partial Differential Equations of Mathematical Physics", Pergamon Press, London.

40. Tang, S. and Yen, D., 1970, "Interaction of a Plane Acoustic Wave with an Elastic Spherical Shell", J. Acoust. Soc. Am. 47, pp. 1325-1333.

41. Thomson, S.W., 1848, "Math and Phys. Papers", vol. 1, pp. 97.

42. Timoshenko, S.P. and Goodier, T.N., 1970, "Theory of Elasticity", McGraw-Hill.

43. Underwood, P.G., and Geers, T.L., 1981, "Doubly Asymptotic, Boundary-Element Analysis of Dynamic Soil-Structure Interaction", Int. J. Solids and Structures, Vol. 17, pp. 687-697.

44. Vasudevan, R., and Ranlet, D., 1982, "Submerged Shock Response of a Linear Elastic Shell of Revolution Containing Internal Structure-Users Manual for the ELSHOK Code", DNA-TR-81-184, Defense Nuclear Agency, Washington, DC.

APPENDIX

FIGURES

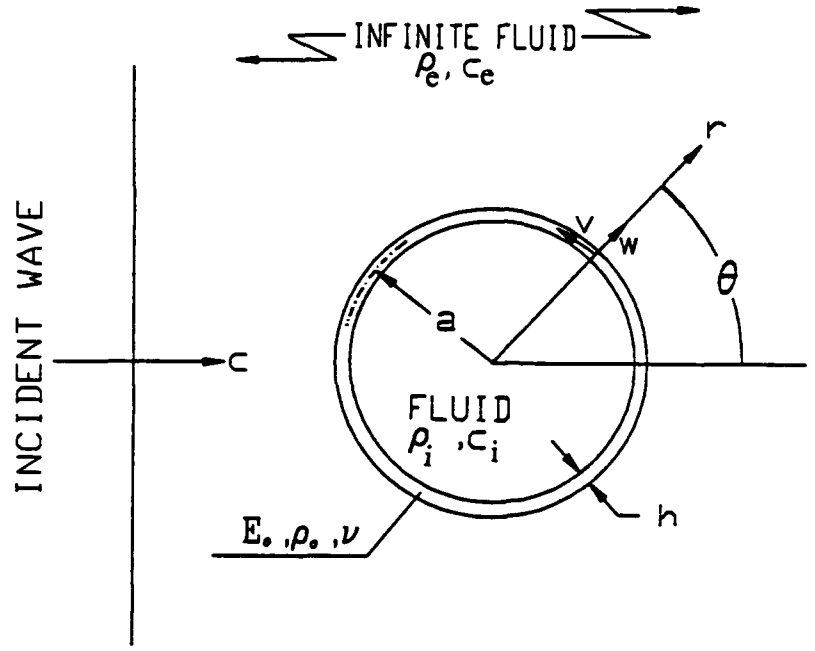

Figure 1. Geometry of the spherical shell problem.

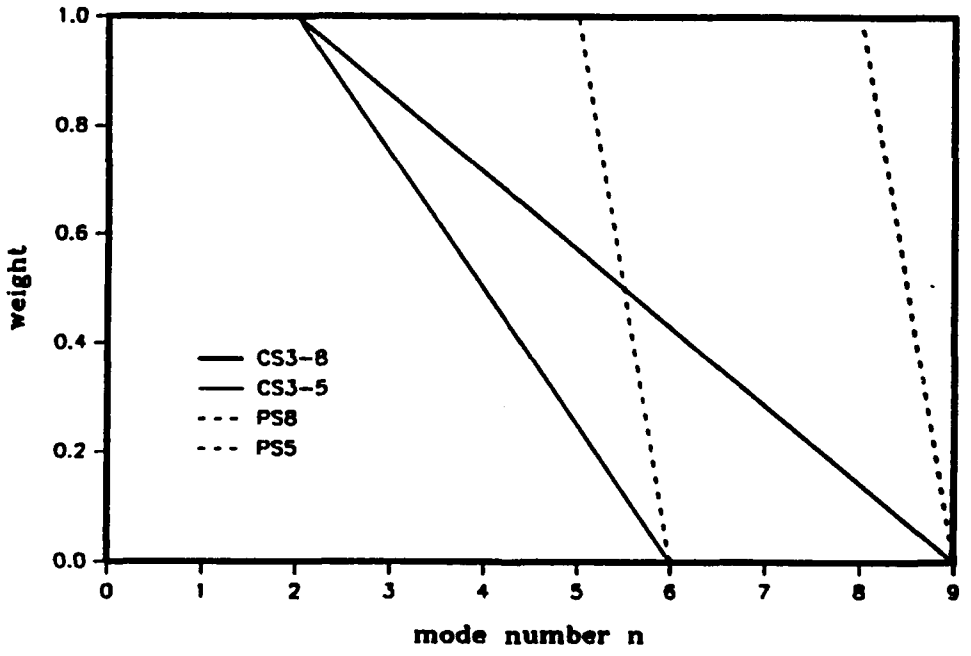

Figure 2. Weighting characteristics of modified Cesàro summation and standard partial summation (CS3-N = Cesàro summation over modes 3 through N; PSN = partial summation over modes 0 through N).

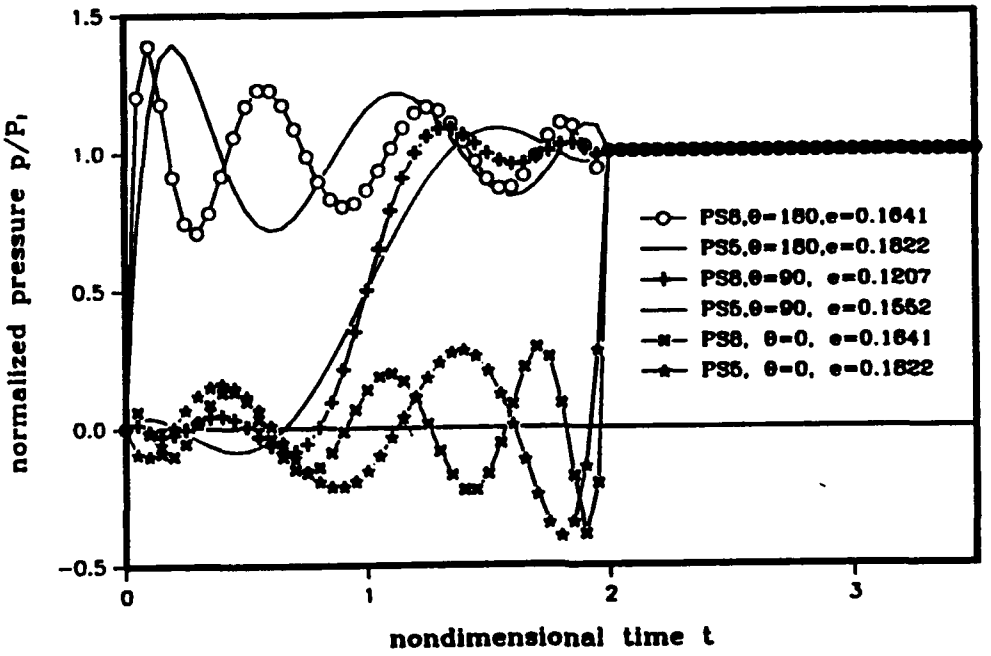

Figure 3. Incident-wave pressure histories produced by standard partial summation (PSN = partial summation over modes 0 through N, e = m-s error over $0 \leq t \leq 2$).

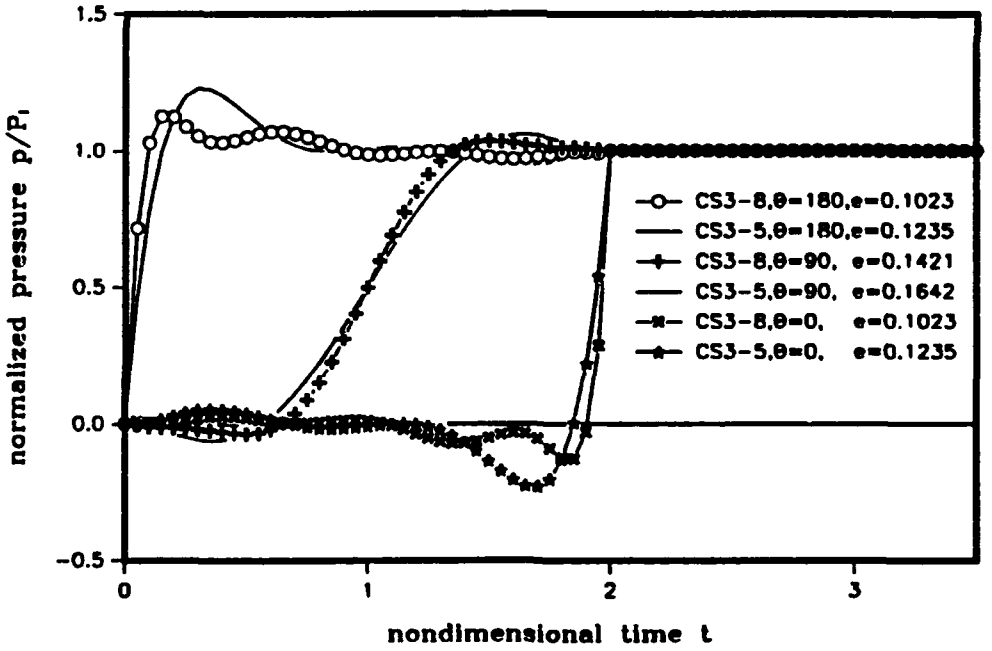

Figure 4. Incident-wave pressure histories produced by modified Cesàro Summation (CS3-N = Cesàro summation over modes 3 through N, e = m-s error over $0 \leq t \leq 2$).

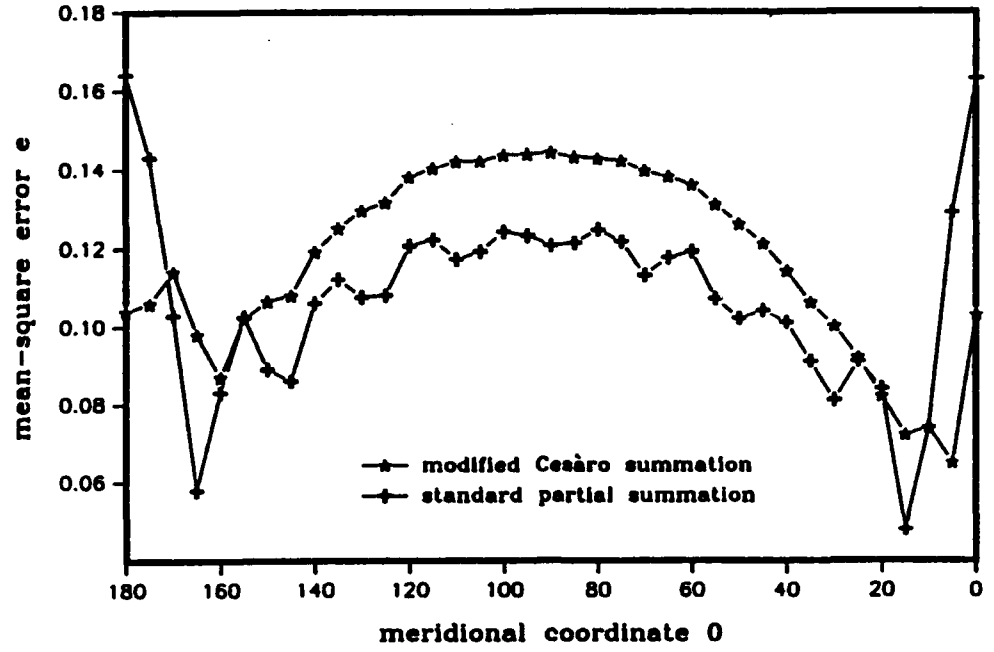

Figure 5. Mean-square error in modal summations for incident pressure histories over $0 \leq t \leq 2$ (N = 8).

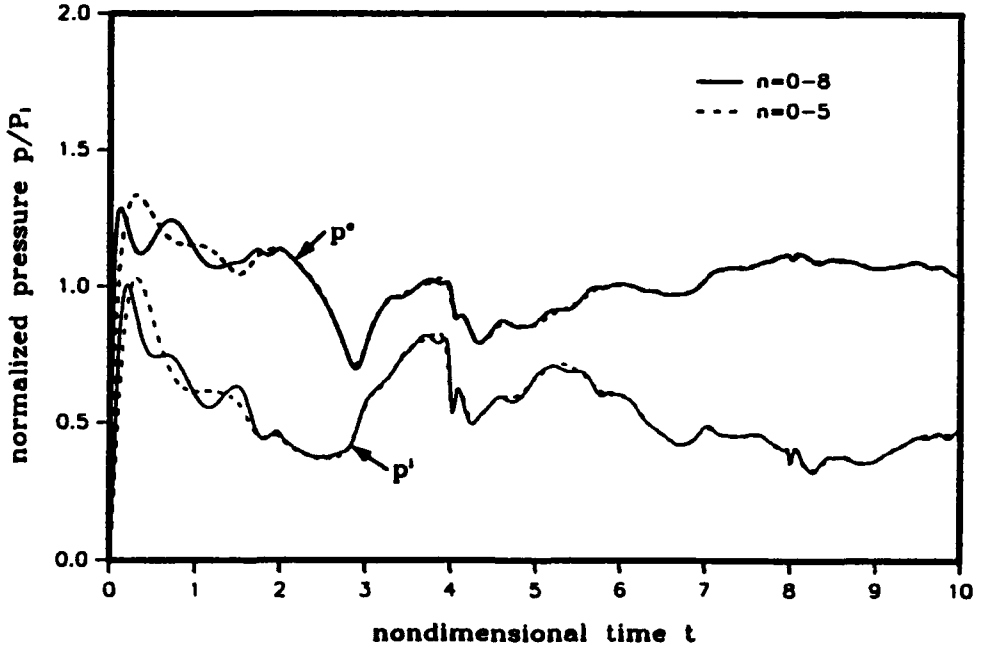

Figure 6. External- and internal-surface pressure histories by modified Cesàro summation (CS) for a steel shell at $\theta = \pi$.

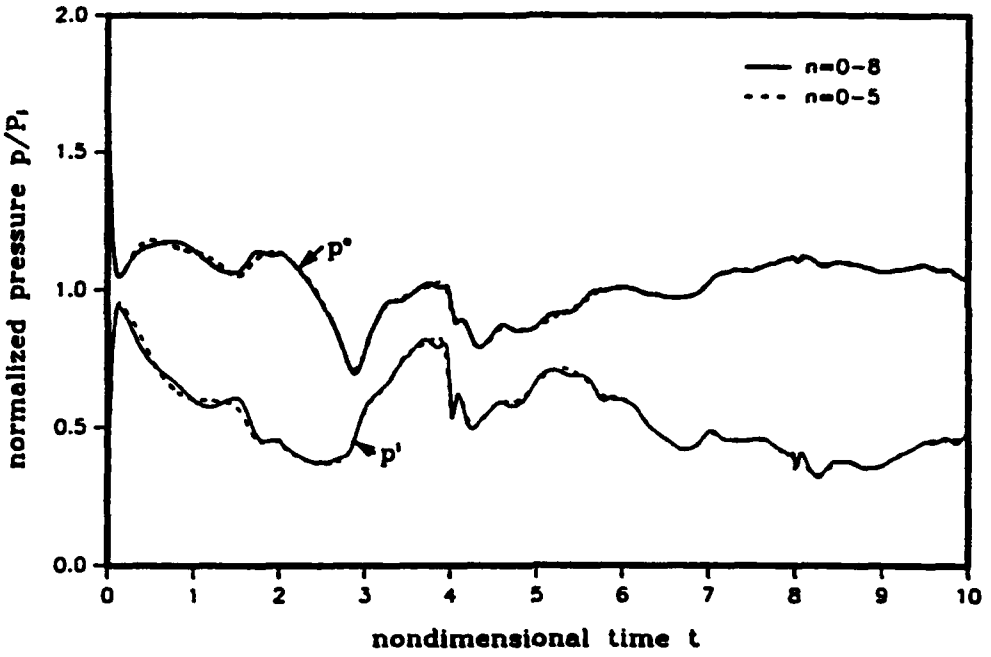

Figure 7. External- and internal-surface pressure histories by modified Cesàro summation (CS) with partial closure (PC) for a steel shell at $\theta = \pi$.

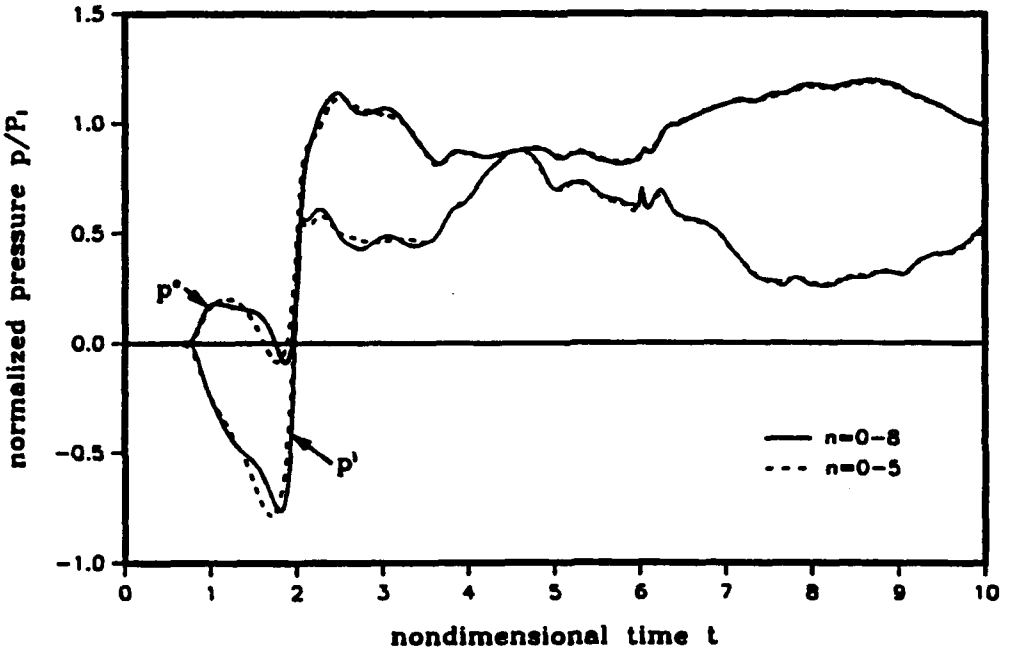

Figure 8. External- and internal-surface pressure histories by CS with PC for a steel shell at $\theta = 0$.

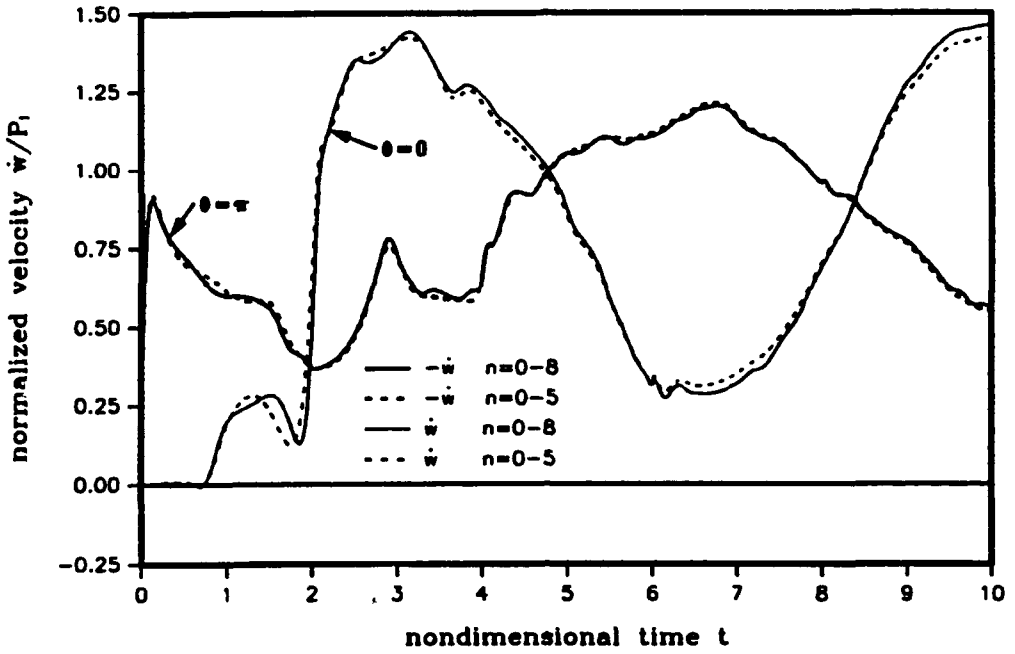

Figure 9. Radial shell-velocity histories by CS with PC for a steel shell at $\theta = \pi$ and $\theta = 0$.

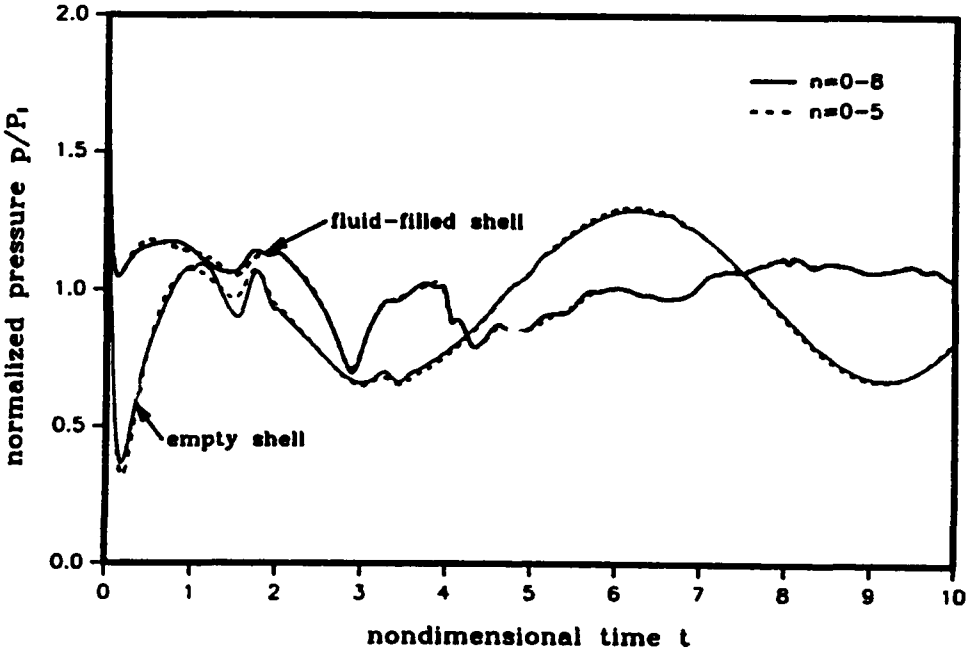

Figure 10. External-surface pressure histories at $\theta = \pi$ for a fluid-filled shell and an empty shell.

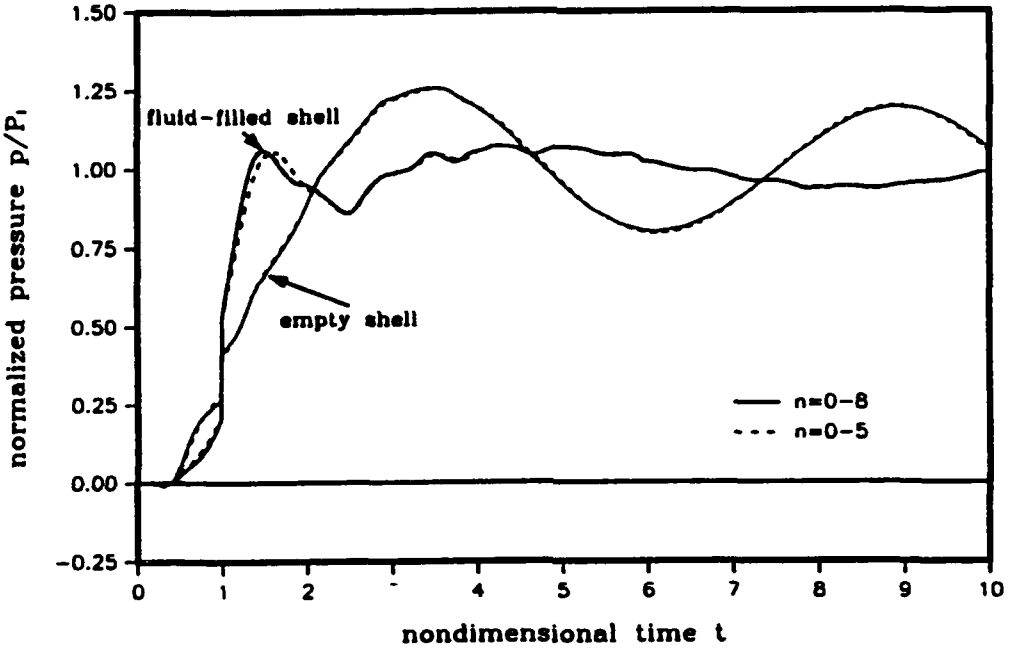

Figure 11. External-surface pressure histories at $\theta = \pi/2$ for a fluid-filled shell and an empty shell.

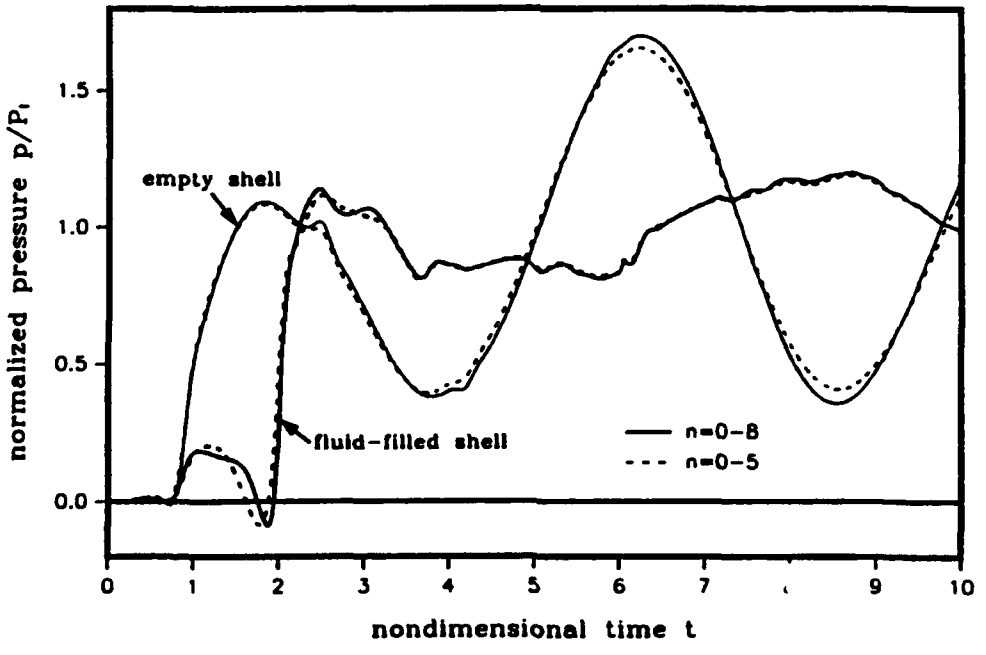

Figure 12. External-surface pressure histories at $\theta = 0$ for a fluid-filled shell and an empty shell.

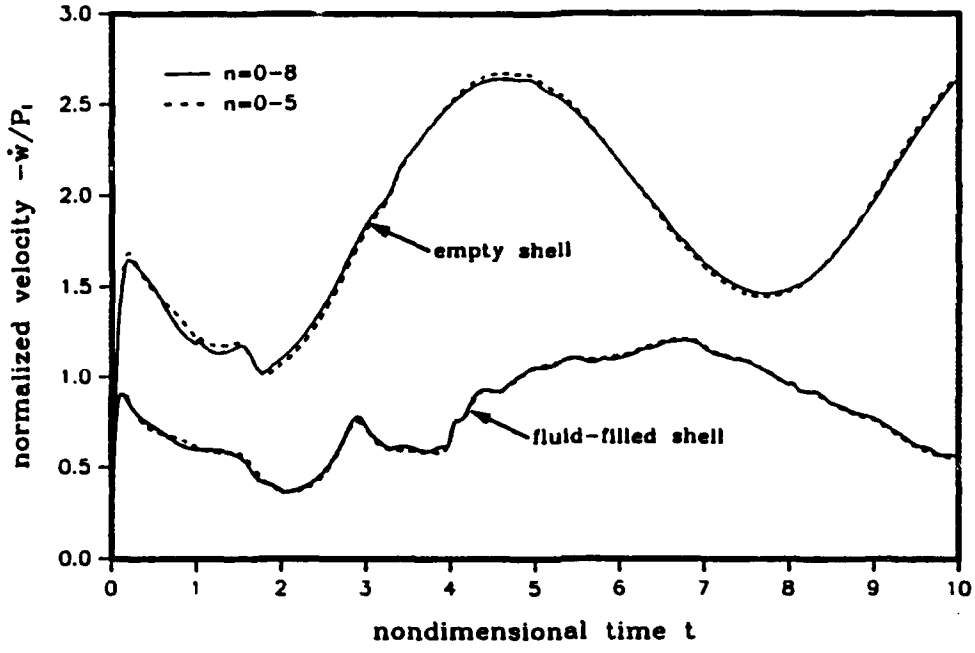

Figure 13. Radial shell-velocity histories at $\theta = \pi$ for a fluid-filled shell and an empty shell.

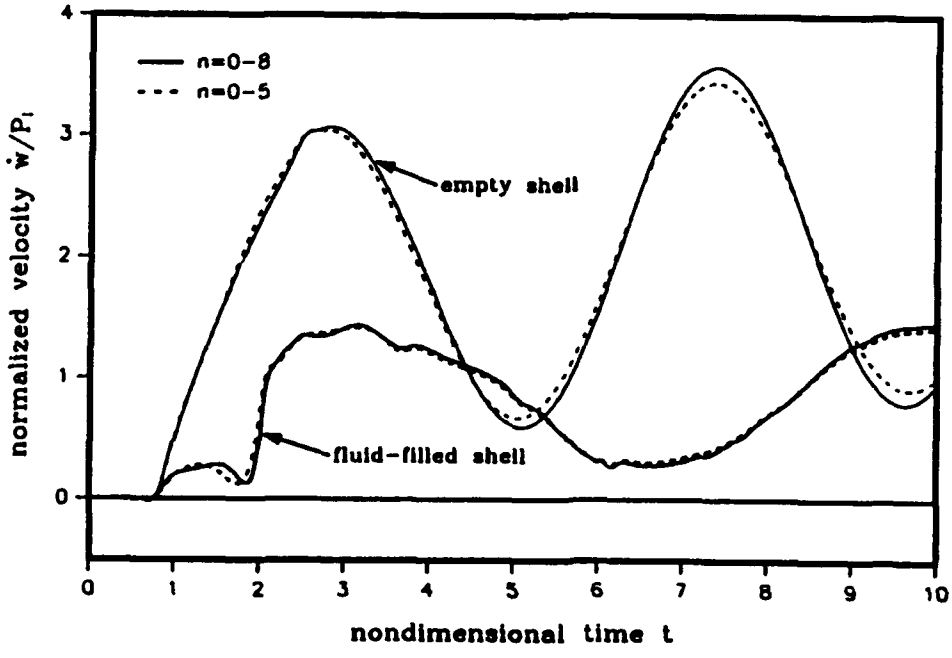

Figure 14. Radial shell-velocity histories at $\theta = 0$ for a fluid-filled shell and an empty shell.

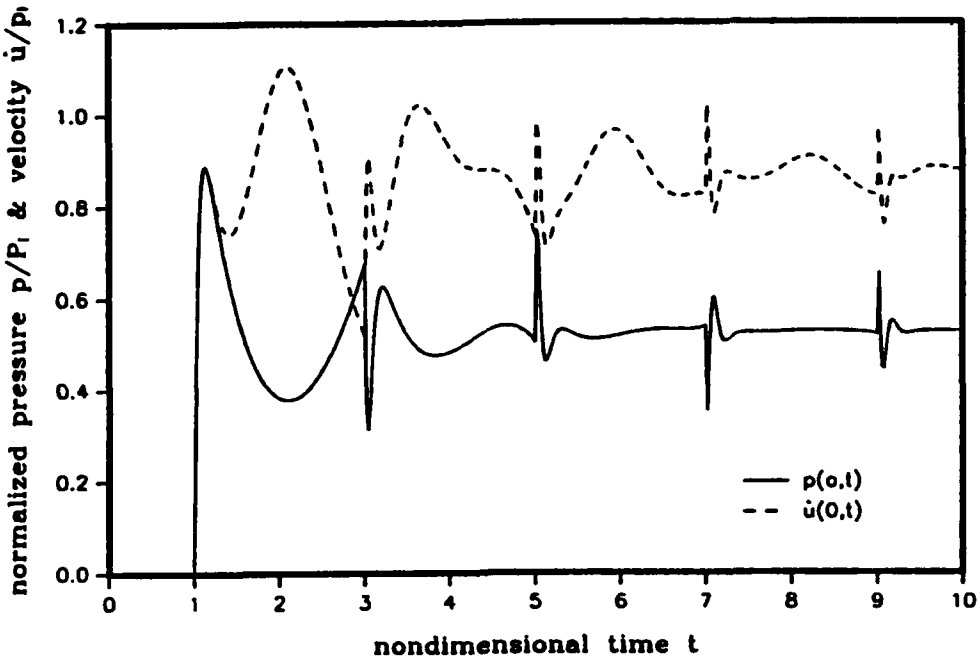

Figure 15. Pressure and fluid-particle-velocity histories at r = 0 inside a steel shell.

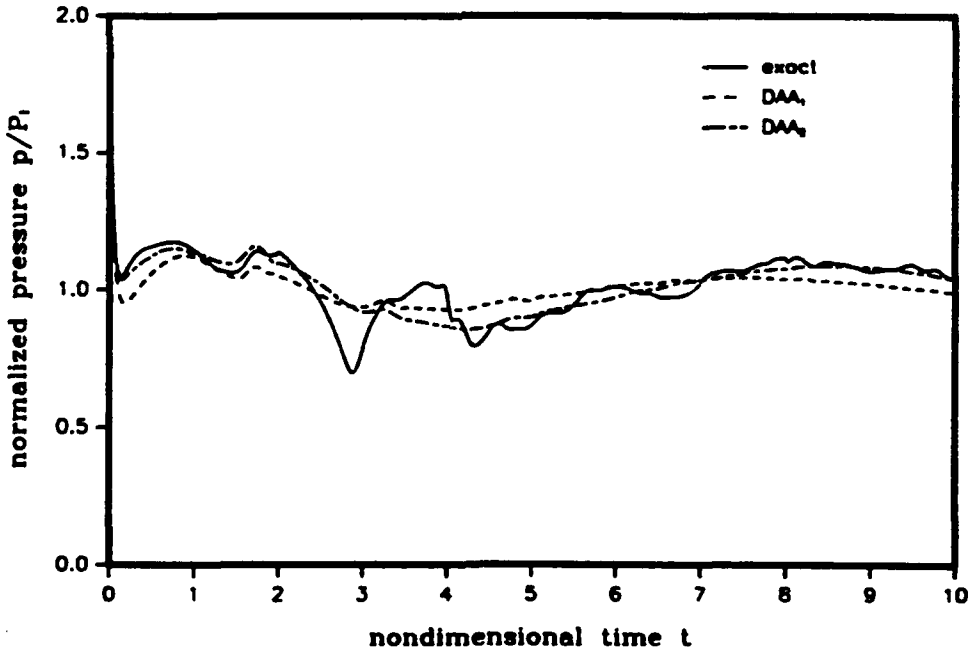

Figure 16. Exact, DAA_1 and DAA_2 external-surface pressure histories at $\theta = \pi$ for a steel shell.

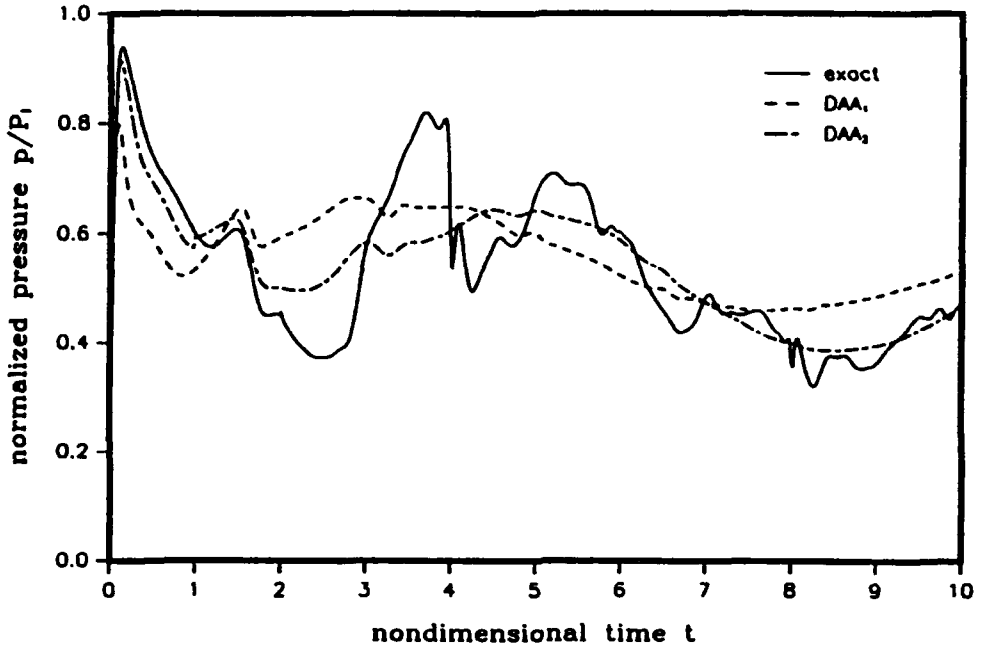

Figure 17. Exact, DAA_1 and DAA_2 internal-surface pressure histories at $\theta = \pi$ for a steel sheel.

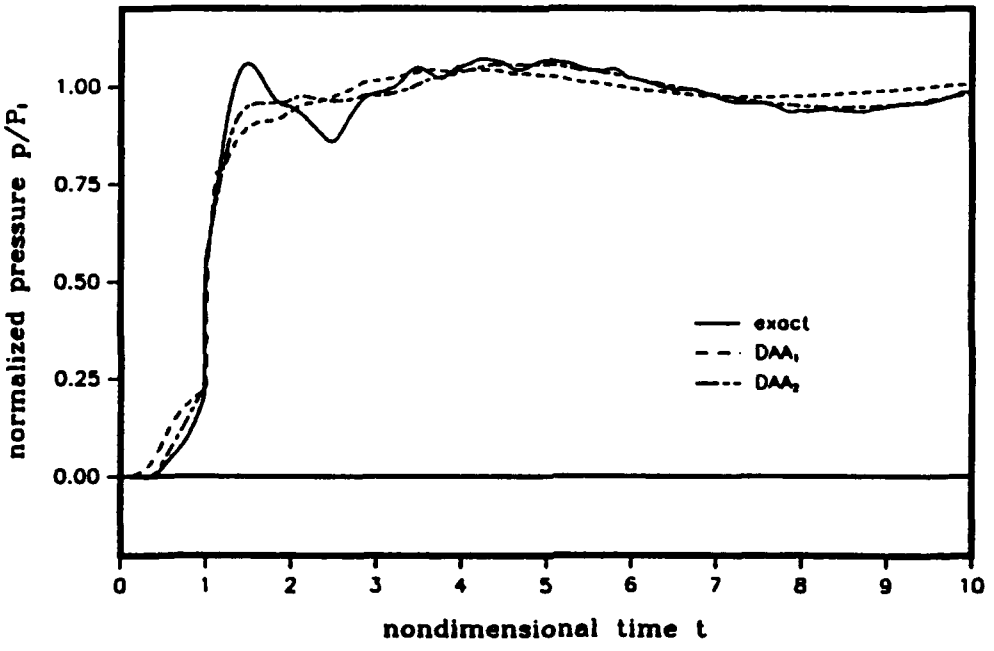

Figure 18. Exact, DAA_1 and DAA_2 external-surface pressure histories at $\theta = \pi/2$.

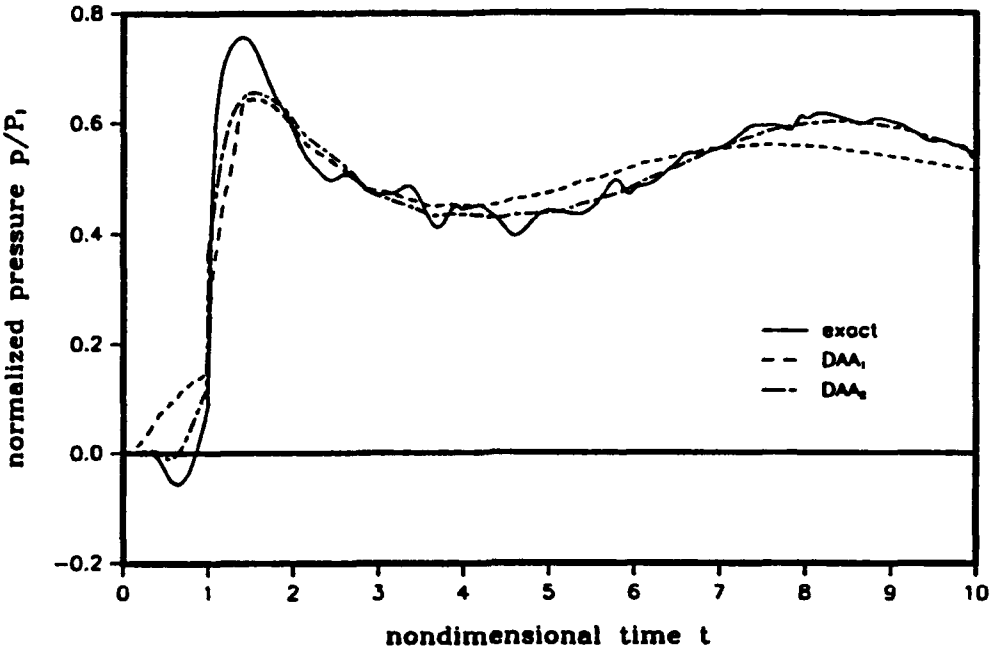

Figure 19. Exact, DAA_1 and DAA_2 internal-surface pressure histories at $\theta = \pi/2$.

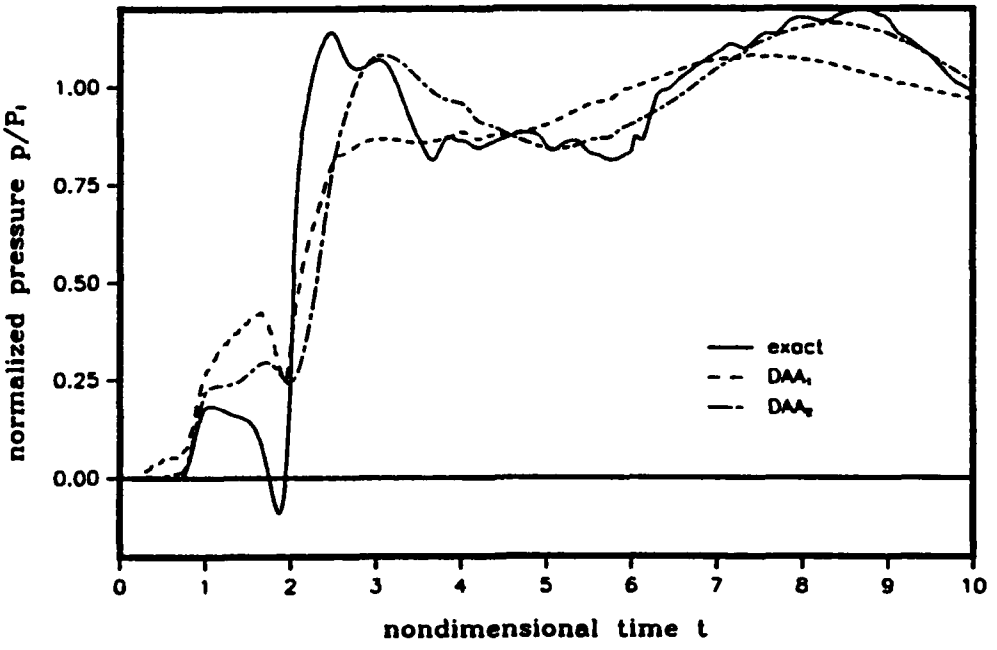

Figure 20. Exact, DAA_1 and DAA_2 external-surface pressure histories at $\theta = 0$.

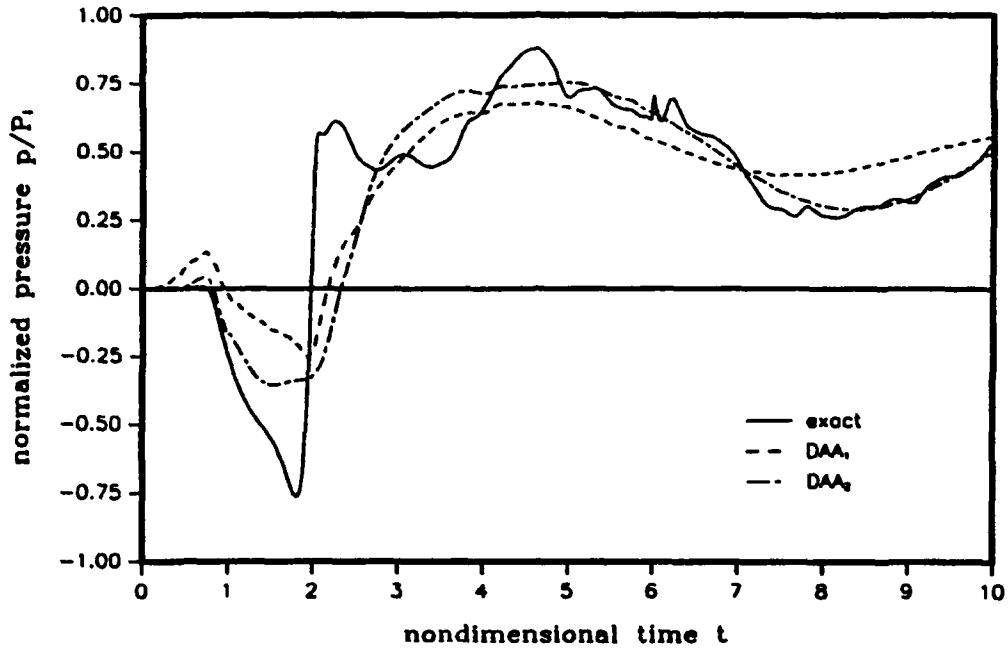

Figure 21. Exact, DAA_1 and DAA_2 internal-surface pressure histories at $\theta = 0$.

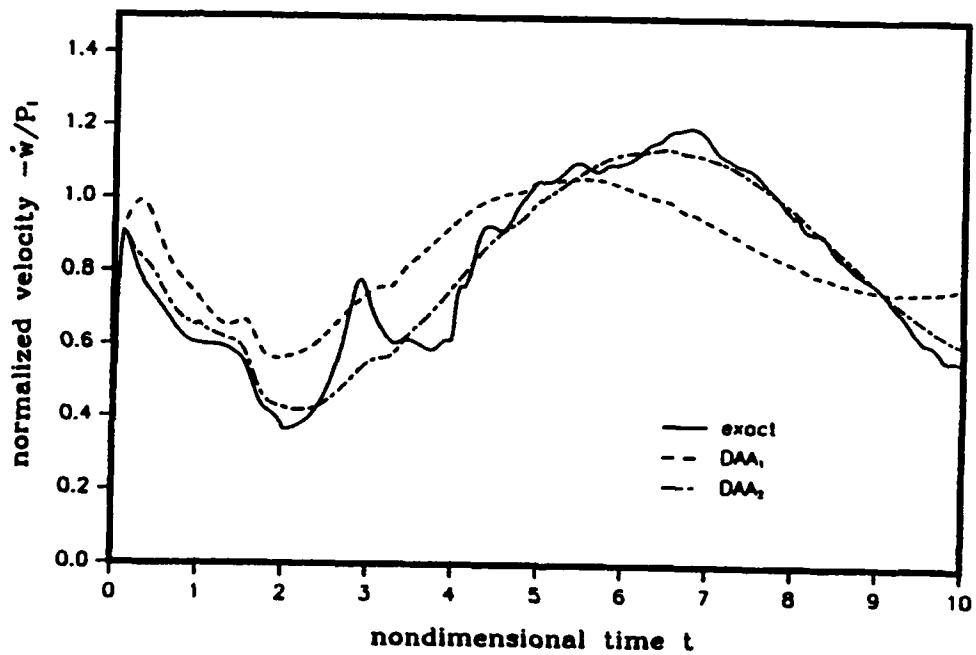

Figure 22. Exact, DAA_1 and DAA_2 radial shell-velocity histories at $\theta = \pi$.

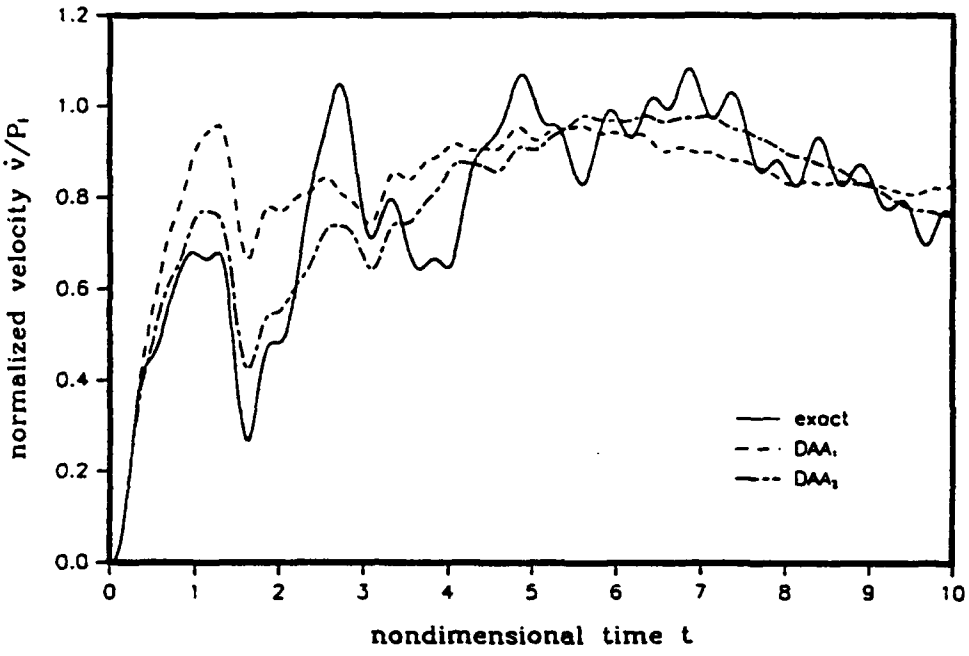

Figure 23. Exact, DAA_1 and DAA_2 circumferential shell-velocity histories at $\theta = \pi/2$.

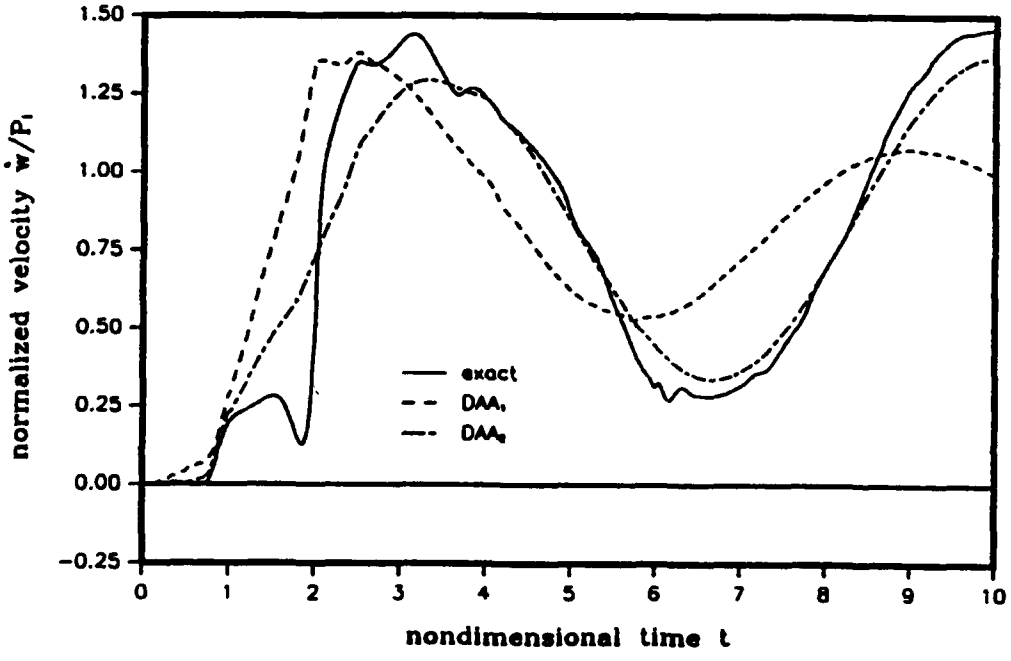

Figure 24. Exact, DAA_1 and DAA_2 radial shell-velocity histories at $\theta = 0$.

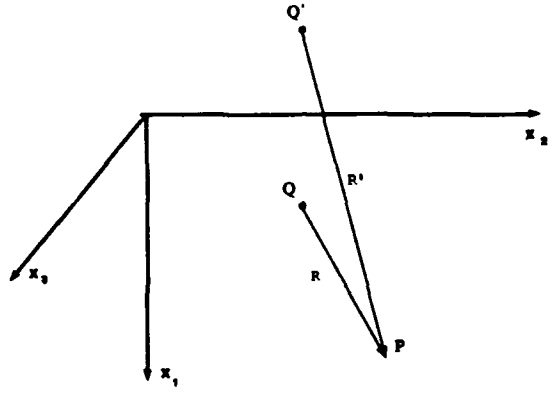

Figure 25. Three–dimensional geometry (in the case of the half–space, the infinite free surface lies in the $x_2 - x_3$ plane).

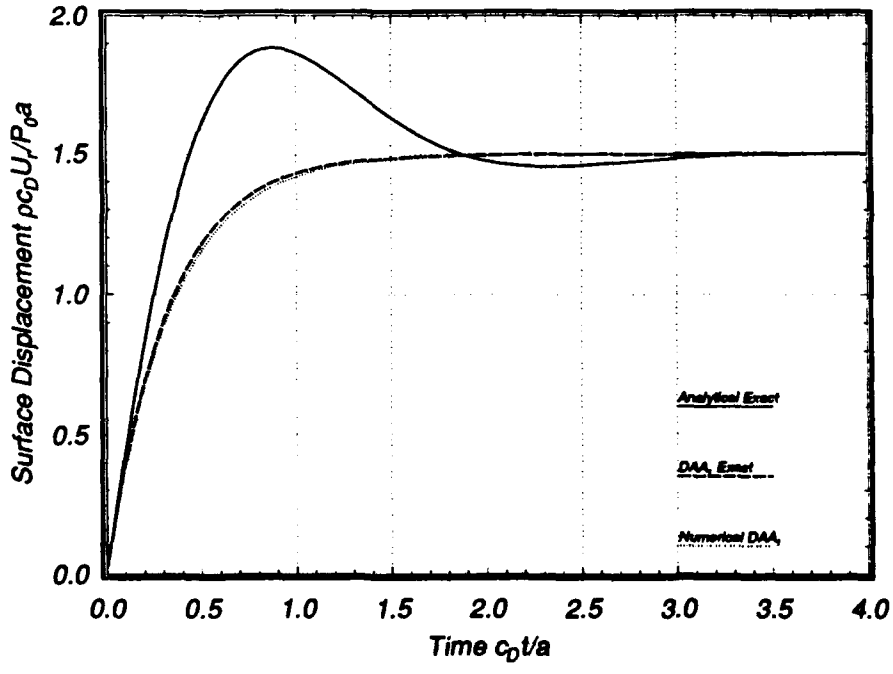

Figure 26. Radial displacement response of a pressurized cavity in an infinite elastic medium.

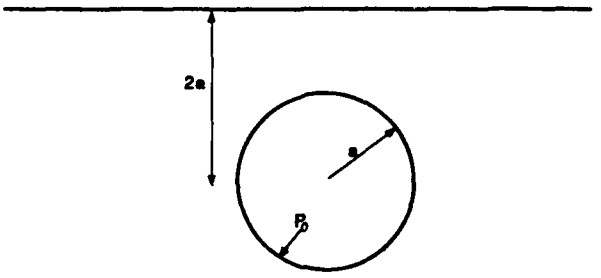

Figure 27. Geometry for a cavity embedded in a semi-infinite elastic medium.

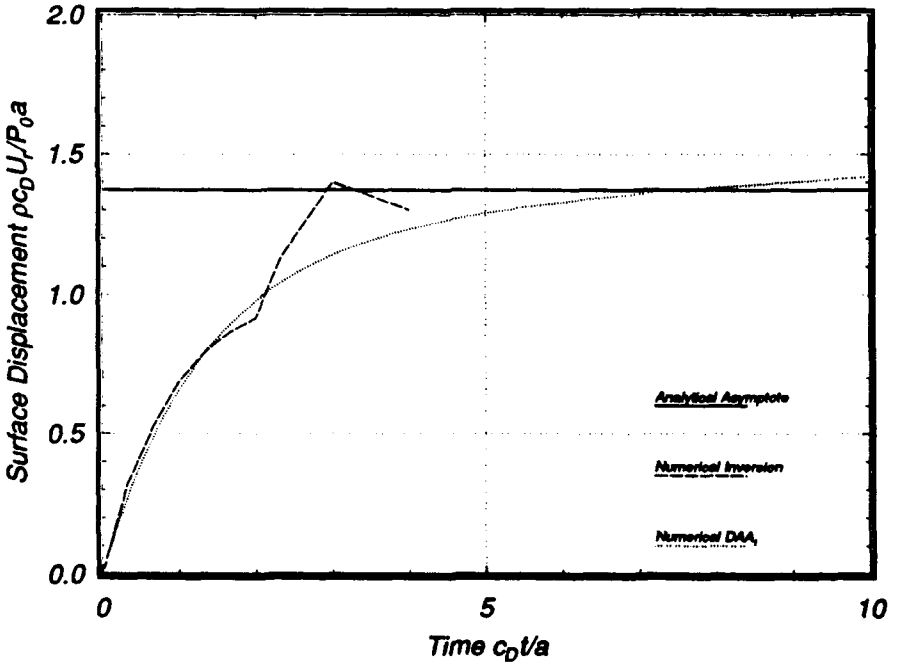

Figure 28. Radial displacement response of a pressurized cavity in a semi-infinite elastic medium ($\theta = 0°$, $d = 2a$).

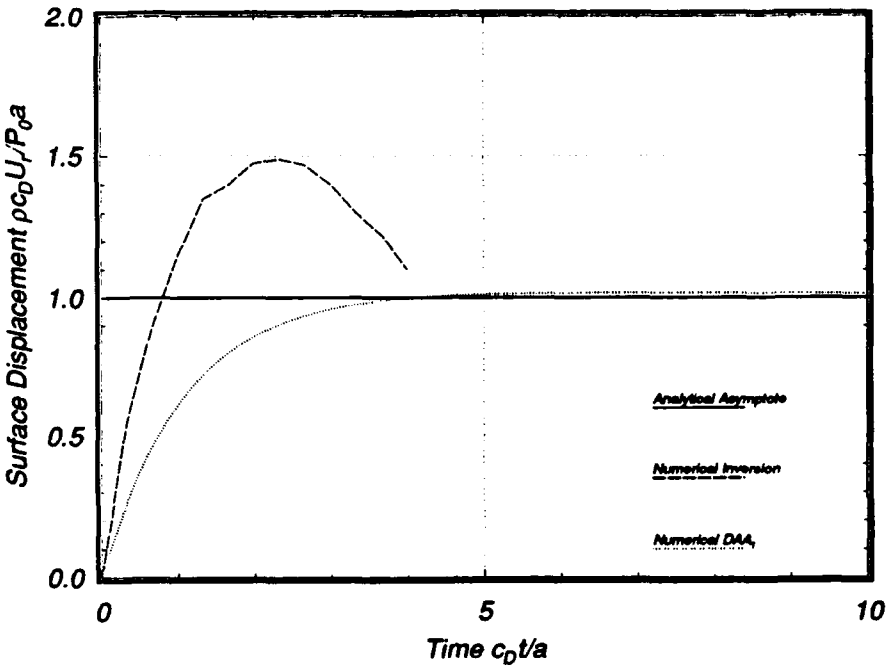

Figure 29. Radial displacement response of a pressurized cavity in a semi-infinite elastic medium ($\theta = 90°$, $d = 2a$).

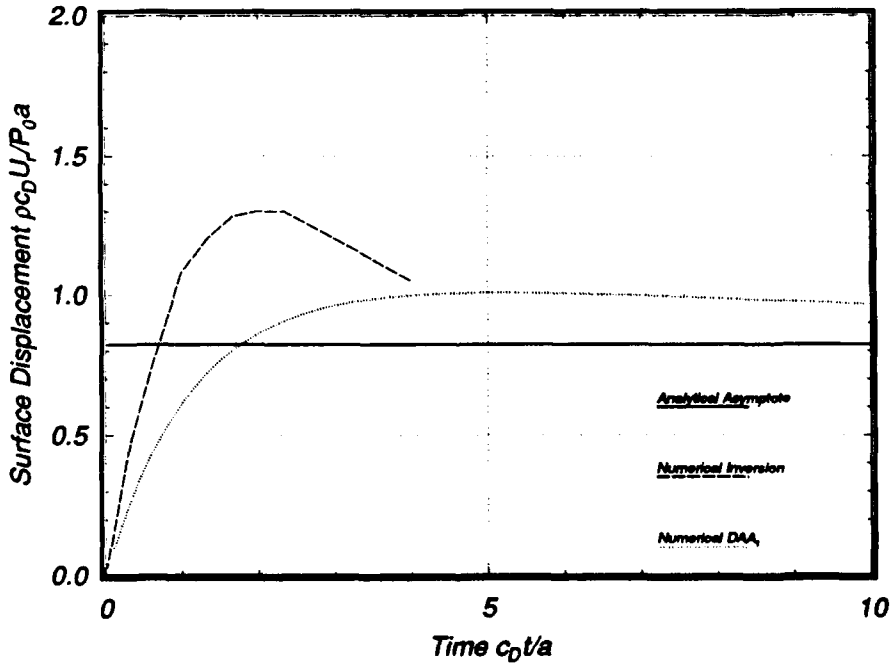

Figure 30. Radial displacement response of a pressurized cavity in a semi-infinite elastic medium ($\theta = 180°$, $d = 2a$).

DISTRIBUTION LIST

DNA-TR-91-69

DEPARTMENT OF DEFENSE

ASSISTANT TO THE SECRETARY OF DEFENSE
ATTN: EXECUTIVE ASSISTANT

DEFENSE INTELLIGENCE AGENCY
ATTN: DB-6E1
ATTN: OGA-4B2

DEFENSE NUCLEAR AGENCY
ATTN: OPNS
ATTN: SPSD
ATTN: SPWE
2 CYS ATTN: TITL

DEFENSE TECHNICAL INFORMATION CENTER
2 CYS ATTN: DTIC/FDAB

FIELD COMMAND DEFENSE NUCLEAR AGENCY
ATTN: FCPR

FIELD COMMAND DEFENSE NUCLEAR AGENCY
ATTN: FCNV

FIELD COMMAND DEFENSE NUCLEAR AGENCY
ATTN: FCNM

THE JOINT STAFF
ATTN: JKC DNA REP
ATTN: JKCS

DEPARTMENT OF THE ARMY

DEP CH OF STAFF FOR OPS & PLANS
ATTN: DAMO-SWN

HARRY DIAMOND LABORATORIES
ATTN: SLCIS-IM-TL

U S ARMY CORPS OF ENGINEERS
ATTN: CERD-L

U S ARMY ENGR WATERWAYS EXPER STATION
ATTN: CEWES J K INGRAM
ATTN: CEWES-SD DR J G JACKSON JR
ATTN: J ZELASKO CEWES-SD-R
ATTN: R WHALIN CEWES-ZT
ATTN: RESEARCH LIBRARY

U S ARMY NUCLEAR & CHEMICAL AGENCY
ATTN: MONA-NU DR D BASH

U S ARMY STRATEGIC DEFENSE COMMAND
ATTN: CSSD-SA-EV
ATTN: CSSD-SL

U S ARMY WAR COLLEGE
ATTN: LIBRARY

USA SURVIVABILITY MANAGMENT OFFICE
ATTN: SLCSM-SE J BRAND

DEPARTMENT OF THE NAVY

DAVID TAYLOR RESEARCH CENTER
ATTN: CODE 172
ATTN: CODE 173
ATTN: CODE 1740
ATTN: CODE 1750
ATTN: CODE 1770
ATTN: CODE 2740

DEPARTMENT OF THE NAVY
ATTN: SEA-08
ATTN: SEA-423
ATTN: SEA-511
ATTN: SEA-55X1
ATTN: SEA-55Y

MARINE CORPS
ATTN: CODE POR-21

NAVAL COASTAL SYSTEMS CENTER
ATTN: CODE 7410

NAVAL DAMAGE CONTROL TRAINING CENTER
ATTN: COMMANDING OFFICER

NAVAL ELECTRONICS ENGRG ACTVY, PACIFIC
ATTN: CODE 250

NAVAL EXPLOSIVE ORD DISPOSAL TECHNOLOGY CENTER
ATTN: CODE 90 J PETROUSKY

NAVAL POSTGRADUATE SCHOOL
ATTN: CODE 1424 LIBRARY

NAVAL RESEARCH LABORATORY
ATTN: CODE 2627

NAVAL SURFACE WARFARE CENTER
ATTN: CODE H21
ATTN: CODE R14
ATTN: CODE R15

NAVAL WEAPONS CENTER
ATTN: CODE 3263 J BOWEN

NAVAL WEAPONS EVALUATION FACILITY
ATTN: CLASSIFIED LIBRARY

NEW LONDON LABORATORY
ATTN: TECH LIBRARY

OFFICE OF CHIEF OF NAVAL OPERATIONS
ATTN: NOP 091
ATTN: NOP 223
ATTN: NOP 225
ATTN: NOP 37
ATTN: NOP 605D5
ATTN: NOP 957E
ATTN: OP 03EG
ATTN: OP 21
ATTN: OP 654
ATTN: OP 73

OFFICE OF NAVAL RESEARCH
ATTN: CODE 1132SM
ATTN: CODE 23

DEPARTMENT OF THE AIR FORCE

AIR FORCE INSTITUTE OF TECHNOLOGY/EN
ATTN: COMMANDER

HQ USAF/CCN
ATTN: AFCCN

DEPARTMENT OF ENERGY

LAWRENCE LIVERMORE NATIONAL LAB
ATTN: D MAGNOLI

LOS ALAMOS NATIONAL LABORATORY
ATTN: REPORT LIBRARY
ATTN: TECH LIBRARY

MARTIN MARIETTA ENERGY SYSTEMS INC
ATTN: DR C V CHESTER

SANDIA NATIONAL LABORATORIES
ATTN: TECH LIB 3141

U.S. DEPARTMENT OF ENERGY
OFFICE OF MILITARY APPLICATIONS
ATTN: OMA/DP-252 MAJ D WADE

OTHER GOVERNMENT

CENTRAL INTELLIGENCE AGENCY
ATTN: OSWR/NED

DEPARTMENT OF DEFENSE CONTRACTORS

AN ANALYSIS & TECHNOLOGY COMPANY
ATTN: V GODINO

APPLIED RESEARCH ASSOCIATES, INC
ATTN: R FRANK

CALIFORNIA INSTITUTE OF TECHNOLOGY
ATTN: T AHRENS

CALIFORNIA RESEARCH & TECHNOLOGY, INC
ATTN: J THOMSEN
ATTN: K KREYENHAGEN

COLUMBIA UNIVERSITY
ATTN: F DIMAGGIO

KAMAN SCIENCES CORP
ATTN: LIBRARY

KAMAN SCIENCES CORP
ATTN: DASIAC
ATTN: E CONRAD

KAMAN SCIENCES CORPORATION
ATTN: DASIAC

KARAGOZIAN AND CASE
ATTN: J KARAGOZIAN

LOCKHEED MISSILES & SPACE CO, INC
ATTN: PHILIP UNDERWOOD

LOCKHEED MISSILES & SPACE CO, INC
ATTN: TECH INFO CTR

PACIFIC-SIERRA RESEARCH CORP
ATTN: H BRODE

S-CUBED
ATTN: K D PYATT JR
ATTN: R SEDGEWICK

SCIENCE APPLICATIONS INTL CORP
ATTN: TECHNICAL REPORT SYSTEM

TELEDYNE BROWN ENGINEERING
ATTN: J RAVENSCRAFT

THE TITAN CORPORATION
ATTN: LIBRARY
ATTN: S SCHUSTER

UNIVERSITY OF COLORADO
2 CYS ATTN: B A LEWIS
2 CYS ATTN: P ZHANG
2 CYS ATTN: T L GEERS

WEIDLINGER ASSOC, INC
ATTN: H LEVINE

WEIDLINGER ASSOCIATES, INC
ATTN: T DEEVY

WEIDLINGER ASSOCIATES, INC
ATTN: M BARON

WESTINGHOUSE ELECTRIC CORP
ATTN: D BOLTON